TAMPERE UNIVERSITY OF TECHNOLOGY

HENRI VÄISÄNEN

$CaCO_3$ SCALE INHIBITION IN PAPER MAKING PROCESSES – EVALUATION OF TESTING METHODS AND INHIBITOR PERFORMANCE

Master of Science Thesis

Examiner: Professor Helge Lemmetyinen
Examiner and topic approved in the Faculty of Science and Environmental Engineering Council meeting on 9 November 2011

ABSTRACT

TAMPERE UNIVERSITY OF TECHNOLOGY
Master's Degree Programme in Science and Engineering
VÄISÄNEN HENRI: $CaCO_3$ scale inhibition in paper making processes – evaluation of testing methods and inhibitor performance
Master of Science Thesis, 77 pages, 18 Appendix pages
December 2011
Major: Chemistry
Examiner: Professor Helge Lemmetyinen
Keywords: calcium carbonate precipitation, scaling problems in paper making, laboratory testing of scale inhibitors

The formation of an adherent layer of inorganic deposition on the surfaces of process equipment is called scaling. Scaling is a major problem in many industries using large quantities of water. One of these industries is the paper making industry and the most common scale forming compound is calcium carbonate. The scaling problem in the paper making industry can be eased or in the best case completely solved by the use of chemical additives referred to as antiscalants or scale inhibitors. The most common antiscalant compounds are phosphonates and polycarboxylates.

The formation of calcium carbonate scale and its inhibition are widely studied themes but few of the studies are linked in the conditions of paper making. The objectives of this thesis are to establish laboratory testing methods for the evaluation of the performance of different scale inhibitors in the paper making conditions and to evaluate the performance of different antiscalants in these conditions. The thesis comprises an extensive literature survey and an experimental part. The literature survey covers the precipitation process of calcium carbonate, factors affecting this process and chemistry of different antiscalants. Also the theory of a computational model of French Creek's WatSIM software is covered. In the experimental part three different laboratory test methods are utilized to conclude the performance of different antiscalants in the conditions of paper making. These laboratory test methods are a static jar test, a dynamic rotating disk procedure, and a dynamic tube blocking procedure. The WatSIM software is utilized to calculate different scaling potential indices in the conditions of paper making.

The results of this thesis show that the differences between different antiscalants can be distinguished with the used laboratory testing methods and that the differences are significant. The phosphonate antiscalants might function better than polycarboxylate antiscalants in certain operating conditions but even a little change in the conditions, for example in the pH or temperature, can completely block the ability of the phosphonate antiscalants to function. The polycarboxylate antiscalants are more resistant to changes in the operating conditions, which extend their range of use. The computational results yielded with WatSIM were somewhat conflicting which indicates that the software is not fully optimized for the conditions of paper making.

TIIVISTELMÄ

TAMPEREEN TEKNILLINEN YLIOPISTO
Teknis-luonnontieteellinen koulutusohjelma
VÄISÄNEN HENRI: $CaCO_3$ saostumien esto paperinvalmistuksen prosesseissa – koemenetelmien ja saostumanestoaineiden toiminnan evaluointi
Diplomityö, 77 sivua, 18 liitesivua
Joulukuu 2011
Pääaine: Kemia
Tarkastaja: Professori Helge Lemmetyinen
Avainsanat: kalsiumkarbonaatin saostuminen, saostumaongelmat paperinvalmistuksessa, saostumanestoaineiden laboratoriokokeet

Epäorgaanisten suolojen muodostamat prosessilaitteisiin tiukasti kiinnittyneet saostumakerrokset aiheuttavat ongelmia monilla teollisuudenaloilla, joissa käytetään suuria määriä vettä. Yksi näistä teollisuuden aloista on paperiteollisuus, jossa yleisin saostumia aiheuttavista suoloista on kalsiumkarbonaatti. Paperiteollisuuden saostumaongelmaa voidaan helpottaa, tai parhaassa tapauksessa se voidaan kokonaan ratkaista, kemiallisten lisäaineiden eli saostumanestoaineiden avulla. Yleisimmin käytettyjä saostumanestoaineita ovat fosfonaatti- ja polykarboksylaattiyhdisteet.

Kalsiumkarbonaatin saostuminen ja saostumisen estäminen ovat laajasti tutkittuja aiheita, mutta harvat tutkimuksista liittyvät suoraan paperinvalmistuksen olosuhteisiin. Tämän työn tavoitteet ovat luoda laboratoriokoemenetelmät eri saostumanestoaineiden vertailuun paperinvalmistuksen olosuhteissa ja arvioida eri saostumanestoaineiden toimintaa näissä olosuhteissa.

Työ koostuu kattavasta kirjallisuusselvityksestä sekä kokeellisesta osuudesta. Kirjallisuusselvityksessä käsitellään kalsiumkarbonaatin saostumista ja siihen vaikuttavia tekijöitä sekä eri saostumanestoaineiden kemiallisia ominaisuuksia. Myös laskennallisen mallin, French Creekin WatSIM -ohjelman, teoria käsitellään kirjallisuusselvityksessä.

Kokeellisessa osuudessa saostumanestoaineiden toimintaa tutkitaan kolmella eri laboratoriomenetelmällä paperinvalmistuksen olosuhteissa. Käytettävät menetelmät ovat staattinen purkkitesti, dynaaminen pyörivä kiekko -menetelmä ja dynaaminen saostumakapillaari -menetelmä. WatSIM -ohjelmaa hyödynnetään erilaisten saostumapotentiaali-indeksien laskemiseen paperinvalmistuksen olosuhteissa.

Työn tulokset osoittavat, että eri saostumanestoaineiden eroja voidaan arvioida käytetyillä laboratoriokoemenetelmillä ja että erot ovat merkittäviä. Fosfonaattiyhdisteet saattavat toimia paremmin kuin polykarboksylaatit tietyissä olosuhteissa, mutta jopa hyvin pieni muutos olosuhteissa, esimerkiksi happamuudessa tai lämpötilassa, voi estää fosfonaattiyhdisteen toiminnan kokonaan. Polykarboksylaatit kestävät paremmin muutoksia toimintaolosuhteissa, mikä laajentaa niiden käyttöaluetta.

WatSIM ohjelmalla saadut laskennalliset tulokset olivat melko ristiriitaisia keskenään, mikä viittaa siihen, että ohjelma ei ole optimoitu paperinvalmistuksen olosuhteisiin.

PREFACE

This study was carried out in Kemira's Fiber and Biorefinery Chemistry laboratory at Kemira's Research & Development Center in Espoo. My sincere gratitude belongs to my supervisors Erkki Räsänen and Jonas Konn for giving me the opportunity to perform this thesis as a part of the Fiber and Biorefinery Chemistry team and for guiding me through the project. I am also grateful for the whole team; I had a great time working with you. I also wish to thank Tapio Honkanen for his help in the project.

In addition, I would like to thank my parents and siblings for supporting me in the course of my studies and my friends for making my student years memorable. Last, but definitely not least, my special gratitude belongs to my girlfriend Noora for being there for me.

Tampere, 28th of November 2011

Henri Väisänen

CONTENTS

ABBREVIATIONS AND SYMBOLS

a	activity
c	concentration
I	ionic strength
J	rate of nucleation
K	equilibrium constant
k	rate constant
K_{sp}	solubility product
m	molality
M_w	weight average molecular weight
R	growth rate
S	supersaturation ratio
S.L.	Saturation Level = supersaturation ratio
γ	activity coefficient
γ'	interfacial tension
ΔG	excess free energy
θ	contact angle
μ	chemical potential
σ	relative supersaturation
τ_{ind}	induction time
τ_{lp}	latent period
v	molecular volume

AA	acrylic acid or acrylate monomer
ACC	amorphous calcium carbonate
AM	acrylamide monomer
ATMP	aminotrimethylenephosphonic acid
B+S model	birth and spread model
BCF theory	Burton-Carbera-Frank theory
BDTMP	butylenediamine tetra(methylene phosphonic acid)
DI-water	deionized water
DSC	differential scanning calorimeter
DTB	dynamic tube blocking
DTPA	diethylene triamine penta acetic acid
EDTA	ethylene diamine tetra acetic acid
EDTMP	ethylenediamine tetra(methylene phosphonic acid)

FAAS	flame atomic absorption spectrometer
HCC	calcium carbonate hexahydrate
HDTMP	hexamethylenediamine tetra(methylene phosphonic acid)
HEDP	1-hydroxyethane-1,1-diphosphonic acid
ICP-OES	inductively coupled plasma-optical emission spectrometer
LSI	Langelier saturation index
MA	maleic acid or maleate monomer
MCC	calcium carbonate monohydrate
MIC	minimum inhibitory concentration
NI	non-ionic monomer
NON model	nuclei on nuclei model
PAA	polyacrylic acid or polyacrylate
PASP	polyaspartic acid or polyaspartate
PBTC	2-phosphono-1,2,4-butanecarboxylic acid
PCC	precipitated calcium carbonate
PDTMP	pentylenediamine tetra(methylene phosphonic acid)
PESA	polyepoxysuccinic acid
PMA	polymaleic acid or polymaleate
ppm	parts per million (mg/kg)
QCM	quartz crystal microbalance
SEM	scanning electron microscopy
SHMP	sodium hexametaphosphate
TDS	total dissolved solids

1. INTRODUCTION

1.1 Background

When a sparingly soluble salt forms a tightly adherent layer of precipitate on the surface, the process is called scaling. The scaling can be caused by many different salts, but one of the most common scale forming salts is calcium carbonate. Scaling causes many problems, such as plugging of the equipment, limited heat transfer, and reduced flow rates in many industrial processes using large quantities of water. These industrial processes include among others many processes of pulp and paper production. [1, p. 1397; 2, p. 345]

The precipitation of calcium carbonate or any other salt results from three mutual processes: supersaturation, nucleation and crystal growth. When a supersaturated solution is formed, the nucleation and crystal growth can take place. The best way to solve the scaling problem is to adjust to process parameters, for example pH and temperature, such way that a supersaturated stage is never generated. This is not always possible, in which case the cleaning of the formed scale or inhibition of the scale formation are the options left. In the case of calcium carbonate, the cleaning can be done for example with an acid boil out. The scale inhibition can be achieved with chemical additives often referred to as antiscalants or scale inhibitors. Most common antiscaling compounds are phosphate, phosphonate, and polycarboxylate antiscalants. The objective of antiscalants is to delay the formation of the precipitate, this is referred to as threshold inhibition, and if the precipitation occurs to modify the formed crystals such way that they do not attach to the surfaces of process equipment, this is referred to as crystal modification and dispersing. The use of antiscalants is commonly a better option than the use of cleaning procedures as the use of antiscalants does not cause down time and limit production. [1; 3; 4]

The alkaline and high temperature conditions of many unit operations of pulp and paper mills are favorable for the formation of the calcium carbonate scale. Calcium is present in the processes from wood and recycled calcium carbonate fillers and carbonate from the cooking chemicals of pulping. The alkaline and high temperature conditions combined with the high total dissolved solids (TDS) content of pulp and paper making streams create extremely difficult conditions for the use of antiscalants compared with many other applications. [5; 6]

In order to specify the performance of different antiscalants in the demanding conditions of pulp and paper mills, it is important that the laboratory test methods are appropriate. Many different methods and standards for the laboratory scale testing exist [7; 8]. The difficulty of choosing right methods comes from the fact that the real process con-

ditions are very hard to simulate in the laboratory. In order to achieve reliable information about the functionality of antiscalants, the methods used should cover as many critical parameters as accurately as possible. Also computational models can be used to achieve additional information about the scaling process and the performance of different antiscalants [9].

The precipitation process of calcium carbonate and the effect of antiscalants on it have been widely studied. The precipitation process of calcium carbonate is for example well covered in the article On Calcium Carbonates: from Fundamental Research to Application [10] by Brečević et al. and the effect of antiscalants on the process is discussed among others in the articles by Rieger et al. [3] and Ketrane et al. [1]. Also the scale problems in pulp and paper mills are well recognized [5; 11].

Although the scale inhibition is a widely studied theme and the problems of pulp and paper mills are known, very few of the studies are directly connected with the conditions of pulp and paper mills. Also the laboratory test methods used in many studies are not suitable for a large scale product testing due to their complexity.

1.2 Objectives

The main objectives of this thesis were to upgrade the fundamental and practical know-how about scaling of calcium carbonate in paper making conditions by:

- evaluating the effect of different test parameters on the scaling process and scale inhibitor performance
- establishing adequate laboratory testing methods for evaluation of calcium carbonate scale inhibition
- gaining information about the functionality of commercially available antiscaling chemistries, as well as new experimental products in the conditions of paper making
- assessing the utility of French Creek's WatSIM software in the conditions of paper making.

1.3 Structure and scope of the study

The study is divided into five chapters. *Chapter 2* is a literature survey covering the theoretical background to the experimental part of the study. The precipitation of sparingly soluble salts is first covered in general. After this the rest of the study focuses merely on the precipitation of calcium carbonate. Also the chemistry of common antiscalants used to solve calcium carbonate scale problems is presented, the options for laboratory test methods are discussed, the theory of the used computational model is covered, and the calcium carbonate scale problems of pulp and paper mills introduced.

Chapters 3 and *4* cover the experimental part of the study. In *Chapter 3* the used research materials and methods are covered in detail. The research methods include a stat-

ic jar test and two different dynamic tests, a rotating disk procedure and a dynamic tube blocking procedure (DTB). In *Chapter 4* the results of the laboratory tests are presented and discussed. The suitability of used test methods is estimated and the performance of different antiscalants discussed. In *Chapter 5* the results of the study are concluded, the achievement of the objectives estimated and the recommendations for further studies suggested.

This study focuses on establishing laboratory test methods for the scale inhibition in paper applications and on estimating the functionality of different antiscalants in these applications. Other applications than those of paper making are left beyond the scope of this study. Nor is the economic point of view included when the suitability of different products for the applications is discussed. In some cases also environmental regulations may rule out the use of certain antiscalants, this is not taken into account in the discussion.

2. THEORETICAL BACKGROUND

The precipitation of sparingly soluble salts, in this case calcium carbonate, is a complex process. Even though the precipitation processes have been studied widely for decades all the phenomena included in the process are not fully understood. [1; 3]

In order to establish adequate testing methods for evaluation of calcium carbonate scale inhibition it is important to understand the mechanisms of the precipitation process, the effect of papermaking conditions, and the effect of inhibitor polymers on this process. In this chapter these matters and computational models of calcium carbonate precipitation in paper making are discussed in further detail.

2.1 Crystallization process of sparingly soluble salts

The precipitation of sparingly soluble salts from aqueous solution requires supersaturated conditions which lead to crystallization. Furthermore, the crystallization involves two stages, nucleation and crystal growth. These processes depend mainly on the equilibrium between mineral phases and aqueous medium. [2; 4]

2.1.1 Concept of supersaturation

Supersaturated conditions are developed when the concentration of salt increases above the equilibrium level. These conditions may be caused by many factors, for example temperature fluctuations or pH change. If the level of deviation from equilibrium is small, the supersaturated solution can be metastable. Metastable solution returns to equilibrium only when the interaction such as the introduction of seed crystal takes place. However, when the level of supersaturation is great enough the supersolubility level is reached and precipitation occurs with or without induction time. [4]

Supersaturation is often expressed as concentration difference between the solute concentration, c, in solution and that at equilibrium, c_∞.

$$\Delta c = c - c_\infty \tag{1}$$

The supersaturation ratio S is defined as

$$S = \frac{c}{c_\infty} = \frac{a}{a_\infty}, \tag{2}$$

where a and a_∞ are the activities of supersaturated solution and equilibrium solution, respectively. It is more relevant to use activities than concentrations, if the concentra-

tions are high. At low concentrations, activities can be assumed to be equal with concentrations. Sometimes also relative supersaturation, σ, is used. It is defined as

$$\sigma = \frac{c - c_\infty}{c_\infty} = S - 1. \tag{3}$$

For salts, $M_{v+}A_{v-}$, it is more appropriate to use mean ionic activities to define the supersaturation ratio, S_a.

$$S_a = \left(\frac{(a_+)_s^{v+} (a_-)_s^{v-}}{(a_+)_\infty^{v+} (a_-)_\infty^{v-}} \right)^{1/v} = \frac{a_{\pm,s}}{a_{\pm,\infty}}, \tag{4}$$

where subscript s refers to supersaturated solution and ∞ to equilibrium conditions. a_+ and a_- are the activities of positive and negative ions, respectively, and $v_+ + v_- = v$. The mean ionic activities are $a_{\pm,s}$ for the supersaturated solution and $a_{\pm,\infty}$ for the equilibrium. The difference in chemical potential $\Delta\mu$ between solute in supersaturated state and equilibrium is the fundamental driving force for the formation of the salt from the supersaturated solution

$$\Delta\mu = \mu_s - \mu_\infty. \tag{5}$$

The chemical potential of the solute can be expressed in terms of standard potential μ° and mean ionic activity $a_\pm$ of the solute

$$\mu_{solute} = \mu^\circ + RT \ln a_\pm^v, \tag{6}$$

where R is the molar gas constant and T the absolute temperature. Substitution of equation 6 to equation 5 gives

$$\frac{\Delta\mu}{RT} = \ln\left(\frac{a_{\pm,s}}{a_{\pm,\infty}} \right)^v = \ln S = v \ln S_a. \tag{7}$$

from which the driving force of salt formation can be calculated. [4, p. 828; 12, pp. 228–230]

2.1.2 Nucleation process

The supersaturated condition alone is not sufficient to cause the formation of crystals. Before crystals can be developed the small centers of crystals, embryos, nuclei or seeds must exist. When the solution reaches supersaturation, the nucleation can take place.

There is no general agreement on nucleation terminology, but usually nucleation is specified to primary and secondary nucleation. Primary nucleation takes place in the absence of other crystallites. When new crystal is generated in the presence of other crystallites, it is identified as secondary nucleation. Primary nucleation can be further distinguished into homogeneous and heterogeneous nucleation. Homogeneous nucleation starts spontaneously and randomly, whereas heterogeneous nucleation occurs catalyzed on the surface of foreign particles. [4, p. 829; 13, p. 181]

According to classical nucleation theories, homogeneous nucleation progresses through bimolecular reactions. First a dimer is formed, which again reacts to a trimer and so on, finally resulting in a cluster with a critical size. When a critical size is reached, the nucleus can grow further to a macroscopic crystallite. This can only occur when supersaturation is locally high. Clusters which do not reach the critical size are unstable and redissolve. If the critical size is reached, the nucleus remains stable under the average supersaturation conditions of the solution. [4, p. 829; 13, p. 182]

This phenomenon can be further discussed by reviewing the overall excess free energy, ΔG, between a small particle of solute and solute in solution. The particle is assumed to be spherical. The overall excess free energy is a sum of surface excess free energy, ΔG_S, and volume excess free energy, ΔG_V. The surface excess free energy is caused by interfacial tension, γ', between the developing crystalline surface and the supersaturated solution. The volume excess free energy is the free energy between a very large particle and the solute in solution.

$$\Delta G = \Delta G_S + \Delta G_V = 4\pi r^2 \gamma' + \frac{4}{3}\pi r^3 \Delta G_v , \tag{8}$$

where r is the radius of the sphere and ΔG_v the free energy change of the transformation per unit volume. The terms ΔG_S and ΔG_V of equation 8 are of opposite signs and differently proportional to r, so the overall excess free energy, ΔG, has a maximum value, ΔG_{crit}, which corresponds to the critical size of the nucleus, r_c. The critical size is obtained by setting $\mathrm{d}\Delta G/\mathrm{d}r = 0$:

$$\frac{\mathrm{d}\Delta G}{\mathrm{d}r} = 8\pi r\gamma' + 4\pi r^2 \Delta G_v = 0 \tag{9}$$

$$r_c = \frac{-2\gamma'}{\Delta G_v} . \tag{10}$$

Substituting equation 10 to equation 8 gives

$$\Delta G_{crit} = \frac{16\pi\gamma'^3}{3(\Delta G_v)^2} = \frac{4\pi r_c^2}{3} . \tag{11}$$

A nucleus formed in a supersaturated solution pursues for a decrease in the free energy, whether it achieves this objective through dissolution or growth is conditional on the size of the cluster. [13, pp. 183–184]

The rate of nucleation, *J*, can be expressed as an Arrhenius equation

$$J = A\mathrm{e}^{\frac{-\Delta G}{\mathrm{k}T}}. \tag{12}$$

where k is the Boltzmann constant, $1.381\times10^{-23}\ \mathrm{J\,K^{-1}}$, T is the absolute temperature, and A the pre-exponential factor. The basic Gibbs-Thomson relationship can be written as

$$\ln S = \frac{2\gamma'\nu}{\mathrm{k}Tr_c}. \tag{13}$$

S is defined by equation 2 and ν is the molecular volume. Connecting equations 10 and 13 gives

$$-\Delta G_v = \frac{2\gamma'}{r_c} = \frac{\mathrm{k}T\ln S}{\nu}. \tag{14}$$

Substituting this to equation 11 gives

$$\Delta G_{crit} = \frac{16\pi\gamma'^3\nu^2}{3(\mathrm{k}T\ln S)^2} \tag{15}$$

and to equation 12

$$J = A\mathrm{e}^{-\frac{16\pi\gamma'^3\nu^2}{3\mathrm{k}^3T^3(\ln S)^2}}. \tag{16}$$

Equation 16 indicates that the rate of nucleation is governed by the temperature, the level of supersaturation and the interfacial tension. For a case of non-spherical nuclei the geometrical factor $16\pi/3$ in equations 11, 15, and 16 must be replaced by an appropriate one. [13, pp. 184–186]

However, the equations above consider the case of homogenous nucleation, which is in fact a rare event. In most cases, especially in papermaking streams, there are foreign particles of appropriate size, which act as heteronuclei leading to heterogeneous nucleation. The most active heteronuclei in liquid solutions are of range 0.1 to 1 μm. The presence of a suitable heteronuclei may induce nucleation at a lower supersaturation ratio

than required for homogeneous nucleation. The critical free energy of a heterogeneous case, $\Delta G'_{crit}$, can be associated to a homogeneous one with the equation

$$\Delta G'_{crit} = \phi \Delta G_{crit} \ , \tag{17}$$

where the factor ϕ is dimensionless and less than unity. [13, pp. 192-193]

The factor ϕ can be expressed as

$$\phi = \frac{(2+\cos\theta)(1-\cos\theta)^2}{4} \ , \tag{18}$$

where θ is the contact angle between the crystalline deposit and the foreign particle. It corresponds to the angle of wetting in liquid-solid systems. The contact angle can be expressed using three interfacial tensions

$$\cos\theta = \frac{\gamma'_{sl} - \gamma'_{cs}}{\gamma'_{cl}} , \tag{19}$$

The interfacial tension are between the foreign solid and liquid γ'_{sl}, between the crystalline phase and the foreign solid γ'_{cs}, and between the crystalline phase and the liquid γ'_{cl}. [13, pp. 192–193]

In the case of secondary nucleation the solution nucleates more easily due to primary crystals present in the solution. This can be explained in two different ways. Either a new surface layer starts to grow on the primary crystal and is then removed by the mechanical shearing of fluid before attached properly into crystal lattice, or small particles can be torn of the primary crystal by collisions or mechanical shearing of fluid. Both cases result in stable embryos which can grow into crystals at a lower supersaturation level than required for the primary nucleation. [13, p. 195; 14]

The nucleation process can be strongly affected by impurities in the solution. Colloidal substances and foreign cations can suppress nucleation. The actions of high molecular weight substances and cations are quite different. High molecular substances, such as antiscalants, probably have their main action on heteronuclei whereas cations, such as Fe^{3+} and Al^{3+}, affect on crystallite structures. [13, pp. 205–206] The effect of impurities will be discussed more in context with the formation of calcium carbonate scale and chemistry of antiscalants.

As mentioned before, there can be an induction time, τ_{ind}, between the formation of supersaturated solution and detection of the first crystals. Induction time consists of the time needed to form a stable nucleus and the time required for the stable nuclei to grow into detectable size. At low supersaturations also a latent period, τ_{lp}, can exist. The la-

tent period is the time between the first crystals detected and a radical change in the supersaturation of the solution due to precipitation. [13, pp. 206–207]

2.1.3 Crystal growth

When the stable nuclei of critical size have been formed, they start to grow into visible crystals. The crystal growth is a complex process and many theories have been formed to describe the crystal growth mechanisms. The most relevant of these theories are the diffusion theories and adsorption-layer theories, which are discussed in this section. [4; 13]

The Gibbs-Volmer theory is based on thermodynamic reasoning. It suggests that a crystal grows by layer to layer induced by two-dimensional surface nucleation. According to this theory, when growth units of crystallizing substance arrive at a crystal face, they are at first loosely connected to the crystal surface forming an adsorption layer. In this layer the growth units are free to migrate by surface diffusion and they link into the crystal lattice in a position, where the attractive forces are the greatest. In an ideal case, a whole layer is completed before the next layer starts to grow. [13, p. 218]

In the new layer, a surface nucleation must first occur before the layer starts to grow. The critical free energy, ΔG_{crit}, of surface nucleation can be expressed in the same manner as for homogeneous three-dimensional nucleation in chapter 2.1.2. The only difference is that in this case the object considered is a disc, whereas in the three-dimensional case it was a sphere. This examination leads to equation 20. [13, p. 219]

$$\Delta G_{crit} = \frac{\pi h \gamma'^2 \nu}{\mathrm{k}T \ln S} . \tag{20}$$

In equation 20 h is the height of the disc. Comparing the equations 15 and 20 with typical values leads to a conclusion that surface nucleation requires lower local supersaturation than three-dimensional nucleation but still rather high values are necessary. [13, pp. 219–220]

Another way to approach the growth of a crystal face is the Kossel model, where a crystal face is assumed to consist of steps of monoatomic height. This model is depicted in *Figure 2.1*.

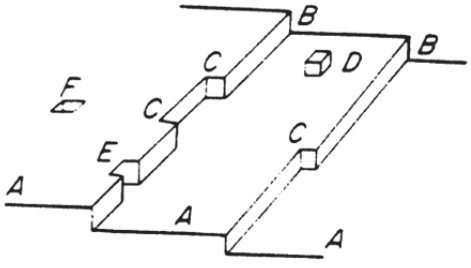

Figure 2.1. Kossel's model of crystal growth. Flat surfaces (A) are separated by steps (B). There are kinks (C), adsorbed growth units (D), edge vacancies (E), and surface vacancies (F) on the steps. [13, p. 220]

The steps may contain kinks and vacancies, where the growth units can be most easily adsorbed. Eventually all the kinks and vacancies are filled leading to full steps and a completed face. A new face starts to grow with surface nucleation. In this model, the growth rate is fastest when the crystal faces are entirely covered with kinks. This condition is not likely to remain long as for example broken crystals have a tendency to repair themselves rapidly and continue to grow at much slower rate. However, many crystals grow quite rapidly even at low supersaturations, which is not consistent with this model. This inconsistency can be explained with the fact that the ideal layer-by-layer growth hardly ever occurs. [13, p. 220]

There are also models based on the surface nucleation, which don't assume the layer-by-layer growth. One of these is birth and spread (B+S) model. This model is based on the idea that several nuclei can be formed on a crystal face and they all spread and is also referred to with other names such as nuclei on nuclei (NON) and polynuclear growth. [13, p. 231] Although theories based on the surface nucleation have some use they don't correspond to empirical experiences of crystal growth rate at low supersaturations. [15]

Instead of surface nucleation other ways to induce crystal growth may be considered. There are dislocations in the crystal face of which screw dislocation is considered important for crystal growth. The concept of screw dislocation is shown in *Figure 2.2*.

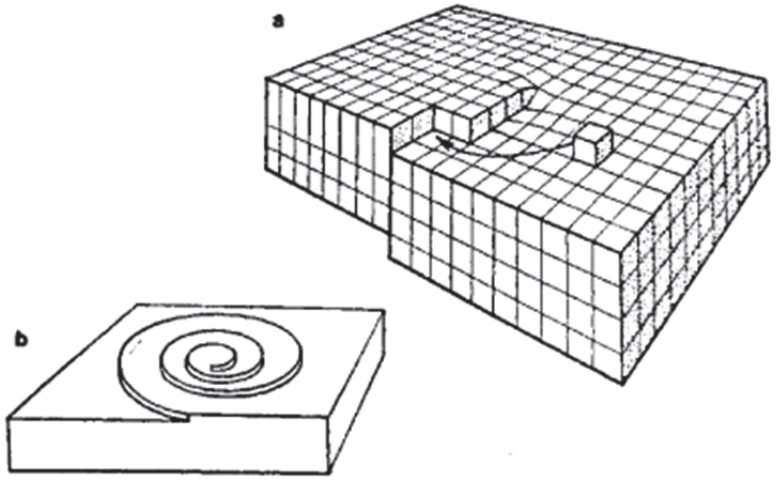

Figure 2.2. (a) Crystal growth induced by screw dislocation. (b) Spiral growth leads to absence of smooth faces. [16]

Screw dislocation causes the crystal to grow in a spiral manner, which leads to absence of smooth faces and surface nucleation is not necessary for the crystal to grow. Burton-Carbera-Frank theory (BCF theory) for spiral growth mechanism states that the curvature of the spiral near its origin is related to distance between successive turns of spirals and the level of supersaturation. The growth rate, R_{BCF}, at any supersaturation is

$$R_{BCF} = \frac{1}{A}\frac{dm}{dt} = A'\sigma^2 \tanh(B'/\sigma), \tag{21}$$

where A is the surface area of the crystal, m is the mass of solid deposition in time t, A' and B' are constants depending on the temperature and step spacings and σ is relative supersaturation. When the level of supersaturation is low equation 21 approximates to $R_{BCF} \propto \sigma^2$ and with high supersaturations to $R_{BCF} \propto \sigma$. This means that the graph of growth rate as a function of relative supersaturation changes from parabolic to linear when the level of supersaturating increases. The BCF theory was developed for vapors, but it can also be used with liquids with different expressions of A and B. However, in liquid solutions the phenomenon is more complex and these factors are difficult to quantify. [4, p. 831; 13, pp. 220–223]

Diffusion-reaction theories are another way to approach the crystal growth process. These theories state that the crystal growth is a two-step process where solute molecules are transported to the crystal surface by diffusion and this is followed by a reaction integrating the molecules into the crystal lattice. The rate equations for this process are

$$R_G = k_d(c - c_i) \qquad \text{(diffusion)} \qquad (22)$$

$$R_G = k_r(c_i - c_\infty)^r \qquad \text{(reaction)} \qquad (23)$$

$$R_G = K_G(c - c_\infty)^g \qquad \text{(overall),} \qquad (24)$$

where k_d and k_r are rate constants for diffusion and reaction. K_G is an overall crystal growth coefficient and c is the concentration of the solute in solution. Subscript i for concentration refers to crystal-solution interface concentration (which is shown to be supersaturated [13, p. 226]) and ∞ to equilibrium saturation. Exponents r and g are the orders of reaction and overall process, respectively. It should be noticed that the term order in this case is not the same as in chemical kinetics conventionally. [13, pp. 225–227]

The overall order of the process, g, is usually 1–2 for the crystallization of inorganic salts. If the reaction is rapid in comparison with diffusion, the overall process is diffusion controlled and $K_G \approx k_d$. This would be the case at relatively low supersaturation levels. Similarly, high supersaturation leads to a case controlled by reaction step, when $K_G \approx k_r$. [13, p. 227]

It should be noted that crystal growth mechanisms are complex and not fully understood. Many of them can occur simultaneously being additive processes or consecutively being competing processes. [13, p. 232] The crystal growth theories represented in this thesis are only a few of those existing. For further orientation Crystallization by J.W. Mullin [13] and Handbook of Industrial Crystallization by A. S. Myerson [15] offer a good starting point.

2.2 Precipitation of calcium carbonate

The precipitation of calcium carbonate occurs basically the same way as described in *Chapter 2.1* for sparingly soluble salts. However, the process is more complex due to several crystalline forms that solid calcium carbonate can have. The temperature, pH, pressure, and the presence of impurities in solution have significant effect on the precipitation behavior of $CaCO_3$.

2.2.1 Equilibrium of $CaCO_3$ in solution

The precipitation reaction of $CaCO_3$ can be written in a general form:

$$Ca^{2+} + CO_3^{2-} \overset{K_{CC}}{\rightleftharpoons} CaCO_3, \quad \text{(I)}$$

where K_{CC} is the equilibrium constant of the reaction. However, the precipitation process is quite complex and the following equilibrium reactions have to be taken into account for carbonate

$$H_2CO_3 \rightleftharpoons HCO_3 + H^+ \quad \text{(II)}$$

$$HCO_3^- \rightleftharpoons CO_3 + H^+ \quad \text{(III)}$$

and for calcium [17, p. 29]:

$$Ca^{2+} + HCO_3^- \rightleftharpoons CaHCO_3^+ \quad \text{(IV)}$$

$$Ca^{2+} + CO_3^{2-} \rightleftharpoons CaCO_3 \quad \text{(V)}$$

$$Ca^{2+}\ OH^- \rightleftharpoons CaOH^+ \quad \text{(VI)}$$

Carbon dioxide also dissolves in water to some extent [17, p. 28]:

$$CO_2\ (g) \rightleftharpoons CO_2\ (aq) \quad \text{(VII)}$$

$$CO_2\ (aq) + H_2O \rightleftharpoons H_2CO_3 \quad \text{(VIII)}$$

The dissolution of carbon dioxide has no major effect in the case of papermaking as the majority of carbonate comes to the process from other sources. In aqueous systems, also the dissociation of water has to be taken into account:

$$H_2O \rightleftharpoons H^+ + OH^- \quad \text{(IX)}$$

Further complexity to the calcium carbonate precipitation process comes from the fact that $CaCO_3$ has several crystalline forms with different physical properties and no single equilibrium constant, K_{CC}, for the formation of $CaCO_3$ can be given. [17, p. 32]

2.2.2 Crystalline forms of $CaCO_3$

Calcium carbonate can precipitate in six different forms, the three anhydrous polymorphs are calcite, aragonite, and vaterite, the three hydrated forms are amorphous calcium carbonates (ACC), calcium carbonate monohydrate (MCC), and calcium carbonate hexahydrate (HCC). Polymorphs differ in lattice structure and have different shapes. They have different physical properties, for example solubility and melting point, but are chemically the same. Polymorphs of $CaCO_3$ (calcite, aragonite and vaterite) are enantiotropic meaning that they can transform from one form to another. According to Ostwald's step rule the least stable crystalline form precipitates first and then transforms into a more stable one. The least stable form also has the highest solubility under the conditions in question. Often hydrated forms of $CaCO_3$ are also referred to as polymorphs, because they have the capability to transform into more stable form, but strictly speaking they are not, as they differ in chemical form. Under standard conditions, calcite is the most stable form of $CaCO_3$ and ACC the most unstable. [10; 13; 17]

ACC is an unstable precursor in precipitation at relatively high supersaturations. It transforms rapidly into more stable anhydrous forms. At low temperatures (10–30 °C) it transforms into vaterite and calcite, at moderate temperatures (40–50 °C) into all three anhydrous forms, and at high temperatures (60–80 °C) into aragonite. ACC exhibits spherical shape with a diameter less than 1 μm. [10, p. 469; 17, p. 33]

HCC ($CaCO_3 \cdot 6H_2O$) is somewhat more stable form than ACC. HCC can stay unmodified at low temperatures (≈ 0 °C) for a few days but decomposes rapidly into anhydrous forms at higher temperatures. The presence of phosphate suppresses the transformation of hydrous forms into anhydrous crystals and enables the growth of HCC. The structure of HCC is monoclinic. HCC is the only crystalline form of $CaCO_3$, which solubility increases with the increase in temperature. [10, p. 470; 17, pp. 33–34]

MCC ($CaCO_3 \cdot H_2O$) is about as stable as HCC. It is a hydrated modification of calcite and its mineral name is therefore monohydrocalcite. Like HCC, also MCC grows in the presence of substances inhibiting the growth of anhydrous forms. These inhibitors can be for example magnesium or other ions and organic matter. The crystal system of MCC is hexagonal. [10, p. 471; 17, p. 35]

Vaterite is the most unstable form of anhydrous polymorphs of calcium carbonate. It transforms rapidly into calcite or aragonite depending on the temperature. However, it is reported that vaterite is often the first solid phase formed in scaling [18]. The crystal system of vaterite is hexagonal. [10, p. 472; 17, p. 36]

Aragonite and calcite are the two most common forms of $CaCO_3$. Under standard conditions calcite is the thermodynamically stable form. However, the difference in the free energy of formation of aragonite and calcite is small and therefore aragonite is also a common form of $CaCO_3$. It transforms slowly into calcite and in the presence of im-

purities aragonite can be a stable form. The structure of aragonite is orthorhombic and the structure of calcite trigonal-rhombohedral. [17, p. 37; 19, p. 137]

2.2.3 Effect of temperature, pH, and pressure on $CaCO_3$

The solubility of inorganic salts is commonly a function of temperature. In the case of calcium carbonate, the solubility of all crystalline forms except HCC decreases with the increase in temperature, which is quite uncommon for inorganic salts. [20, p. 2227] The solubility products of different crystalline forms of $CaCO_3$ as a function of temperature at 1 atm are presented in *Table 2.1*.

Table 2.1. Equations for solubility products of different calcium carbonate crystalline forms at 1 atm and the temperature range in which they are valid. [21; 22; 23; 24]

Crystalline form	log K_{sp} (T in K and t in °C)	Temperature range (°C)
ACC	-6.1987 - 0.00053369*t - 0.0001096*t^2	10–55
HCC	0.1598 - 2011.1/T	0–25
MCC	-7.050 - 0.000159*t^2	15–50
Vaterite	-172.1295 - 0.077993*T + 3074.688/T + 71.595*log T	0–90
Aragonite	-171.9773 - 0.077993*T + 2903.293/T + 71.595*log T	0–90
Calcite	-171.9065 - 0.077993*T + 2839.319/T + 71.595*log T	0–90

The solubility products of ACC, vaterite, aragonite and calcite from *Table 2.1* are presented in *Figure 2.3*.

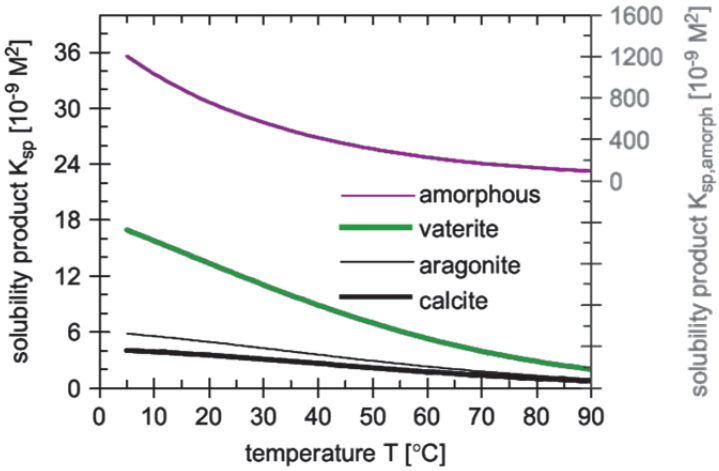

Figure 2.3. Solubility products of ACC, vaterite, aragonite, and calcite as a function of temperature. [20]

A noteworthy matter in the solubility products of calcium carbonate polymorphs is that at higher temperatures the differences in their solubility products are smaller as seen in *Figure 2.3*. Therefore, the stabilities of aragonite and vaterite increase compared with calcite.

In the case of calcium carbonate, another factor affecting the solubility is the value of pH. The effect of pH on solubility is much greater than the effect of temperature due to the diprotic nature of carbonate. The carbonate species as a function of pH is presented in *Figure 2.4*.

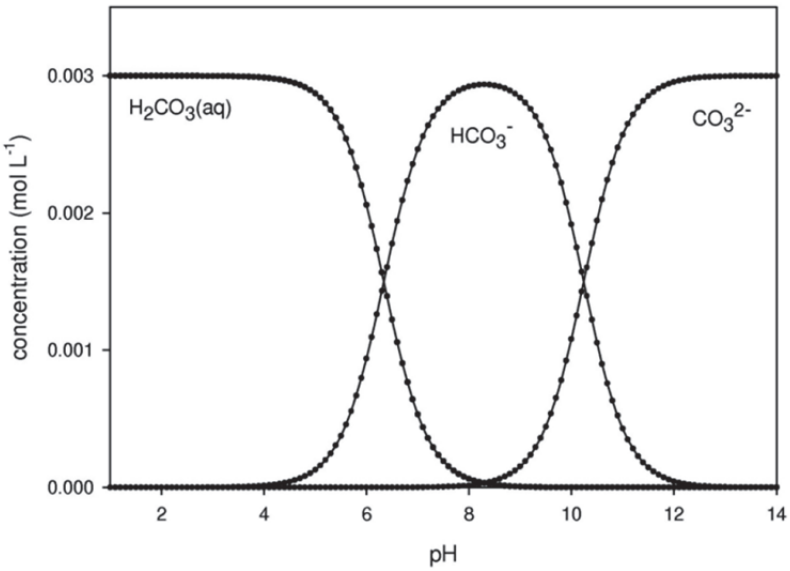

Figure 2.4. The presence of different carbonate species as a function of pH. [17, p.31]

As seen in *Figure 2.4*, $CaCO_3$ is soluble in acid solutions as the equilibrium of the equation II shifts to the carbonic acid. When pH increases, bicarbonate and carbonate are also present. In strongly basic solutions only carbonate ions exist as the equilibrium of the equation III shifts to carbonate and $CaCO_3$ is insoluble. Although the solubility of $CaCO_3$ changes with pH, it should be noted, that this is due to a decrease of the carbonate concentration with the decrease of pH and the solubility product remains unchanged, being only a function of temperature and pressure [25; 26].

The solubility of $CaCO_3$ increases with the increasing pressure. The pressure dependence of the solubility product is complex issue and will not be discussed more here. This dependence is described in detail in many publications [26; 27]. Also the partial pressure of CO_2 in the ambient air affects the solubility of $CaCO_3$. An increase in the partial pressure of CO_2 shifts the equilibrium of the reactions VII and VIII to the right side, which leads to decrease in the pH due to increment in the amount of carbonic acid. This causes an increase in the solubility of $CaCO_3$. [27]

2.2.4 Other factors affecting the $CaCO_3$ precipitation process

Impurities, such as foreign ions and molecules, influence the precipitation process. They can have effect on the rate of the precipitation and the crystalline form of calcium car-

bonate. Impurities can be inorganic or organic and act as inhibitors or promoters of precipitation. [10; 19]

Foreign metal ions, for example Mg^{2+}, Mn^{2+}, Fe^{3+}, Zn^{2+}, and Cu^{2+}, have been reported to make aragonite the thermodynamically stable form of $CaCO_3$ under conditions that normally favorite calcite. The presence of these metal ions has also been reported to promote bulk precipitation and delay nucleation and crystal growth. [19, pp. 137–138] The mechanisms behind these phenomena are not easy to define, but some suggestions can be made. It is probable that the promotion of bulk precipitation is due to formation of heteronuclei containing these foreign ions, for example $ZnCO_3$ or $Zn(OH)_2$. These heteronuclei compete as growth centers with the metallic surface and reduce the precipitation on the surface. The delay of nucleation can be explained by the interaction of the foreign metal ions with the calcium carbonate embryos below the critical size and the delay of crystal growth by the adsorption of the ions on the growth sites of calcium carbonate crystal. The replacement of calcium ions in the crystal lattice with ions of smaller ionic radius and higher hydration energy than calcium results in retardation of the crystal growth rate of aragonite and the transformation to calcite is blocked. [19, pp. 143–144]

The effect of inorganic anions on calcium carbonate precipitation is less significant than the effect of cations. Anions such as SO_4^{2-}, NO_3^-, and Cl^-, have some influence on the content of the corresponding metal ion in the calcium carbonate lattice. Magnesium content of calcite, for example, has been reported to decrease in the order $MgSO_4$ > $Mg(NO_3)_2$ > $MgCl_2$ [10; 28] Anions alone have a little effect on the $CaCO_3$ morphology. Only sulfate ions have been reported to cause aggregation of crystals at moderate and high relative supersaturations. This can be explained with the tetrahedron structure of sulfate ion. For example NO_3^- has a planar sp^2 hybrid structure like CO_3^{2-}. When incorporated in the crystal lattice of $CaCO_3$, sulfate ions cause more disturbances because they are of a wrong shape. [10, p. 480; 28]

Organic substances can also affect the $CaCO_3$ precipitation. Most of them act as inhibitors of the precipitation and if the precipitation occurs they often act as promoters of a certain polymorph. Simple organic molecules like propionic acid have no significant effect on calcium carbonate precipitation but more complex molecules like citric acid and fulvic acid have reported to inhibit the precipitation on nucleation and growth stages. These more complex carboxylic acids adsorb on the positively charged growth sites of $CaCO_3$ crystals and disable their growth. [10, p. 481]

Another factor affecting the precipitation process is the tendency of small solid particles in aqueous systems to form clusters due to attractive van der Waals forces. These forces can cause particles to attach permanently if the particles are small enough for the van der Waals forces to overcome the gravitational forces. This process is called agglomeration and it can boost scaling. [13, p. 316] Agglomeration has influence on the precipitation kinetics and particle size distribution of calcium carbonate crystals. At low supersaturation levels agglomeration has a minor role. At higher supersaturation levels

greater amount of small particles is present and agglomeration plays an increasing role. [29; 56]

2.3 Chemistry of antiscalants

$CaCO_3$ precipitation can be prevented with chemical additives often referred to as antiscalants or scale inhibitors. Commonly used antiscalants are polyphosphates, phosphonates and polycarboxylates. Also chelating agents, for example aminocarboxylates such as ethylenediaminetetraacetic acid (EDTA) and diethylene triamine pentaacetic acid (DTPA), can be used for scale inhibition, but they function mainly by complexing calcium in the solution. This is impractical because their use requires stoichiometric amounts with calcium ions and is therefore uneconomical at high calcium level. Polyphosphates, phosphonates and polycarboxylates function on a much lower dosage. Usually the used dosages vary from a few to some dozen parts per million. The inhibitors functioning at dosages below the stoichiometric level are often referred to as "threshold inhibitors" [1; 31]

These threshold inhibitors can affect the precipitation process in three different ways [5]:

1. Threshold inhibition: The nucleation and crystal growth stages are retarded by the antiscalant.
2. Dispersing: The antiscalant affects the attractive forces between particles and prevents agglomeration.
3. Crystal modification: The antiscalant modifies the crystal structure such way that the surface area of crystal is reduced, which limits the ability of the crystal to attach to surfaces and other crystals.

The same antiscalant can affect the precipitation process with more than one of these mechanisms. The performance of different antiscalants is influenced by the temperature, pH, supersaturation ratio, and the presence of other ions in the solution. In the case of polymer antiscalants, the molecular weight of the polymer can play an important role [32].

2.3.1 Inhibition mechanisms

As the crystallization process of $CaCO_3$ is relatively complex and interactions between the antiscalant and forming nuclei are challenging to study, it is difficult to draw conclusions about the specific inhibition mechanisms involved. However, it is evident that the threshold inhibition, dispersing and crystal modification are all based on the adsorption of the negatively charged antiscalant on the surfaces of the developing nuclei and on the positively charged growth sites of the growing crystals.

The threshold inhibition can be defined as the adsorption of the inhibitor on the surface of ion clusters on the nucleation stage of the crystallization process. The adsorption

on the surfaces of these clusters causes them to be unstable and redissolve rather than grow into visible size (see C*hapter 2.1.2*) which delays the formation of crystals. The threshold inhibition is basically the capability of the antiscalant to extend the induction time, τ_{ind}, between the formation of the supersaturated state and detection of the first crystals. [31; 33]

Eventually, the crystals start to grow. In the crystal growth stage, the inhibitors adsorb on the growth sites of the crystals causing the crystal modification and the retardation of crystal growth. These distorted crystals are much less capable of adhering on the metal surfaces and cause tightly adherent scale deposits. If the adherent inhibitor has an electrostatic charge, it also has dispersing properties due to the electrostatic repulsion of particles with the charge of the same sign. This repulsion disables the crystals to agglomerate. [33]

Phosphonates and polycarboxylates both exhibit threshold inhibition and crystal modification properties. Generally phosphonates are better threshold inhibitors, whereas polycarboxylates are better dispersants. The selection of the used scale inhibitor depends on the conditions of the application. It can be supposed that at low supersaturation levels phosphonates may be sufficient treatment due to their threshold properties and at higher supersaturation levels, where the complete inhibition of precipitation is unlikely, polycarboxylates may be better due to their dispersing properties. Also blends of phosphonates and polycarboxylates can be used. [33; 34] The suitability of different compounds at different applications will be discussed more in context with research results. The differences of different antiscalant groups (polyphosphates, phosphonates and polycarboxylates) are discussed next.

2.3.2 Polyphosphates

Polyphosphates are inorganic polymers consisting of phosphate groups PO_4 which are linked together by shared oxygen atoms. They can be either cyclic or linear compounds. The structure of a commonly used polyphosphate antiscalant, sodium hexametaphosphate (SHMP) is shown in *Figure 2.4.*

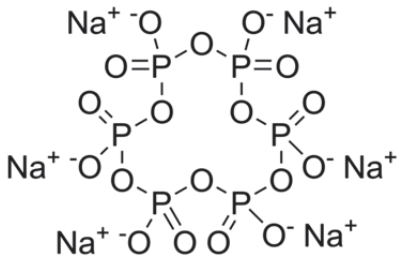

Figure 2.4. Structure of sodium hexametaphosphate (SHMP). The phosphate groups are linked together by shared oxygen atoms. [35]

Polyphosphates act as threshold inhibitors. They are efficient at the pH range of 8–10, but only at temperatures near the room temperature. At higher temperatures, the P-O linkages undergo hydrolysis and long polymer chains are broken to shorter ones. This

suppresses the inhibition efficiency and increases the risk of calcium phosphate precipitation. [1, pp. 1398] Due to the hydrolysis at higher temperatures there is a little use of polyphosphates in the papermaking processes.

2.3.3 Phosphonates

Phosphonates are organic compounds containing one or more phosphonic acid, C-$PO(OH)_2$ or C-$PO(OR)_2$ groups. Phosphonates can be separated into aminophosphonates and other phosphonates. Compared with polyphosphates, the C-P-C and P-C-N-C-P bonds of phosphonates are more stable against hydrolysis than the P-O-P bonds of polyphosphates and therefore phosphonates are useful also at higher temperatures. Phosphonates have negatively charged dissociated phosphonic acid groups in aqueous solutions. [1, p. 1398]

Aminophosphonates contain an amine group attached to phosphonate group. For example, *Figure 2.5,* aminophosphonates ethylenediamine tetra(methylene phosphonic acid) (EDTMP), butylenediamine tetra(methylene phosphonic acid) (BDTMP), pentylenediamine tetra(methylene phosphonic acid) (PDTMP), and hexamethylenediamine tetra(methylene phosphonic acid) (HDTMP) are used as antiscalants and compared with their aminocarboxylate analogs. Also the structure of aminotrimethylenephosphonic acid (ATMP) which is a commonly used antiscalant is presented in *Figure 2.5*.

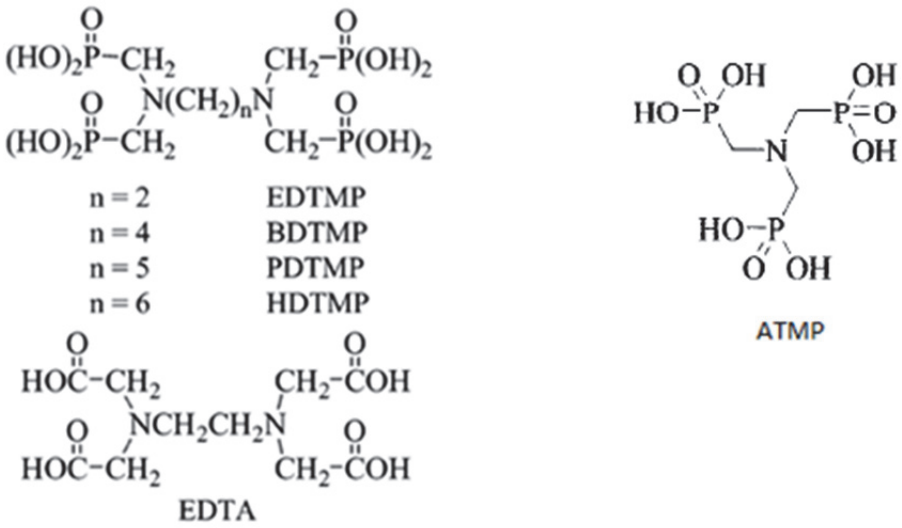

Figure 2.5. The structures of some aminophosphonates. EDTA is the aminocarboxylate analog of EDTMP. [31, p. 5412; 36, p. 152]

Despite the analogy in the structure of aminophosphonates and aminocarboxylates, their antiscaling mechanisms are different. When aminocarboxylates sequester calcium ions at stoichiometric dosages, aminophosphonates inhibit the precipitation of $CaCO_3$ at sub-stoichiometric quantities, which indicates that their scale inhibition efficiency is mostly based on the adsorption of the negatively charged phosphonic acid groups on the nuclei and growth sites of crystals as described in *Chapter 2.3.1*. However, at larger quantities aminophosphonates also act as complexing agents like aminocarboxylates. [31]

Other phosphonates used for scale inhibition are for example 2-phosphono-1,2,4-butanecarboxylic acid (PBTC) and 1-hydroxyethane-1,1-diphosphonic acid (HEDP). Their structures are presented in *Figure 2.6*.

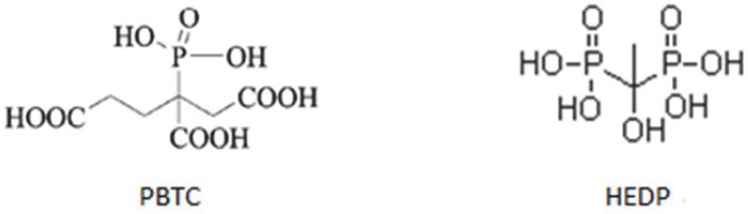

Figure 2.6. The structures of the PBTC and HEDP phosphonates, which are commonly used as scale inhibitors. [36, p. 3230; 35]

The efficiency of phosphonates as scale inhibitors is the best when the molecule size is small. EDTMP, for example, has been reported having better efficiency than amino-phosphonates with more methyl linkages (BDTMP, PDTMP and HDTMP). This indicates that the spacing of phosphonate groups is important for the ability to inhibit scaling. In the case of phosphonates the adsorption on the $CaCO_3$ growth sites can be quite selective leading to the blockage of specific growth sites. This leads to the fact that the increase in the dosage of the phosphonate inhibitor does not improve the threshold inhibition after a certain dosage because there are a limited number of specific growth sites. Aminophosphonates can also precipitate as calcium salts if the dosage is increased too much. [1, p. 1398; 31, pp. 5413–5414]

2.3.4 Polycarboxylates

Polycarboxylates are linear or cyclic polymers containing carboxylic acid groups, RCOOH. Polycarboxylates are polyelectrolytes, which means that their carboxylic acid groups dissociate in aqueous solutions and results in negatively charged polyanions with carboxylate groups, $RCOO^-$. The efficiency of polycarboxylates as scale inhibitors is based on these negatively charged regularly spaced carboxylate groups. Polyacrylic acid (PAA), polymaleic acid (PMA), polyaspartic acid (PASP), and polyepoxysuccinic acid (PESA) are some of the polycarboxylates used as antiscalant. Also copolymers like maleic acid/acrylic acid (MA/AA) copolymer and terpolymers like maleic acid/acrylic acid/acrylamide (MA/AA/AM) terpolymer are used. In the terpolymers one of the monomers is usually non-ionic. This non-ionic part can be for example acrylamide and its purpose is to increase the dispersing properties of the polymer by enhancing steric hindrance between particles. [1; 37; 38; 41] Structures of some polycarboxylates used in antiscalants are presented in *Figure 2.7*.

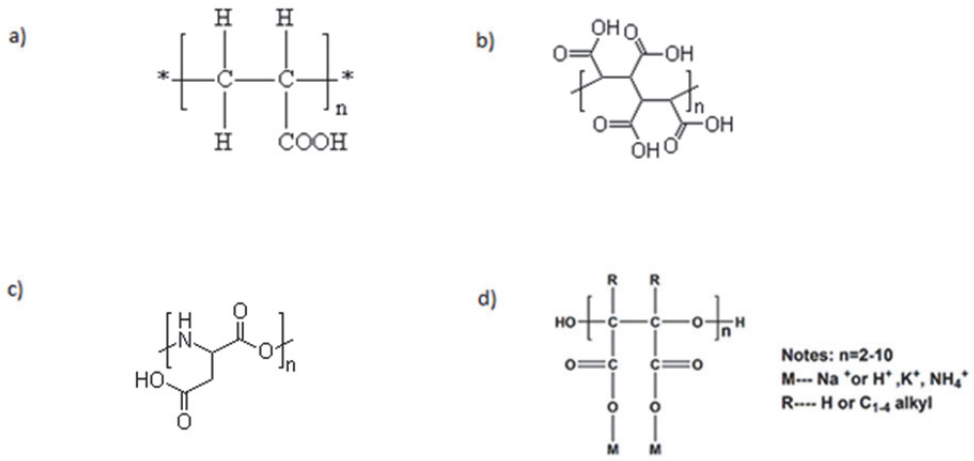

Figure 2.7. The structures of polycarboxylates. a) PAA, b) PMA, c) PASP, d) PESA. [35; 39]

Polycarboxylates are good crystal modifiers and dispersants but they can also exhibit threshold inhibition properties. [1; 3]

Rieger et al. [3] have studied the effect of polycarboxylates on $CaCO_3$ precipitation by x-ray microscopy to achieve better understanding about the inhibition mechanism of polycarboxylates. They concluded that precursors of calcite crystallization, $CaCO_3$ nanoparticles, are fixed in a network of polymers bridged by Ca^{2+}-ions. This is shown in *Figure 2.8.*

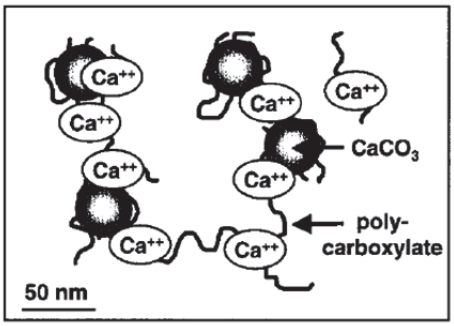

Figure 2.8. The effect of polycarboxylate on $CaCO_3$ precipitation. The polycarboxylate is adsorbed on the surfaces of $CaCO_3$ nanoparticles forming a network of polymers bridged by Ca^{2+}-ions. [3, p. 8305]

If the amount of polymer is sufficient to cover the nanoparticles entirely, they are stabilized. If the amount of polymer is not sufficient, the nanoparticles dissolve and recrystallize to calcite. In this case the morphology of the calcite is affected by the polycarboxylate.

Compared with phosphonates, the adsorption of polymeric species on the $CaCO_3$ growth sites does not require selective interactions in order to act as growth blocker. This means that the efficiency relative to phosphonate inhibitors increases with an increasing dosage (dosages over ~20 ppm). [31, p. 5414] With an increasing dosage also the complex formation interactions between carboxylate groups and calcium ions play an increasing role. It can be assumed that two carboxylate groups are required to complex one calcium ion. [32]

As mentioned before, the molecular weight of an antiscalant polymer can play an important role in the inhibition performance. Loy et al. [32] have studied the influence of the molecular weight of PAA on its inhibition efficiency. They came to the conclusion that an optimal molecular weight range exists. It has been reported that this range is 2000–20000 g/mol [31; 40]. The reason for this is not completely understood. It is probable that the charged polymers with lower molecular weight diffuse faster in the solution and their adsorption rate is high, whereas polymers with higher molecular weight adsorb to a greater extent. It has also been suggested that higher number concentration on the interface with smaller polymer species has benefits and that the bridging potential between crystals, which is promoted by larger polymer species, has effect on the inhibition performance. These assumptions could explain the existence of the ideal range. Polymers inside the range have a good compromise of the properties of small and large components. [32]

Loy et al. [32] also concluded that under competitive conditions between smaller and larger polymer components the smaller components adsorb first, but are replaced by the larger components later. This indicates that the polydispersity of the polymer also plays an important role in the inhibition process. They also reported that at low dosages the inhibition performance for the mixtures of polymers with different molecular weight distributions can be predicted from the performances of the individual distributions. [32, p. 1883]

2.3.5 Factors affecting the performance of antiscalants

Other factors besides supersaturation that have effect on the performance of antiscalants are the temperature, pH, pressure, and the presence of impurities such as iron and aluminum ions in the solution. Even a little change in these factors can have significant impact on the scale inhibitor.

The performance of the scale inhibitor can sometimes be a function of pH. The level of alkalinity can have effect on the dissociation state and stereochemistry of the inhibitor molecule. Also the charge and shape of the inhibitor can change with varying pH. [9]

Temperature has effect on the supersaturation level of $CaCO_3$ but in addition it affects the inhibitor. Especially in high temperature applications with relatively long residence times, for example boilers and digesters, the thermal stability of the antiscalant plays an increasing role. [9; 40; 41] In high temperature applications, particularly when combined with high alkalinity, phosphonates are at risk of reversion to orthophosphates [41, p. 3]. As is well known, also polymers undergo thermal degradation when treated long times with high temperatures. Polycarboxylates can lose their calcium carbonate inhibition ability if they lose molecular weight or carboxylic acid groups due to high temperature. Elevated pressures have the same kind of effect on the scale inhibitors than elevated temperature. [40; 41]

Some impurities additional to calcium carbonate can have major effect on the antiscalant. Small amounts of iron and aluminum ions can drastically lower the perfor-

mance of calcium carbonate scale inhibitors by deactivating their functional acid groups. [41, p. 2]

2.4 Antiscaling testing methods

The antiscaling testing methods can be distinguished by the test conditions to static and dynamic or by the analytical methods to online and offline methods. In this chapter, alternative testing methods are discussed. The operational principles of different methods are described and their advantages and disadvantages estimated.

2.4.1 Static methods

Static methods for testing different antiscaling products are usually very straightforward. The static jar test used in this work is quite simple and described in *Chapter 3*. Some standards for the scale inhibitor performance in static conditions exist, for example the NACE Standard TM0374-2007 [7]. The problem with these standards is that in addition to the standard method they also standardize the test conditions and obviously the conditions vary with different applications and different products perform differently in varying conditions.

In the static methods, the supersaturation, which is needed for the precipitation to occur, can be created with several different methods. The simplest way is to mix an anionic carbonate or bicarbonate solution with cationic calcium solution. The advantage of this method is the simplicity and it is suitable when a large amount of samples is prepared. Also the carbonate/calcium ratio can be easily adjusted. Other ways are to induce the supersaturation to undersaturated solution by increasing the pH of the test solution electrochemically or with other methods. The advantages of these methods include among others the isolation of different kinetic stages. A good overview of these methods can be found in the article Evaluation method for the scaling power of water by F. Hui et al. [8].

The difficulty in the static methods is to choose the right way to measure and monitor the precipitation process. The online options are to measure the free calcium ion concentration by calcium selective electrode or the mass of the precipitated calcium carbonate by quartz crystal microbalance (QCM). Also indirect methods can be used, for example the pH can be monitored as the pH of the solution changes when calcium carbonate precipitates or the current can be monitored as the current decreases when the precipitation occurs induced electrochemically on the surface of the electrode. These methods also come with advantages and disadvantages. The pH of the solution, for example, will not radically change if there is excess carbonate compared with calcium. The QCM technique is accurate but impractical when the amount of samples is large. Also the combination of two or more of these methods is possible. For example the combination of QCM and calcium selective electrode is often used. [8; 42]

An alternative for the real time measurements is to choose a reaction period and analyze the sample afterwards. In this case the determination of the free calcium could be

performed by a simple EDTA titration method [43] but the reliability of this method is questionable as the unprecipitated calcium can be partly bound by the antiscalant and therefore is not seen as free calcium by the method. Alternative ways to analyze the free or precipitated calcium amount are for example inductively coupled plasma (ICP) and flame atomic absorption spectrometer (FAAS) [38; 44]. These analytical methods offer reliable results but are slower and more expensive to use.

The static tests are usually good for large scale screening tests but are quite far away from the real applications. In many static methods only the inhibition percentage is calculated. The information received from the static methods can be increased if also the bulk precipitation and adherent deposition are analyzed. Also an addition of metal surface would bring the static test closer to real applications. The bulk precipitation can be considered as homogeneous nucleation and the adhesion on the surface as heterogeneous nucleation. [44]

2.4.2 Dynamic methods

Usually at the real applications the conditions are rather dynamic than static. The dynamic conditions can be added quite easily to the jar test with stirring. Magnetic or other stirrer can add the stirring. A metallic rotating disk electrode, for example, can be used to add dynamic conditions and metal surface to an electrochemical method. [44] The problem with the addition of the stirring is that the system can be very delicate to the dynamic conditions. The equilibrium between free calcium, bulk precipitation and adherent deposition can change even with a little change in the stirring which affects the reproducibility of the test. [45] Another way to test antiscaling products in the dynamic conditions is to use a more complicated system to study the precipitation. In this thesis, the dynamic tube blocking procedure performed on a Process Measurement and Control (PMAC) Systems Ltd instrument is used.

The PMAC instrument is once through constant flow system. The basic principle of the system is to mix cationic and anionic solutions in a scaling coil and to monitor the pressure difference over the scaling coil. The test is started with high amount of scale inhibitor and the dosage is then decreased stepwise. The scale formation in the test coil causes an increase in the differential pressure. The operational principle of the system is presented in *Figure 2.9*.

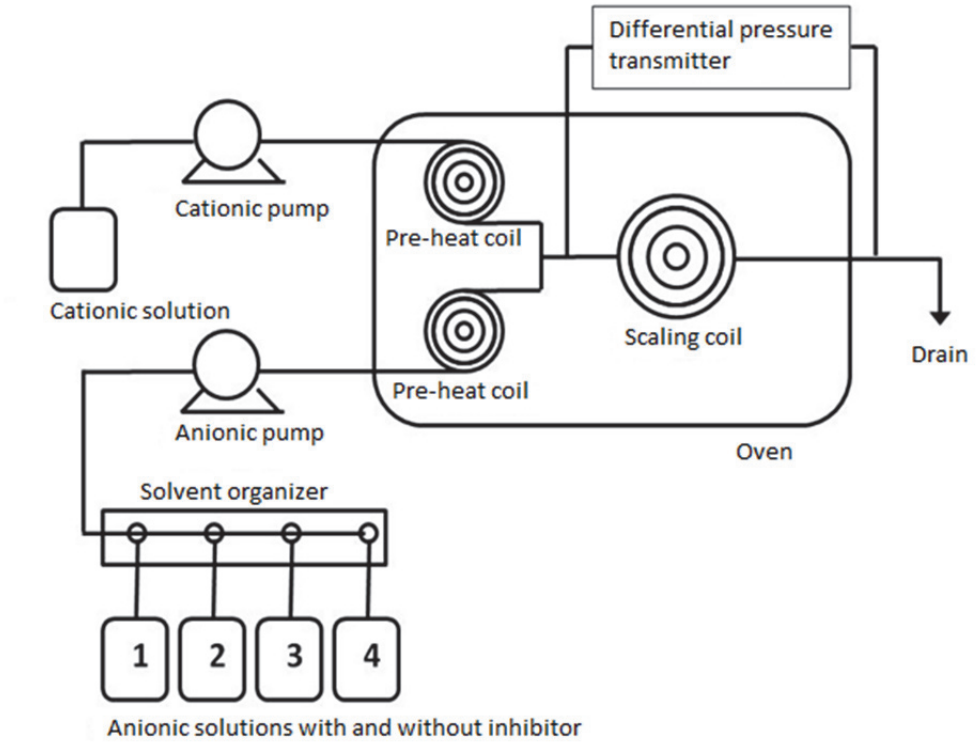

Figure 2.9. Operational principle of the PMAC instrument.

The cationic and anionic pumps are HPLC piston pumps. The solvent organizer before the anionic pump makes it possible to adjust the scale inhibitor dosage. In the solvent organizer there is an anionic solution without the inhibitor, anionic solution with desired amount of inhibitor, cleaning solution, and deionized water. The inhibitor dosage is controlled by mixing of the two anionic solutions. The cleaning solution and water are used to clean the system. The maximum flow rate of each pump is 10 ml/min. The anionic and cationic solutions are pre-heated before they are mixed in the inlet of the scaling coil. The material of the scaling coil can be chosen between stainless steel and Monel. [46]

The operational parameters are set with the PMAC DSL computer software and during the test run the differential pressure, system pressure, and fluid temperature are monitored and recorded by the same software. The operation of the instrument is covered in more detail in *Chapter 3*. [46]

The advantages of the PMAC system are that the progress of the test can be monitored real time, the system is highly automated, and the temperature and pressure can be set to actual pulp and paper making conditions. With this instrument, the scaling test can be operated at temperatures up to 250 °C, and pressures up to 200 bar. On the other hand, the system is a once through system, which is not the case in the pulp and paper making as many of the pulp and paper making processes include long residence times or closure of water circuits. The only way of controlling the residence time with PMAC instrument is the flow rates of the pumps. Nor is the high amount of suspended solids present in the paper making streams possible to simulate with this system. [46]

2.4.3 Additional methods

It is noteworthy that it is not possible to attain real process conditions in the laboratory scale. The precipitation process in the real applications can be very slow and it is necessary to speed up the process in the laboratory. When there is no single laboratory test method that represents real conditions, it is reasonable to use several methods in order to achieve knowledge of the performance of different products.

In addition to methods already presented, it is possible to achieve more information on the scaling process and performance of the antiscalants with several methods. The morphology of the formed scale, for example, can be studied with scanning electron microscope (SEM), X-ray microscopy and particle size distribution measurements. [3; 44] The thermal stability of the antiscalants can be studied with differential scanning calorimetry (DSC).

Requirements for a good laboratory method are the adjustability of the test conditions, reliability and reproducibility. If one test method is not sufficient to cover the conditions of the real applications, several methods should be used in order to study as many of the critical parameters as possible.

2.5 Computational models of scaling

Many computational models have been developed for predicting the scaling potential of aqueous systems. These models are usually based on the thermodynamic calculations of the supersaturation ratio by means of activities of ion species present in the system. The differences in these models come from the method that is used for ionic activity calculations. The software used in this work is French Creek WatSIM. The models related to this software are discussed in more detail. [30]

2.5.1 Scaling potential indices

The WatSIM is developed for the determination of the scaling potential of common sparingly soluble salts in municipal applications. It calculates several scaling potential indices when the concentrations of specific ions, pH and temperature are known. These indices include among others the Langelier saturation index, Saturation Level and Momentary Excess. [47]

The Langelier saturation index is a commonly used indicator for scaling potential of calcium carbonate in aqueous systems. It is an equilibrium model derived from the theoretical concept of saturation. The model is described in detail in the literature [48]. The problem of the Langelier saturation index is that it does not account for common ion effect or non-carbonate alkalinity, so it predicts incorrect scaling potential in high TDS (total dissolved solids) systems and when other alkalinity than carbonate alkalinity is present. [30; 47]

Another and probably the most useful scaling potential indicator which the WatSIM calculates is the saturation level, *S.L.,* which is the same as the supersaturation ratio de-

fined with the equation 2. It can also be presented using the solubility product of the salt, in this case calcite.

$$S = S.L. = \frac{a_{Ca^{2+}} * a_{CO_3^{2-}}}{K_{sp,calcite}} \quad (25)$$

In equation 25 $a_{Ca^{2+}}$ and $a_{CO_3^{2-}}$ are the activities of calcium ion and carbonate ion, respectively. $K_{sp,calcite}$ is the solubility product of calcite at the temperature and pressure under study. The WatSIM software uses ion association model to calculate the saturation level. This model is covered in *Chapter 2.5.2*. [30]

The Momentary Excess index describes the amount of the sparingly soluble salt which would have to precipitate to bring the solution to the equilibrium. It is the only index of WatSIM which describes the amount of scale, not only the driving force. It is not certain that all of the salt will precipitate but the Momentary Excess index gives an estimation of the quantity of the scale. For example, the saturation level can be the same for a solution with high carbonate and low calcium concentration and a solution with equal parts of calcium and carbonate but the Momentary Excess gives larger value for the latter case. [47, p. 11] The calculation method of Momentary Excess is covered in the literature [49].

2.5.2 Ion association model

The ion association model takes into account the interactions between different ions and is therefore reliable also in high TDS systems. Instead of using the total analytical values of calcium and carbonate, the saturation level is calculated based on the free ion concentrations. For example, in the case of $CaCO_3$ the equilibrium of the reactions II–IX is checked. The process is iterative consisting of the following steps:

1. Checking the water for electro neutrality via cation-anion balance and balancing with appropriate ion.
2. The estimation of ionic strength, calculation and correction of activity coefficients and dissociation constants for the temperature, and correction of alkalinity for non-carbonate alkalinity.
3. Calculation of the distribution of species in the water using the equilibrium constants.
4. Checking the water for balance and adjusting ion concentrations to agree with total analytical values.
5. Repeating the steps 1–4 until the change in the values is insignificant.
6. Calculation of the supersaturation ratio based on the free ion concentrations.

The most challenging part of this process is the calculation of activities of single ions. The activity of single ion is formally defined as

$$a_i = \gamma_i m_i, \tag{26}$$

where a_i is the activity, γ_i (kg/mol) is the activity coefficient and m_i (mol/kg) the molality of a single ion. [30; 50, pp. 5–6]

Single ion activities or single ion activity coefficients cannot be determined thermodynamically or exactly measured or calculated. Therefore non-thermodynamic models have to be used to calculate single ion activity coefficients. The ion association model of WatSIM is based on the WATEQ program [50], which uses the Debye-Hückel equations and the MacInnes assumption to calculate the activity coefficients. [47; 50, p. 6]

The Debye-Hückel theory was developed to explain the non-ideal behavior of electrolyte solutions. It considers the effect of electrical interactions between oppositely charged ions. The original equation states that a single ion activity coefficient, γ, can be calculated with equation

$$\log \gamma = -\frac{Az^2\sqrt{I}}{1+Ba\sqrt{I}}, \tag{27}$$

where A and B are constants, z is the ionic charge, I is the ionic strength, and a is the hydrated ion size that is estimated from experimental data.

The ionic strength, I, is defined as

$$I = \frac{1}{2}\sum_i (m_{i+} z_{i+}^2 + m_{i-} z_{i-}^2), \tag{28}$$

where m is the molality and z the charge of the ith ion. [12, p. 232] The constants A and B are calculated by the equations

$$A = \frac{1.82483 \times 10^6 \sqrt{d}}{(\varepsilon T)^{3/2}} \ \mathrm{kg}^{1/2}\ \mathrm{mol}^{-1/2} \tag{29}$$

$$B = \frac{50.2916 \times 10^8 \sqrt{d}}{(\varepsilon T)^{1/2}} \ \mathrm{kg}^{1/2}\ \mathrm{mol}^{-1/2}\ \mathrm{cm}^{-1}, \tag{30}$$

where d is the density of water, T is the absolute temperature and ε is the dielectric constant of water. [50, p. 8]

However, the original form of the equation is only valid for very dilute solutions. In more concentrated solutions, the extended form of the equation can be used.

$$\log \gamma = -\frac{Az^2\sqrt{I}}{1+Ba\sqrt{I}} + bI. \tag{31}$$

In the extended form of the equation a second adjustable parameter, b, is added. This parameter takes into account the decrease in the concentration of solvent in concentrated solutions. [50, p. 7]

The information about the behavior of single ion activities at higher concentrations is needed to fit the parameters of the extended Debye-Hückel equation. It is necessary to determine the variation of single ion activity coefficients with ionic strength to assign the parameters *a* and *b* in equation 31. For many salts the mean ionic activity coefficients, $\gamma_{\pm}$, are experimentally determined. If the activity of one ion can be calculated, then others can be derived from it. This can be done with the MacInnes assumption, which states that the ion activity coefficients of K^+ and Cl^- are equal to each other and to the mean ionic activity coefficient of KCl,

$$\gamma_{K^+} = \gamma_{Cl^-} = \gamma_{KCl}. \tag{32}$$

The mean ionic activity coefficient is defined as

$$\gamma_{\pm}^{v} = \gamma_{+}^{v_+}\gamma_{-}^{v_-}. \tag{33}$$

Using the equations 32 and 33,

$$\gamma_{Na^+} = \frac{\gamma_{\pm\,NaCl}^2}{\gamma_{\pm\,KCl}}, \tag{34}$$

$$\gamma_{Ca^{2+}} = \frac{\gamma_{\pm\,CaCl_2}^3}{\gamma_{\pm\,KCl}^2} \text{ and so on.} \tag{35}$$

When deriving these single ion activity coefficients, one must be careful to avoid solutions in which the ions are associated. The activity coefficient for CO_3^{2-} , for example, cannot be calculated using the mean ionic activity coefficient of H_2CO_3 because of the formation of the HCO_3^- ion pair. [50, pp.8–9]

After the ion activity coefficients are solved, the mass action and mass balance equations can be solved. The chemical model in the WatSIM solves the distribution of solution species using total analytical concentrations, experimental solution equilibrium constants, mass balance equations and measured pH. First the distribution of anionic weak acids (silicate, phosphate, borate, and sulfide species) is calculated using total analytical concentrations, the pH and activity coefficients. The carbonate species calculation requires the alkalinity determination in addition. This procedure is covered in detail in the literature. [50, pp. 10–11]

The distribution of ion pairs is calculated with similar procedure than the distribution of anionic weak acids. Only the analyzed or calculated anion concentrations are used in place of the pH. The free ion concentrations of calcium is, for example, calculated with the equation

$$m_{Ca^{2+}} = \frac{m_{Ca\ total}}{1 + \gamma_{Ca^{2+}} \left(\frac{K_{IV} a_{HCO_3^-}}{\gamma_{CaHCO_3^+}} + \frac{K_V a_{CO_3^{2-}}}{\gamma_{CaCO_3}} + \frac{K_{VI} a_{OH^-}}{\gamma_{CaOH^+}} \right)}. \quad (36)$$

In equation 36 K_{IV}, K_V, and K_{VI} are the equilibrium constants of the reactions IV, V, and VI. In WatSIM this equation also includes sulfate and phosphate species. The derivation of the equation 36 is presented in the literature. [50, pp.11–13]

The concentrations of ion pairs affect the ionic strength and the activity coefficients as they were originally calculated with total analytical concentrations. The corrected values are calculated by iteration. When the sums of all weak acids, complex ions and free ions for all anions differ less than 0.5 percent from the analytical values, the iteration is completed. [50, p. 13]

The equilibrium constants, K, used in the calculations are expressed as a function of the absolute temperature, T.

$$\log K = A + BT + \frac{C}{T} + D \log\ T, \quad (37)$$

where A, B, C and D are experimental coefficients from which one or more may be zero. The equilibrium constants for crystalline forms of calcium carbonate are expressed in this form in *Table 2.1* but the coefficients used in the WatSIM may vary from those. If experimental data at only a few temperatures is available, the equilibrium constants can be expressed using Van't Hoff relation.

$$\log K = \log K_{Tr} - \frac{\Delta H_{Tr}}{2.3\ R} \left(\frac{1}{T} - \frac{1}{T_r} \right), \quad (38)$$

where ΔH_{Tr} is the enthalpy change of the reaction at reference temperature, T_r, which is usually 298.15 K and R is the gas constant. The effect of pressure is not taken into account in the calculations of WatSIM. [50, p. 16–17]

2.5.3 Scale inhibitor dosage models

In addition to predicting scaling potential, the scale inhibitor dosages can be modeled with WatSIM. These models are based on the idea that the scale inhibitors extend the induction time. This means that the crystal modification and the dispersing properties of the antiscalants are not modeled. The induction time, τ_{ind}, can be described with an equation

$$\tau_{ind} = \frac{1}{k\ (S-1)^{P-1}}, \quad (39)$$

where k is a temperature dependent constant, S is the saturation level and P is the critical number of molecules in a cluster prior to phase change. The temperature dependent constant, k, correlates well with the Arrhenius relationship

$$k = A\mathrm{e}^{-E_a/RT}. \tag{40}$$

In equation 40 A is a pre-exponential factor, E_a is the activation energy, R is the gas constant and T is the absolute temperature. [30]

The dosage models of WatSIM are based on empirical laboratory and field data. The equation 39 can be modified by adding the inhibitor dosage, D, as a factor to the right side.

$$\tau_{ind} = \frac{D^M}{k\,(S-1)^{P-1}}, \tag{41}$$

where M is an experimental coefficient. The dosage can be solved from this equation. The time used in the place of induction time is the residence time in the application, and saturation level is calculated with the ion association model. Other coefficients are estimated using regression analysis. [9]

The database used in determining the required dosages for different applications must cover several critical parameters in order to be reliable. These parameters are the temperature, time, supersaturation ratio and pH. For example, there is no use of a dosage model for a system operating at 90 °C, if the data is available only for the temperature range 20–50 °C. Even if all the parameters are covered, the dosages proposed by the software may vary from those actually needed, because all systems are different and not all the parameters can be taken into account. For example, the amount of suspended solids affects the precipitation process by promoting heterogeneous nucleation and the conditions in practical systems may be more or less dynamic whereas the data used in the software is based mainly on static laboratory tests. [9; 30]

2.6 Scaling in pulp and paper making

Scaling is a common problem throughout pulp and paper making processes due to large quantities of water used. The recent trend of closing up of the process water circuits induced by stricter environmental demands can make the scaling an even more severe problem. The deposition of the calcium carbonate scale is present in the alkaline processes of pulp and paper mills. Scaling can cause a number of operational problems such as plugging of equipment, inefficient usage of chemicals, and lost production due to downtime. The most common ways of resolving scale problems in papermaking processes include the optimization of operating conditions, cleaning of equipment from scale build up, and prevention of scale formation with antiscalants. [5; 6]

2.6.1 Pulp mills

Several pulping unit operations are moderately or highly alkaline with high temperatures. As calcium and carbonate are present in the pulping process, these conditions are favorable for the formation of the calcium carbonate scale. Also the high amounts of dissolved and suspended solids complicate the function of the antiscalant and promote scaling. The calcium comes to the process from wood and carbonate is present in the cooking liquor. Most of the calcium is present in the bark and cambial layer of the wood and one way of eliminating the scaling of calcium carbonate would be the use of more effective barking procedures. Calcium carbonate scale depositions can be formed in various areas in the pulp mill, including the digester, the black liquor evaporators and the bleach plant. [5]

The most challenging part is the digester where the high pH of 12 to 14, temperature around 170 °C and pressure up to 15 bar combined with relatively long residence time set very difficult conditions for the scale inhibitors. In these conditions, the complete inhibition of calcium carbonate precipitation is unlikely and the crystal modification and dispersing properties of the inhibitor have more importance as the main objective is to prevent the adherence of the precipitation. Two possible ways of dealing with digester scale are the use of phosphonate and polycarboxylate antiscalants or various cleaning methods. The use of antiscalants is preferred as the cleaning methods create additional costs. [11; 51]

In the black liquor evaporation systems water-soluble scales can be formed which also promotes the growth of the calcium carbonate scale. The scale deposition reduces the efficiency of the evaporation process due to decrease in heat transfer. The black liquor is generally evaporated to 60–80 % solids content. The higher the solids content the more severe is the scaling problem. Black liquor evaporators are usually multiple effect evaporators which commonly have from four to eight effects in series. Generally, the calcium carbonate scaling occurs only in one or two of these effects. A common way of dealing with this scale is a hot acid boil out. However, the boil out affects the production and can cause corrosion problems, which makes the use of antiscalants a viable option. [5; 11; 51]

In the bleach plant the extreme pH swings caused by the acid and alkaline bleaching and washing stages create ideal conditions for scale formation. Calcium carbonate scale forms in the stages where pH exceeds 8. The temperature in the bleaching is not as high as in previous pulping processes, which leaves more options for the use of antiscalants. [5]

2.6.2 Paper mills

Calcium carbonate scale is also common in neutral paper making processes. It is encountered in many locations around and on the paper machine affecting the performance of the paper machine. The sources of calcium and carbonate in paper mills are virgin

and secondary fiber, fresh water, and process additives such as calcium carbonate filler. [5; 6]

The closure of water circuits combined with the increased use of precipitated calcium carbonate (PCC) as a filler and coating pigment has made the calcium carbonate scaling problem especially severe on the mills using recycled fibers as raw material. Although the overall process is slightly alkaline, there might be some acidic chemicals and dilution waters which cause the dissolution of the filler. This way the otherwise stable and harmless PCC filler enters the process water as a solute and can precipitate in another stage of the paper making process and cause scale deposition. [6; 52]

In paper mills the scaling can be inhibited or reduced by the use of antiscalants. In the alkaline paper making the pH is in the range of 7 to 9 and temperature near 50 °C. In these conditions the performance of many antiscalants is good. Also the solutions for the limitation of pH shocks can reduce the scaling problems. One of these is the use of carbon dioxide instead of alum and sulphuric acid for neutralizing kraft pulp and controlling paper machine stock pH. The pH shock is limited due to the buffer capacity of the $CO_2/H_2CO_3/HCO_3^-$ system. [53]

3. RESEARCH METHODS AND MATERIALS

In order to determine the performance of scale inhibitors as accurately as possible it is important to test the product with both static and dynamic laboratory tests with varying test conditions. It is also important that the tests are quite easy and quick to perform yet giving enough information to conclude the performance of the antiscalant. Additional information or evaluation of laboratory test results can be achieved with computational models.

In this chapter the research methods used in this thesis are described and discussed. The static test used was a quite common static jar test. The dynamic tests were a rotating disk procedure and a dynamic tube blocking procedure. Computational model utilized comes from French Creek's WatSIM software.

3.1 Materials

The following solutions were needed to perform the laboratory tests:

- **0.1, 0.2 and 0.3 M Na_2CO_3**
- **0.1, 0.2 and 0.3 M $NaHCO_3$**
- **4 M NaCl**
- **4 M NaCl containing 0.5 M NaOH**
- **80 ppm, 160 ppm and 320 ppm Ca^{2+}-ions (0.002 M, 0.004 M and 0.008 M $CaCl_2$)**
- **10 mg/ml inhibitor as solids**
- **7 % and 14 % HNO_3**

Analytical grade reagents were used. Using the carbonate and bicarbonate solutions, test conditions of four different pH values were created to correspond with the process conditions of pulp and paper making. The pH values and the ratios of used solutions are presented in *Table 3.1*.

Table 3.1. The percentage values of the carbonate and bicarbonate solutions in the samples with different pH values.

pH	Sodium carbonate solution (%)	Sodium bicarbonate solution (%)
8.8	10	90
9.2	40	60
10.7	90	10
12.7	100	0

Table 3.1 tells the ratio of the Na_2CO_3 and $NaHCO_3$ solutions used to make the sample. This determines the final pH of the sample, the total concentration of the carbonate in the sample is insignificant at least in the range used in this work. In the samples of pH 12.7, the 4 M NaCl solution containing 0.5 M NaOH was used in addition to achieve high enough pH. In all the other pH values the 4 M NaCl solution without NaOH was used.

A large number of scale inhibitors were used in the tests. All the antiscalants used in this study and their properties are listed in *Table 3.2*.

Table 3.2. The antiscalants used in the antiscaling tests.

Antiscalant	Composition	M_w(Da)
Polyacrylate	PAA	2500
Polymaleate	PMA	600
Polyaspartate 1	PASP	3000
Polyaspartate 2	PASP	5000
Polyaspartate 3	PASP	10000
Phosphonate 1	ATMP	
Phosphonate 2	HEDP	
Phosphonate 3	PBTC	
Copolymer 1	MA:AA	1600
Copolymer 2	MA:AA	1900
Copolymer 3	MA:AA	3050
Copolymer 4	MA:AA	6100
Copolymer 5	MA:AA	50000
Copolymer 6	MA:NI	7450
Terpolymer 1	MA:AA:NI	2900
Terpolymer 2	MA:AA:NI	2700
Terpolymer 3	MA:AA:NI	2850
Terpolymer 4	MA:AA:NI	2850
Terpolymer 5	MA:AA:NI	2700
Terpolymer 6	MA:AA:NI	2300

The antiscalants of *Table 3.2* were chosen to represent different antiscaling chemistries. The molecular weights of the polymers are expressed as the weight average molecular weights, M_W. In the Copolymers and Terpolymers the proportions of the monomeric species and the molecular weights vary. The abbreviation NI in stands for non-ionic monomer. The used non-ionic polymer compounds are not specified.

3.2 Static methods

In the static jar method, the test conditions can be assumed to represent homogeneous nucleation conditions, as the presence of foreign heteronuclei is minor. The aim of the static tests was to determine the repeatability of this method and to compare the static results with dynamic results in order to understand what information these tests actually give and is it necessary to do also other tests. The test results were also utilized to determine the performance of different types of polymers and to compare the performance of different antiscaling chemistries in different conditions.

The samples of the static jar tests were prepared by weighing into a lidded 250 ml glass jar. The size of one sample was 200 g. The variables in the test preparation were the pH from *Table 3.1*, the total amount of calcium and the total amount of carbonate. Only the concentration of NaCl was held constant in all the tests representing the high TDS conditions of paper making streams. At first 50 g of the carbonate and bicarbonate ions containing solution was weighed into the jar, then 50 g of the 4 M NaCl solution was added and finally 100 g of the solution containing calcium ions was added. All the used conditions are presented in *Table 3.3*.

Table 3.3. Compositions of different static samples.

pH	Ca^{2+} (ppm)	CO_3^{2-} (ppm)
8.8	80	3000
9.2	40	3000
	80	1500
		3000
		4500
	160	3000
10.7	80	3000
12.7	80	3000

The final NaCl concentration of all the samples was 1 M. *Table 3.3* describes the blank samples without inhibitor solution. Four different inhibitor dosages were used: 5, 10, 18 and 30 ppm as solids. These were prepared by adding 100, 200, 360 and 600 µl of 10 mg/ml inhibitor solutions into the samples in the middle of adding the NaCl solution, so that the final size of the sample was still 200 g. The samples containing 40 ppm calcium ions were prepared using an 80 ppm calcium containing solution, the samples contain-

ing 80 ppm calcium ions were prepared using a 160 ppm calcium containing solution and the samples containing 160 ppm calcium ions were prepared using a 320 ppm calcium containing solution. The samples containing 1500 ppm carbonate ions were prepared using 0.1 M solutions of Na_2CO_3 and $NaHCO_3$, the samples containing 3000 ppm carbonate ions were prepared using 0.2 M solutions and the samples containing 4500 ppm carbonate ions using the 0.3 M solutions.

The samples were then placed in a water bath for a desired reaction period. Three different temperatures, 50, 75, and 95 °C and four different reaction periods, 1.5, 5, 20, and 48 hours were used. The temperatures were chosen to correspond with the conditions of pulp and paper mill (see *Chapter 2.6*) with the limitation that 100 °C could not be exceeded as the tests were performed at the pressure of 1 atm.

After the reaction period, the jar was inverted ten times and 100 ml of the sample was taken with a syringe and filtered through a 0.2 µm hydrophilic polypropylene (GHP) filter. After the filtration, three different parts of the sample were further treated. The "filtrate" sample containing the free calcium was prepared by adding 10 ml of filtered sample into a 50 ml volumetric flask. 25 ml of the 14 % HNO_3 solution was added and the sample was made to the mark with deionized water (DI-water). The "membrane" sample representing the precipitated calcium carbonate dispersed in the solution was prepared by pushing 50 ml of the 7 % HNO_3 solution through the same syringe filter used for filtering the original sample. The third part, "adherent", represents the precipitated calcium carbonate attached to the surfaces of the jar. This sample was prepared by disposing the rest of the original sample and rinsing the jar with acetone in order to make it dry. After letting the jar dry for about 5 minutes, 50 ml of the 7 % HNO_3 solution was added in the jar to dissolve the attached calcium carbonate. This procedure results in three different samples in 7 % HNO_3. The intention of the acid solution is to preserve the sample and prevent the calcium carbonate from further precipitation. The calcium contents of these three samples were measured with the Perkin-Elmer Optima 5300 DV ICP-OES (inductively coupled plasma-optical emission spectrometer).

The ICP results show the distribution of calcium to different parts of the original sample. In addition the inhibition percentage can be calculated.

$$\%\ Inhibition = \frac{[Ca^{2+}]_{sample} - [Ca^{2+}]_{blank}}{[Ca^{2+}]_{control} - [Ca^{2+}]_{blank}}, \tag{42}$$

where $[Ca^{2+}]_{sample}$ is the calcium concentration of the "filtrate" of an inhibited sample, $[Ca^{2+}]_{blank}$ is the calcium concentration of the "filtrate" of a blank, representing uninhibited conditions, and $[Ca^{2+}]_{control}$ is the calcium concentration of the "filtrate" of a sample containing no carbonate, representing 100 % inhibition.

3.3 Dynamic methods

Two different dynamic methods were used to determine the performances of different antiscaling products. These methods were a rotating disk procedure and a dynamic tube blocking procedure performed on a Process Measurement and Control (PMAC) Systems Ltd instrument. In both of these methods, a metal surface is present and a prescale or seeding stage is used so that the tests represent heterogeneous or secondary nucleation conditions. The aim of the dynamic test was to compare the results of these tests with each other and with the results of static tests and to evaluate the reliability and repeatability of the methods. Also information about the performance of different chemistries in dynamic conditions was gained.

3.3.1 Rotating disk procedure

In the rotating disk procedure, the conditions of the static jar test were basically transferred to dynamic conditions. In addition, a seeding stage was added at the beginning of the test in order to make the conditions represent heterogeneous nucleation conditions and to accelerate the kinetics of the crystal growth. In the rotating disk procedure a stainless steel disk with a diameter of 51 mm and thickness of 3.1 mm attached to a stirrer was immersed in the test solution and rotated at 250 rpm for 90 minutes. The tests were performed in a polystyrene cup, which was heated with a water bath. For the detailed procedure, see Appendix 1. The test set-up is shown in *Figure 3.1*.

Figure 3.1. Test set-up used in the rotating disk procedure.

In the rotating disk test the used temperature was 50 °C. Higher temperatures could not be used due to the open water bath. In order to keep the variables at a minimum the same disk was always used with the same stirrer. The stirrers and disks were numbered from 1 to 3 starting from left.

The treatment of the sample after the reaction period was similar to the static method. The only differences were in the preparation of the "adherent" sample. 100 ml of the 7 % HNO_3 was used instead of 50 ml and the dissolution process was performed with the disk spinning for 15 minutes in the 7 % HNO_3 solution. Also the possible calcium carbonate precipitated on the surface of the polystyrene cup was included in the "adherent" sample.

3.3.2 Dynamic tube blocking procedure

The same $CaCl_2$, $NaHCO_3$, Na_2CO_3, and NaCl solutions that were used in the static tests and rotating disk tests were also used with the DTB. The solutions were filtered with 0.2 µm Merck Millipore GSWP filter paper before operation as the HPLC pumps of the DTB instrument are sensitive to impurities. The $CaCl_2$ solution was used as a cationic solution and the $NaHCO_3$, Na_2CO_3 and NaCl solutions were mixed in advance to form an anionic solution. The pH of the test was again controlled by the carbonate/bicarbonate ratio. Also an anionic solution containing 200 ppm of antiscalant was prepared. 5 % acetic acid was used as a cleaning solution. These solutions were attached in the pumps of DTB instrument according to *Figure 2.9*.

The parameters, which can be chosen for the test run, are the temperature, the pressure, the flow rates of the pumps, and the length of steps between the decreases of the inhibitor dosage. The test can be started with a clean test coil or the first step of the test run can be a prescale step, where the coil is partially blocked with the scale before the actual test starts. The idea of the prescale step is similar to the seeding stage of the rotating disk procedure and it also describes better the real applications than a completely clean system. The prescale step ends when the differential pressure exceeds a chosen value. Also the actual test ends, and the cleaning program starts when a chosen value of differential pressure is exceeded. This value is usually higher than the value at which the prescale ends. In the cleaning program, the system is first flushed with the 5 % acetic acid solution and then with DI-water.

The results of DTB runs are presented graphically by plotting the differential pressure as a function of time. A typical graph is shown in *Figure 3.2*.

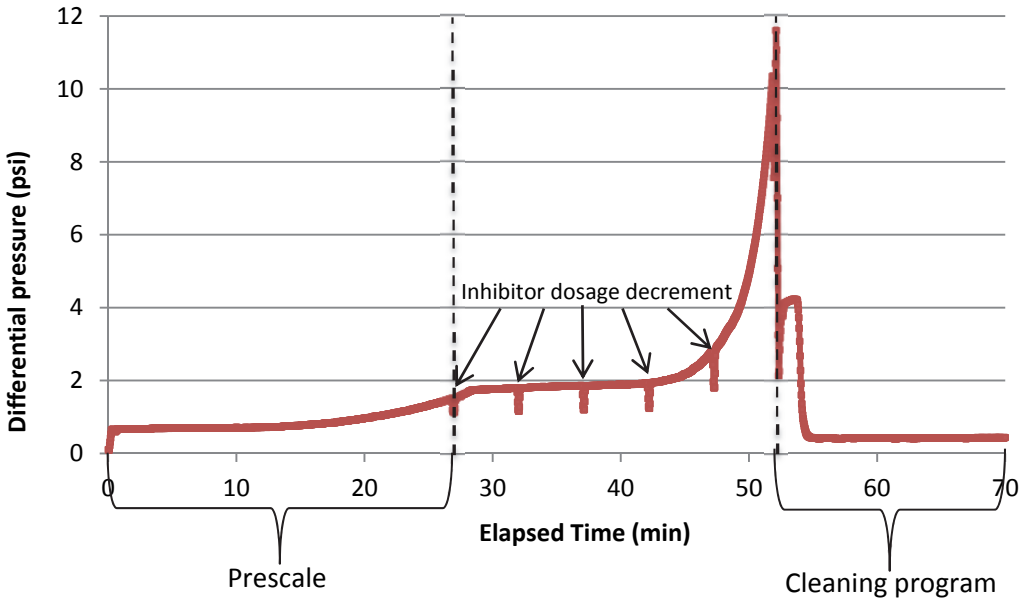

Figure 3.2. A typical graph from a dynamic tube blocking (DTB) test run.

In the case of *Figure 3.2* the prescale was set to end at differential pressure 1.5 psi and the cleaning program started at differential pressure 10 psi. The anionic pump of the DTB instrument is momentarily shut down when the solvent organizer changes the proportions of the anionic solutions with and without the inhibitor. This can be seen as a differential pressure and system pressure drop in the recorded data and the inhibitor dosage decrements can be easily identified from the graph.

If the performance of an antiscalant is wanted to be expressed as a single value, the minimum inhibitory concentration *MIC* can be determined from the graph. The *MIC* value is the last inhibitor concentration at which the scaling is prevented. In *Figure 3.2*, the *MIC* value would be the inhibitor dosage used between 37 minutes and 42 minutes. It is advisable to repeat the test with this inhibitor concentration in order to confirm the value [46].

3.4 Computational methods

In order to utilize the French Creek's WatSIM software, the M and P alkalinities had to be determined for the test solutions. This was done for the samples of pH 9.2 and 10.7 containing 3000 ppm CO_3^{2-}. The samples were prepared otherwise similarly with static jar test samples but water was added instead of $CaCl_2$. A 10 ml sample was titrated with 0.1 M (=0.1 N) HCl. The titration yields two end points, the first is P endpoint and the second is M endpoint. The alkalinity is then calculated with the equation

$$Alkalinity\ (\text{mg/l}\ as\ CaCO_3) = \frac{N_{Acid} \times V_{Acid}}{V_{Sample}} \times eq.wt.(CaCO_3) \times 1000, \qquad (43)$$

where N_{Acid} is the normality of the acid, V_{Acid} is the volume of the used acid at desired endpoint in milliliters, V_{Sample} is the volume of the sample in milliliters, and *eq. wt.*($CaCO_3$) is the equivalent weight of calcium carbonate.

This is all that is required for the French Creek to calculate supersaturation ratios, but also the distributions of HCO_3^-, CO_3^{2-} and OH^- ions can be determined from the alkalinity titrations. The alkalinity relations are presented in *Table 3.4*.

Table 3.4. Alkalinity relationships [54].

Result of titration	Hydroxide Alkalinity	Carbonate alkalinity	Bicarbonate alkalinity
P = 0	0	0	M
P < 1/2M	0	2P	M - 2P
P = 1/2M	0	2P	0
P > 1/2M	2P - M	2(M - P)	0
P = M	M	0	0

The total carbonate amount of the sample can be verified with the relationships of *Table 3.4*. When using the relationships of *Table 3.4*, one must be careful in the conversions between the alkalinities of mg/l as $CaCO_3$, mg/l as CO_3^{2-}, and mg/l as HCO_3^-.

The molecular weight of $CaCO_3$ is 100 g/mol and the molecular weight of CO_3^{2-} ion is 60 g/mol. Therefore, each milligram of $CaCO_3$ contains 0.6 milligrams of CO_3^{2-}. So the conversion between carbonate alkalinities is

$$Alkalinity\ as\ CO_3^{2-}\ (\mathrm{mg/l}) = 0.6 \times Alkalinity\ as\ CaCO_3(\mathrm{mg/l}). \quad (44)$$

When making the conversion between alkalinity as $CaCO_3$ and alkalinity as HCO_3^-, the following reaction must be considered [55]

$$CaCO_3 + H_2O + CO_2 \rightarrow Ca(HCO_3)_2. \quad (X)$$

This means that each mol of $CaCO_3$ corresponds to two mols of HCO_3^- ions. HCO_3^- ion has a molecular weight of 61 g/mol, so each milligram of $CaCO_3$ corresponds to $\frac{2\times 61\ \mathrm{g/mol}}{100\ \mathrm{g/mol}} = 1.22$ milligrams of HCO_3^-. The conversion between bicarbonate alkalinities can be written

$$Alkalinity\ as\ HCO_3^-\ (\mathrm{mg/l}) = 1.22 \times Alkalinity\ as\ CaCO_3(\mathrm{mg/l}). \quad (45)$$

4. RESULTS AND DISCUSSION

In this chapter the results of the laboratory tests are presented and discussed. First the results of the static tests are covered and then the results of dynamic tests are discussed and compared with the static ones. The tests were started with a large scale screening test of different antiscalants with the static method described in the previous chapter. Five antiscalants of different chemistries were then chosen for further study. The variables covered with the tests were the inhibitor dosage, temperature, pH, reaction time, and saturation level. Also the effect of total ionic strength is discussed.

4.1 Results of the static tests

In the static tests the performance of different antiscaling chemistries and the reliability of the method were studied. The ICP results of the "filtrate", "membrane", and "adherent" parts of the sample were calculated to parts per million (ppm = mg/kg) in the original sample. The sum of these three parts should yield the concentration of the control sample's "filtrate" part. Also the inhibition percentages were calculated.

4.1.1 Screening test

In the screening test several different antiscalants were tested with the test conditions of pH 9.2, temperature of 50 °C, and reaction period of 48 hours. The calcium concentration of these tests was 80 ppm as Ca^{2+} and carbonate concentration 3000 ppm as CO_3^{2-}. A NaCl concentration of 1 M was used to represent the high TDS conditions. These were held as reference conditions throughout the tests. Based on the screening test results, five antiscalants were chosen for further study.

A selection of the results of the screening test is presented in *Table 4.1*. All results of the screening test can be found in Appendix 2.

Table 4.1. Results from the screening test. Inhibitor dosage of 18 ppm was used.

Sample	Filtrate (ppm as Ca^{2+})	Membrane (ppm as Ca^{2+})	Adherent (ppm as Ca^{2+})	Total (ppm as Ca^{2+})	% Inhibition
Blank	5.0	27.6	49.5	82.1	0 %
Control	82.4				100 %
Polyacrylate	5.3	1.5	69.8	76.6	0 %
Polymaleate	56.0	0.8	19.7	76.5	66 %
Polyaspartate 1	6.6	9.8	65.8	82.2	2 %
Polyaspartate 2	5.5	12.3	66.5	84.3	1 %
Polyaspartate 3	5.2	24.1	46.5	75.7	0 %
Phosphonate 1	83.6	1.8	0.2	85.6	102 %
Copolymer 3	62.0	4.2	18.7	84.9	74 %
Copolymer 5	41.7	6.9	37.4	86.0	47 %
Terpolymer 1	64.3	4.3	11.5	80.0	77 %
Terpolymer 2	62.6	3.6	15.3	81.5	74 %

The inhibitor dosage of these results was 18 ppm as solids. Due to large amount of samples, duplicates were not made for each sample. If the duplicates were made, the average value of the results was used in *Table 4.1*. All the results of the screening test including duplicates can be found in Appendix 2. The repeatability, reliability and error sources of this method are discussed more under a separate chapter. The inhibition percentages were calculated with equation 42. The inhibition percentage of Terpolymer 1 is calculated as an example,

$$\%\ Inhibition\ (Terpolymer\ 1) = \frac{64.3\ ppm - 5.0\ ppm}{82.4\ ppm - 5.0\ ppm} \times 100\ \% = 76.6\ \%.$$

When calculating inhibition percentages with this method, it is possible to get inhibition percentages over 100 %, like in the case of Phosphonate 1. This is due to the inaccuracies of the method.

The results of *Table 4.1* are presented graphically in *Figure 4.1*.

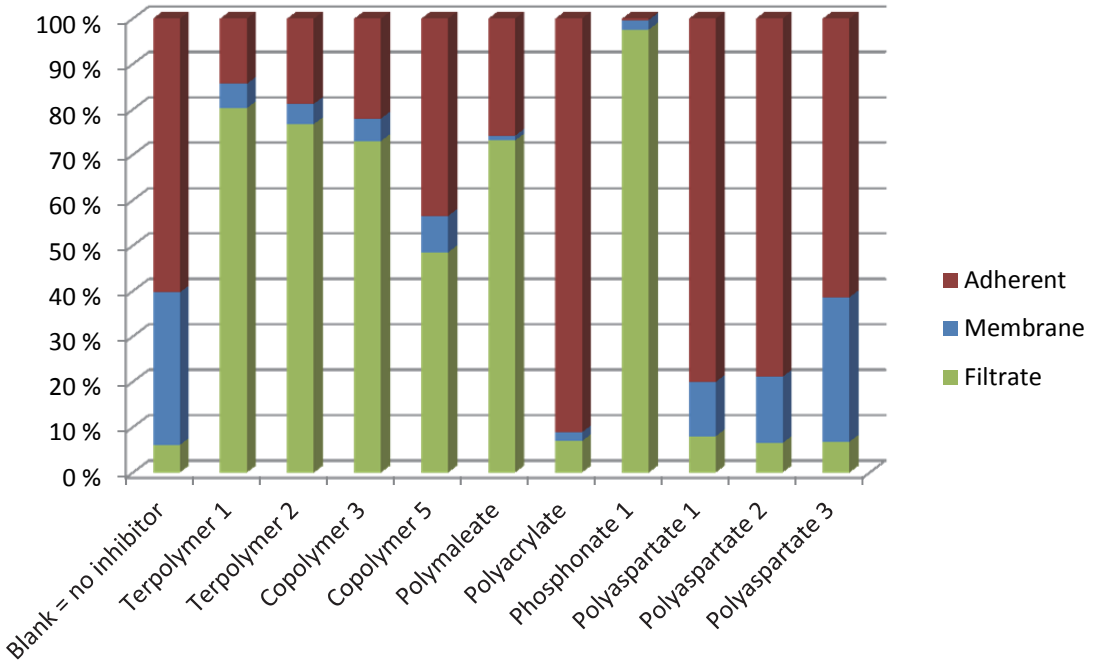

Figure 4.1. Performance of different antiscalants in the screening test.

Terpolymer 1 and Copolymer 5 are commercially available products. Both products are known to perform well in specific real process applications. Terpolymer 2 and Copolymer 3 are new experimental antiscaling polymers. Also three different polyaspartate (PASP) antiscalants of different molecular weighs were tested.

According to the screening test, both the commercially available Terpolymer 1 and the experimental product Terpolymer 2 performs equally well. The performance of Copolymer 2 compared with Copolymer 4 indicates that the lower molecular weight of Copolymer 2 improves the performance. This result is consistent with the conclusion made in *Chapter 2.3.4* that an optimal molecular weight range exist being 2000–20000 g/mol. The molecular weight of Copolymer 2 is 3050 g/mol whereas the molecular weight of Copolymer 4 is 50000 g/mol. The Polymaleate (maleate homopolymer) performs quite like the Copolymer 2 whereas the Polyacrylate (acrylate homopolymer) does not exhibit any inhibition in these conditions. Also the performances of all three different Polyaspartates are poor. The increase in the adherent precipitation compared to blank in the cases of Polyaspartates and Polyacrylate can be explained with the promotion of the nucleation on the glass surface of the jar. Although these antiscalants perform poor in the 48 h test it is likely that they delay the precipitation process in the beginning and the nucleation is promoted at the irregularities of the glass surface. This leads to adherent precipitation rather than bulk precipitation. The best performing antiscalant in the screening test was the Phosphonate 1, which is an ATMP antiscalant. It was the only antiscalant that could completely inhibit the precipitation at 50 °C in the 48 h test with the dosage of 18 ppm.

According to the screening test, the performances of different antiscalants can be distinguished with the static jar method. The static tests were carried on with five an-

tiscalants. The selected antiscalants were Terpolymer 2, Polymaleate, Polyacrylate, Phosphonate 1, and Polyaspartate 3. The Terpolymer 2 was chosen for further study as the performance of the new terpolymer antiscalant was of great interest. Polymaleate, Polyacrylate, Polyaspartate 3, and Phosphonate 1 were chosen to represent basic antiscaling chemistries. The PASP chosen was the Polyaspartate 3 with the highest molecular weight as it might show some dispersing properties according to the screening test. ATMP was chosen from the phosphonates as it had the best performance in the screening test. The properties of these antiscalants can be found in *Table 3.2*.

4.1.2 The effect of the inhibitor dosage

The effect of the inhibitor dosage for five selected inhibitors was studied at the same conditions as in the screening test. The studied dosages were 5, 10, 18, and 30 ppm as solids. The results of these tests are shown in *Table 4.2*.

Table 4.2. Results of the static tests with varying inhibitor dosage. Tests were carried out at 50 °C for the test period of 48 h.

Sample	Dosage (ppm)	Filtrate (ppm as Ca^{2+})	Membrane (ppm as Ca^{2+})	Adherent (ppm as Ca^{2+})	Total (ppm as Ca^{2+})	% Inhibition	% Filtrate
Terpolymer 2	5	32.5	1.0	44.3	77.8	36 %	42 %
	10	43.1	1.6	29.3	73.9	49 %	58 %
	18	62.6	3.6	15.3	81.5	74 %	77 %
	30	77.3	3.6	0.6	81.4	93 %	95 %
Polymaleate	5	15.0	1.2	57.5	73.8	13 %	20 %
	10	39.7	1.1	33.1	73.9	45 %	54 %
	18	56.0	0.8	19.7	76.5	66 %	73 %
	30	77.3	1.3	0.6	79.3	93 %	97 %
Polyacrylate	5	6.7	1.8	69.4	77.9	2 %	9 %
	10	3.6	1.3	68.2	73.0	-2 %	5 %
	18	5.3	1.5	69.8	76.6	0 %	7 %
	30	3.9	2.7	68.0	74.5	-1 %	5 %
Phosphonate 1	5	5.9	36.7	34.0	76.6	1 %	8 %
	10	8.4	45.2	22.9	76.5	4 %	11 %
	18	83.6	1.8	0.2	85.6	102 %	98 %
	30	75.5	0.7	0.4	76.5	91 %	99 %
Polyaspartate 3	5	8.6	48.0	19.8	76.4	5 %	11 %
	10	4.4	25.7	36.7	66.8	-1 %	7 %
	18	5.2	24.1	46.5	75.7	0 %	7 %
	30	4.8	7.6	61.0	73.5	0 %	7 %

Duplicates of all samples were not made in these tests. Only the screening test results of inhibitor dosage 18 ppm were confirmed and the average values were used in *Table 4.2*. The increasing dosage was assumed to increase the inhibition and the samples with different inhibitor dosages could be considered as parallel samples.

In *Table 4.2* also the percentage value of free Ca^{2+} (filtrate) per total Ca^{2+} (sum of the filtrate, membrane, and adherent) was calculated and labeled as % filtrate. The % filtrate value of Terpolymer 2 with the inhibitor dosage of 5 ppm is calculated as an example,

$$\%\ filtrate\ (Terpolymer\ 2) = \frac{32.5\ \text{ppm}}{77.8\ \text{ppm}} \times 100\ \% = 41.8\ \%.$$

This way the inhibition percentages of over 100 % and below 0 % could be avoided. The relative performance of the antiscalants is the same with both percentage values apart from some exceptions. The use of % filtrate value is also better as most of these samples are from the same series, where the ICP result of the control sample was only 78 ppm. Also most of the total calcium values are close to this value. In this case, the use of % inhibition value yields larger errors than the use of % filtrate value, as the control concentration used in these calculations was the average of all the control samples made (82.4 ppm). The test made with the 30 ppm dosage of Phosphonate 1, for example, yields more logical percentage value when the % filtrate is calculated. It should be noted that the % filtrate values are generally larger than the % inhibition values as there is also few ppms of free calcium in the blank. In the sample with 10 ppm of Polyaspartate 3, the sum value is so much below the control value that some sort of error might have happened in the sample treatment. The test was not repeated as it seemed obvious that the performance of this product was poor.

The % filtrate values are plotted as a function of the inhibitor dosage in *Figure 4.2*.

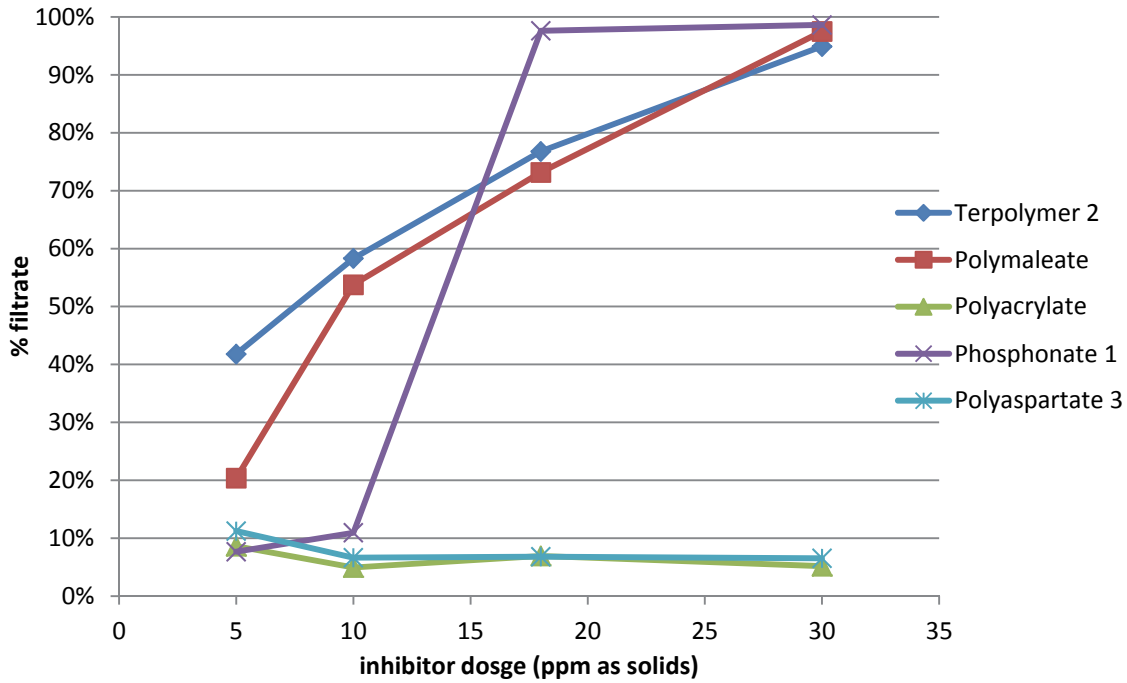

Figure 4.2. The performance of the antiscalants as a function of inhibitor dosage. Tests were carried out at 50 °C for the test period of 48 h.

It can be seen from *Figure 4.2* that the polymer antiscalants Terpolymer 2 and Polymaleate improve their performance more linearly compared with phosphonate antiscalant Phosphonate 1, which performs poorly with lower dosages but improves rapidly when the dosage exceeds certain value. This finding is not completely consistent with the conclusions made in the theoretical part (see *Chapter 2.3*) but can be explained with the more specific interactions of the phosphonates. When the test period is long the low dosage of phosphonate can block only some of the growth sites while others continue to grow. When the dosage is increased, at some point it is sufficient to block all the growth sites and the precipitation does not occur during the 48 h test period. The linear behavior of polymers can be explained by their less specific interactions. The performance is based more on blocking of growth sites and steric hindrance with their relative large molecule size. At the lowest dosage of 5 ppm, the Terpolymer 2 is superior to the other antiscalants in this test. This can be assumed to be due to the non-ionic compound in the polymer. The non-ionic part of the polymer may keep the polymer backbone straight and the functionality of the carboxylate groups is maintained whereas the pure maleate and acrylate polymers tend to coil around the calcium in high ionic strength conditions like in these tests and the functionality is lost more rapidly.

The poor performance of Polyaspartate 3 and Polyacrylate even with higher dosages is interesting. It seems that the test conditions are too harsh for these antiscalants to work. When looking at the membrane results of *Table 4.2*, at a lower dosage the Polyaspartate 3 seems to have more dispersing properties than with higher dosages. The reason for this is hard to explain.

4.1.3 The effect of the temperature

The next variable in the static tests was the temperature. The other conditions were again held constant and the inhibitor dosage used was 18 ppm as solids. Terpolymer 2, Polymaleate, and Phosphonate 1 were chosen for these tests. This time duplicates of each sample were made. The results are presented in *Table 4.3*.

Table 4.3. Results of the static tests with varying temperature. Tests were carried out with inhibitor dosage of 18 ppm for the test period of 48 h.

Sample	Temperature (°C)	Filtrate (ppm as Ca^{2+})	Membrane (ppm as Ca^{2+})	Adherent (ppm as Ca^{2+})	Total (ppm as Ca^{2+})	% filtrate
Terpolymer 2	50	67.8	4.2	15.2	87.1	78 %
		57.4	3.0	15.4	75.8	76 %
	Average	62.6	3.6	15.3	81.5	77 %
	75	32.6	16.7	27.9	77.3	42 %
		34.1	4.2	44.6	83.0	41 %
	Average	33.4	10.5	36.3	80.1	42 %
	95	11.6	19.6	48.2	79.4	15 %
		10.0	34.5	36.8	81.4	12 %
	Average	10.8	27.0	42.5	80.4	13 %
Polymaleate	50	55.5	0.9	19.0	75.4	74 %
		56.5	0.7	20.4	77.7	73 %
	Average	56.0	0.8	19.7	76.5	73 %
	75	34.5	4.4	39.2	78.1	44 %
		31.3	11.6	31.1	74.0	42 %
	Average	32.9	8.0	35.2	76.1	43 %
	95	2.0	5.3	76.7	84.1	2 %
		1.0	39.6	28.5	69.0	1 %
	Average	1.5	22.5	52.6	76.6	2 %
Phosphonate 1	50	78.7	1.4	0.2	80.2	98 %
		88.5	2.3	0.3	91.1	97 %
	Average	83.6	1.8	0.2	85.6	98 %
	75	8.7	5.1	50.7	64.4	13 %
		6.2	22.6	66.9	95.7	6 %
	Average	7.4	13.8	58.8	80.0	9 %
	95	1.5	18.5	25.7	45.7	3 %
		0.5	40.3	28.8	69.6	1 %
	Average	1.0	29.4	27.3	57.6	2 %

From the data of *Table 4.3* can be seen that the parallel tests yield consistent results for the filtrate value but at higher temperatures than 50 °C the values of membrane and adherent parts of the sample differ increasingly. The differences in the membrane values are due to bigger crystals and agglomerates that are formed at higher temperatures in the presence of antiscalant. In this case, the sample cannot be made homogeneous by inverting the jar after the test and the 100 ml of the sample which is filtrated can include varying amounts of the agglomerates. For this reason there are quite big differences also in the calculated total amounts of calcium in the samples. This problem could be solved by filtering the whole sample instead of 100 ml. This would require more time for each

test. The differences in the adherent parts of the sample can be explained with the fact that at increasing temperature the equilibrium between bulk precipitation and adherent depositions becomes more delicate as the solubility of other polymorphs than calcite approach the solubility of calcite (see *Figure 2.3*). However, the filtrate parts of the sample are reliable and they can be plotted as a function of temperature. This is done in *Figure 4.3*.

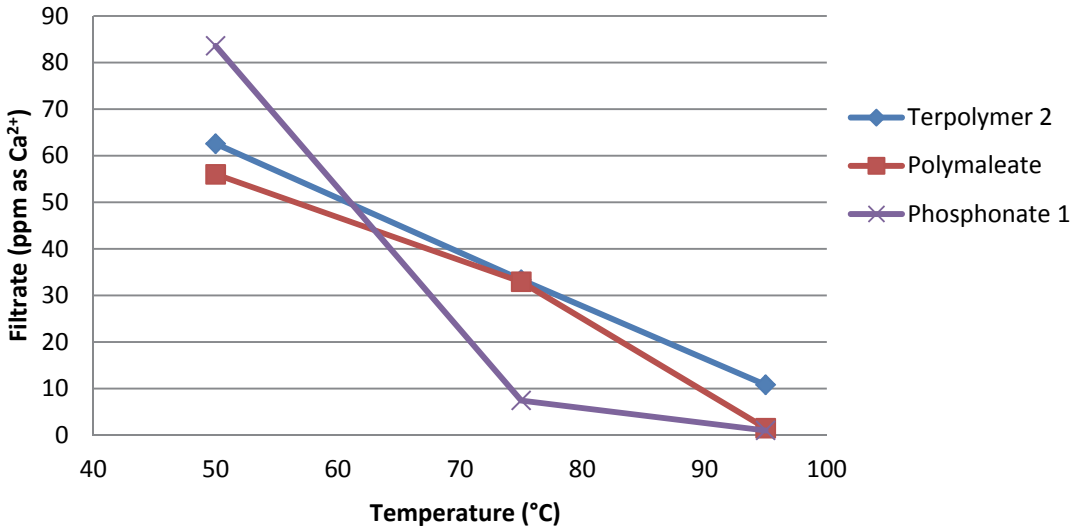

Figure 4.3. Performance of chosen antiscalants as a function of the temperature. Tests were carried out with inhibitor dosage of 18 ppm for the test period of 48 h.

It appears that the temperature has drastic effect on the performances of antiscalants. Increasing the temperature from 50 °C to 75 °C decreases the amount of free calcium almost to half in the case of Terpolymer 2 and Polymaleate. In the case of Phosphonate 1 the free calcium concentration at 75 °C is under 10 % from the free calcium concentration at 50 °C. At 95 °C the Terpolymer 2 is the only one of these three antiscalants that can keep even a small part of calcium from precipitating.

It seems that even a quite small increase in the temperature with long residence time causes the thermal degradation of the polymer antiscalants and the hydrolysis of the phosphonate antiscalant. Another explanation for the rapid failing of inhibition at higher temperatures, especially in the case of the Phosphonate 1, could be the increasing percentage of aragonite in the forming precipitate. The differences in the crystal structure of calcite and aragonite could cause the phosphonate group spacing of ATMP to be mismatched with the crystal growth sites when the percentage of aragonite increases. However, this is pure speculation as the morphology of the precipitate was not studied.

4.1.4 The effect of the reaction time

The effect of the residence time was studied with Terpolymer 2 and Phosphonate 1. The inhibitor dosage used for Terpolymer 2 was 18 ppm as solids and for Phosphonate 1 10 ppm as solids. The lower dosage for Phosphonate 1 was chosen because the inhibition with the 18 ppm dosage was complete even after 48 hours. The reaction times of 1.5 h,

5 h, and 20 h were used. The other conditions were held the same as in the screening test. Duplicates of each sample were made and the results are presented in *Table 4.4*.

Table 4.4. Results for the tests with different reaction times. The tests were carried out at 50 °C.

Sample	Time (h)	Filtrate (ppm as Ca^{2+})	Membrane (ppm as Ca^{2+})	Adherent (ppm as Ca^{2+})	Total (ppm as Ca^{2+})	% filtrate
Terpolymer 2 (18 ppm)	1.5	78.2	2.5	1.6	82.3	95 %
		75.1	1.2	1.6	77.8	96 %
	Average	76.7	1.8	1.6	80.1	96 %
	5	68.5	2.4	7.9	78.8	87 %
		70.8	0.9	0.3	72.0	98 %
	Average	69.6	1.7	4.1	75.4	92 %
	20	63.2	3.1	13.7	80.0	79 %
		63.2	1.0	13.2	77.4	82 %
	Average	63.2	2.0	13.5	78.7	80 %
Phosphonate 1 (10ppm)	1.5	82.2	1.3	0.5	84.0	98 %
		86.2	1.3	0.5	88.1	98 %
	Average	84.2	1.3	0.5	86.0	98 %
	5	82.7	1.1	2.4	86.2	96 %
		82.0	1.2	1.9	85.0	96 %
	Average	82.3	1.1	2.2	85.6	96 %
	20	5.5	38.5	30.9	74.9	7 %
		5.0	39.1	33.9	78.1	6 %
	Average	5.3	38.8	32.4	76.5	7 %

The results presented in *Table 4.4* show that the duplicates yield consistent results apart from the second sample of Terpolymer 2 in the test with reaction time of 5 hours. In this sample adherent result can be assumed to be incorrect as all the other adherent results show expected behavior with increasing reaction time. The % filtrate values are plotted as a function of reaction time in *Figure 4.4*. For the 5 h test of Terpolymer 2 the value of the first test (87 %) is used instead of the average.

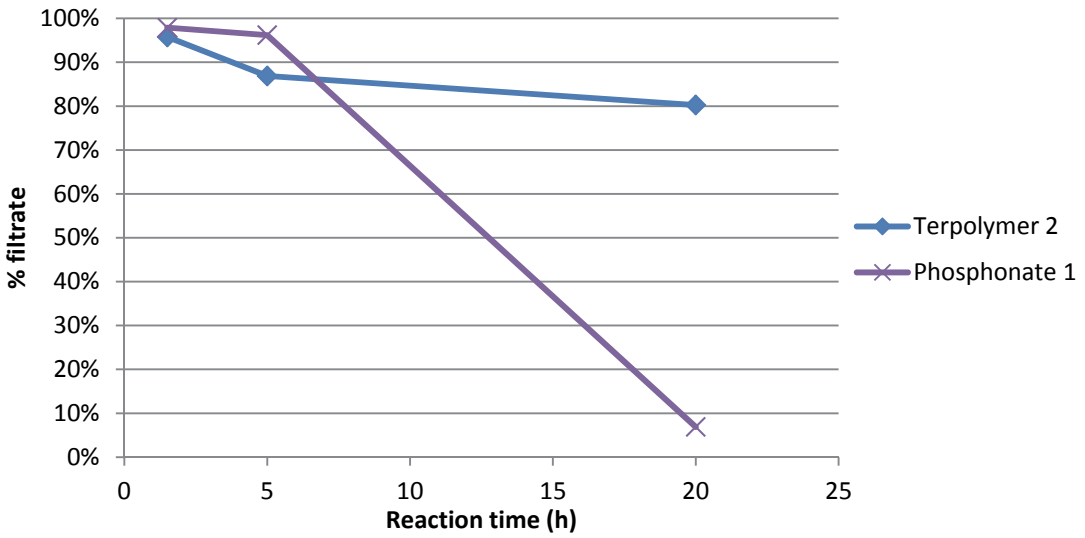

Figure 4.4. Performance of chosen antiscalants as a function of the reaction time. The used dosage of Terpolymer 2 was 18 ppm and the dosage of Phosphonate 1 10ppm. Tests were performed at 50 °C.

These results confirm the earlier speculations that with shorter reaction time the Phosphonate 1 is capable of inhibiting the precipitation well but cannot keep the calcium carbonate from precipitating when the residence time is increased. In the results of Terpolymer 2 can be seen that a good polymer antiscalant can better retard and delay the precipitation after the nucleation has taken place compared with a phosphonate antiscalant, which can longer delay the nucleation process but fails rapidly when the crystal growth begins.

4.1.5 The effect of the pH

Next variable in the static tests was pH. Other conditions were again held constant. The temperature was 50 °C and reaction time 48 h. The used pH values were 8.8, 9.2, 10.7, and 12.7. The results for blanks in these conditions are presented in *Table 4.5*. Duplicates were made for each blank.

Table 4.5. Results of the blanks with varying pH. Tests were carried out at 50 °C with the reaction period of 48 h.

Sample	pH	Filtrate (ppm as Ca^{2+})	Membrane (ppm as Ca^{2+})	Adherent (ppm as Ca^{2+})	Total (ppm as Ca^{2+})
Blank	8.8	4.0	9.5	69.6	83.1
		3.6	4.8	72.8	81.2
	Average	3.8	7.1	71.2	82.1
	9.2	4.6	23.4	51.7	79.7
		1.5	21.8	49.8	73.1
	Average	3.1	22.6	50.8	76.4
	10.7	0.9	68.1	7.0	76.0
		1.0	73.5	6.7	81.2
	Average	0.9	70.8	6.9	78.6
	12.7	3.6	73.2	7.5	84.3
		1.8	76.5	7.4	85.8
	Average	2.7	74.9	7.5	85.0

The results of *Table 4.5* show that with increasing pH the amount of adherent precipitate is decreased and the amount of precipitate in the solution is increased. This is due to the increased supersaturation ratio with increasing pH. When the supersaturation is increased the precipitation in the solution occurs faster and the growth on the surface is diminished. The results of the parallel samples in *Table 4.5* are consistent and it was decided that it was not necessary to do duplicates for each sample with an inhibitor. The results of all five inhibitors with varying pH are summed up in *Table 4.6*.

Table 4.6. Results of different antiscalants with varying pH. Tests were carried out at 50 °C with the reaction period of 48 h and inhibitor dosage of 18 ppm.

Sample	pH	Filtrate (ppm as Ca^{2+})	Membrane (ppm as Ca^{2+})	Adherent (ppm as Ca^{2+})	Total (ppm as Ca^{2+})	% filtrate
Terpolymer 2	8.8	80.2	2.7	0.3	83.2	96 %
	9.2	67.8	4.2	15.2	87.1	78 %
	10.7	51.8	4.3	27.5	83.6	62 %
	12.7	64.5	11.8	10.3	86.6	75 %
Polymaleate	8.8	82.8	1.4	0.3	84.5	98 %
	9.2	56.5	0.7	20.4	77.7	73 %
	10.7	38.4	1.7	46.0	86.1	45 %
	12.7	37.3	1.6	42.6	81.5	46 %
Polyacrylate	8.8	5.5	10.1	63.5	79.1	7 %
	9.2	5.0	1.4	72.4	78.8	6 %
	10.7	3.9	4.4	75.9	84.2	5 %
	12.7	3.5	68.0	14.6	86.2	4 %
Phosphonate 1	8.8	83.0	1.4	0.2	84.5	98 %
	9.2	78.7	1.4	0.2	80.2	98 %
	10.7	5.5	27.9	48.4	81.9	7 %
	12.7	76.8	2.2	4.2	83.2	92 %
Polyaspartate 3	8.8	8.2	2.6	70.7	81.4	10 %
	9.2	4.5	24.8	49.6	78.9	6 %
	10.7	7.2	29.2	49.1	85.5	8 %
	12.7	4.7	66.9	14.6	86.3	6 %

At pH 8.8, all the other antiscalants can practically completely inhibit the calcium carbonate from precipitating except Polyacrylate and Polyaspartate 3, which display very little inhibition even at the lowest pH. The adherent and membrane parts of these two antiscalants differ from the blanks to some extent, yet having the same trend of the increasing percentage of the membrane part with increasing pH. In the results of Terpolymer 2, Polymaleate, and Phosphonate 1 the trend of the % filtrate value seems logical until the pH 12.7. This is demonstrated by plotting the % filtrate values as a function of pH in *Figure 4.5*

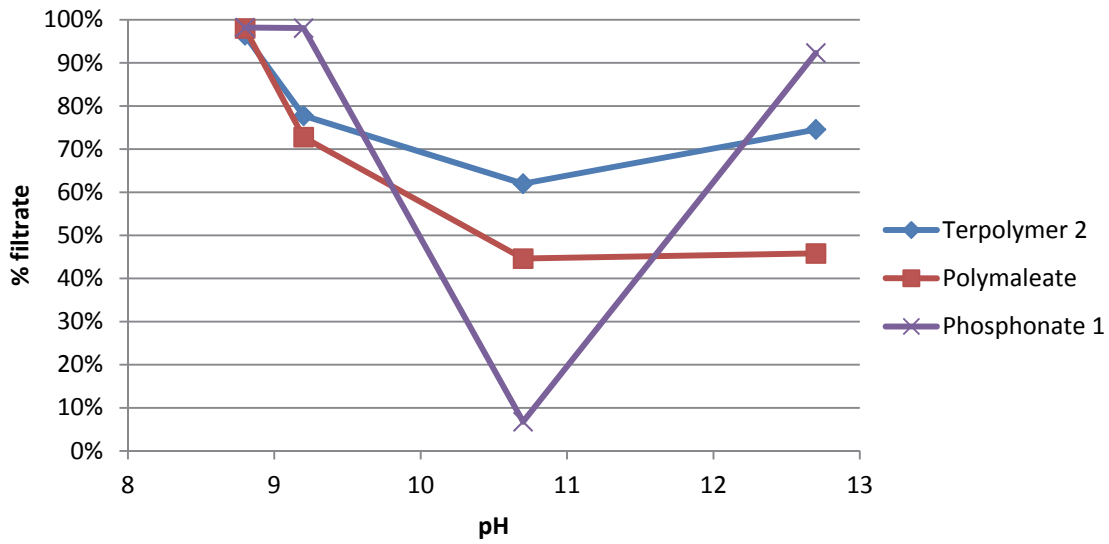

Figure 4.5. Performance of chosen antiscalants as a function of pH. Tests were carried out at 50 °C with the reaction period of 48 h and inhibitor dosage of 18 ppm.

The behaviors of the antiscalants in the tests with the pH values of 8.8, 9.2, and 10.7 are consistent with the previous results. As the pH and supersaturation increase, the performances of the polymer antiscalants sink less drastically than the performance of the phosphonate antiscalant. The improvement of the performance at pH 12.7 with all three antiscalants is surprising. The test results for Phosphonate 1 were repeated a few times at pH values 10.7 and 12.7 in order to make sure that the result was correct. The same behavior took place in the repeated tests.

As the possibility of a false result was excluded, there are two reasons for this kind of behavior that could be thought of. First possibility that came to mind was that the increased ionic strength due to added NaOH in order to increase the pH value to 12.7 could decrease the activities of calcium and carbonate ions and decrease the supersaturation ratio. The increase in the sodium ion concentration was about 3000 ppm due to the NaOH addition in the samples of pH 12.7 which seemed insignificant as the total sodium ion concentration was about 25000 ppm in the samples with lower pH values. However, this possibility could easily be checked by increasing the sodium ion concentration of the pH 10.7 sample to the same level with an addition of NaCl. This was done for a blank, Terpolymer 2, and Phosphonate 1. The results with increased sodium level are presented in *Table 4.7*.

Table 4.7. Repeated tests with increased sodium ion concentration.

Sample	pH	Filtrate (ppm as Ca^{2+})	Membrane (ppm as Ca^{2+})	Adherent (ppm as Ca^{2+})	Total (ppm as Ca^{2+})	% filtrate
Blank	10.7	4.6	55.0	25.5	85.1	5 %
Terpolymer 2	10.7	54.4	6.7	27.1	88.2	62 %
Phosphonate 1	10.7	6.6	49.9	13.6	70.2	9 %

When comparing these results with the results of *Table 4.5* and *Table 4.6*, it seems that the increased sodium ion concentration was not the main reason for the good perfor-

mance of the antiscalants at pH 12.7. The results of the blank in *Table 4.7* differ slightly from the earlier blanks at the same pH as the relative amount of adherent precipitate is increased but the results of Terpolymer 2 and Phosphonate 1 are very similar to earlier results at the same pH.

The second potential explanation is that the morphology of the scale is changed at pH 12.7 compared with other pH values which improves the performances of the antiscalants at this pH. The validity of this explanation has not been evaluated.

4.1.6 The effect of the supersaturation ratio

The effect of different calcium and carbonate levels on the performance of Terpolymer 2 and Phosphonate 1 was studied. For the Phosphonate 1 calcium levels below 80 ppm and carbonate levels below 3000 ppm were not studied as the inhibition percentage was practically 100 % at these levels. These tests were performed at pH 9.2 and temperature 50 °C with the inhibitor dosage of 18 ppm and reaction period of 48 h. The results are summarized in *Table 4.8*.

Table 4.8. Results of the static tests with different calcium and carbonate levels. Tests were carried out with inhibitor dosage of 18 ppm for the test period of 48 h at 50 °C and pH 9.2.

Sample	Ca^{2+} (ppm)	CO_3^{2-} (ppm)	Filtrate (ppm as Ca^{2+})	Membrane (ppm as Ca^{2+})	Adherent (ppm as Ca^{2+})	Total (ppm as Ca^{2+})	% inhibition
Blank	40	3000	4.5	29.8	5.1	39.4	0 %
	80	3000	4.6	23.4	51.7	79.7	0 %
	160	3000	2.0*	24.4	113.2	139.6	0 %
	80	1500	3.3	12.5	61.6	77.4	0 %
	80	4500	1.5*	28.8	32.9	63.2	0 %
Control	40	0	41.9			41.9	100 %
	80	0	82.4			82.4	100 %
	160	0	162.5			162.5	100 %
Terpolymer 2	40	3000	39.3	1.7	0.2	41.2	93 %
	80	3000	57.4	3.0	15.4	75.8	68 %
	160	3000	39.6	61.3	53.3	154.3	23 %
	80	1500	80.4	2.8	0.2	83.4	97 %
	80	4500	51.9	3.6	21.8	77.2	62 %
Phosphonate 1	80	3000	78.7	1.4	0.2	80.2	95 %
	160	3000	10.2	3.9	142.1	156.3	5 %
	80	4500	7.7	29.7	35.4	72.8	8 %

* The concentration was below the lowest calibration value of the ICP and not as accurate as other results

The results of *Table 4.8* seem logical as the increased supersaturation reduce the inhibition percentage values of the antsicalants. This time the % inhibition was chosen to be calculated instead of % filtrate because many different blanks were used for different calcium and carbonate levels. For example, the % filtrate value of the blank with 40 ppm calcium and 3000 ppm carbonate is 12 % whereas the % filtrate value for the blank

with 160 ppm calcium and 3000 ppm carbonate is only 1 %. For this reason the % filtrate values at different calcium levels for samples including inhibitors would not be comparable. The percentage distributions of calcium in the samples of *Table 4.8* are graphically presented in *Figure 4.6* and *Figure 4.7*. In *Figure 4.6* the carbonate level is held constant at 3000 ppm as CO_3^{2-} and in *Figure 4.7* the calcium level is held constant at 80 ppm as Ca^{2+}.

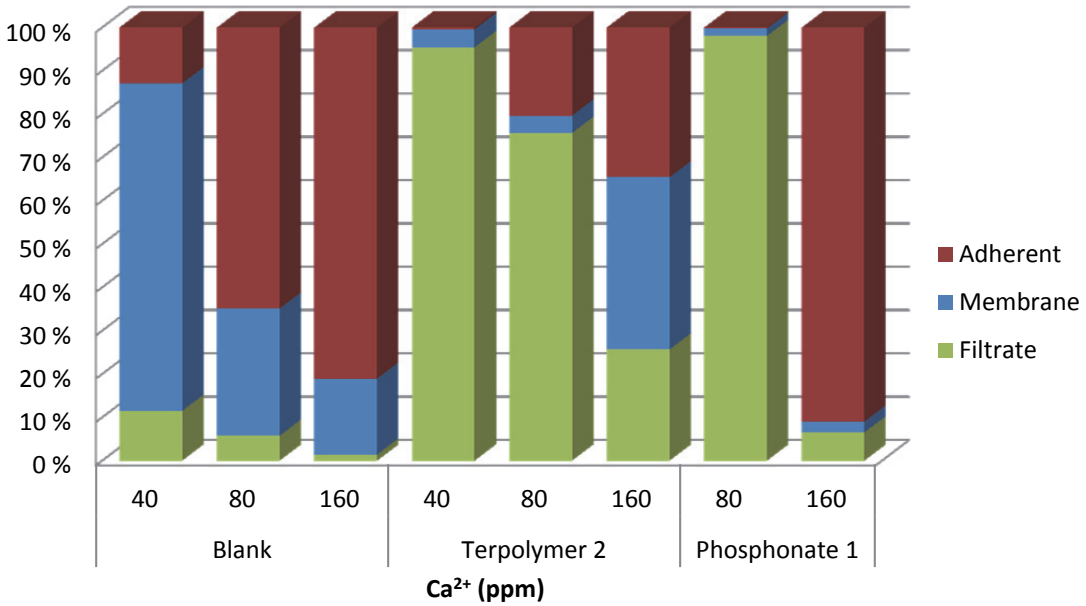

Figure 4.6. The effect of different calcium levels on the calcium distribution of the sample in absence and presence of scale inhibitor. The carbonate level was held constant at 3000 ppm as CO_3^{2-}. Tests were carried out with inhibitor dosage of 18 ppm for the test period of 48 h at 50 °C and pH 9.2.

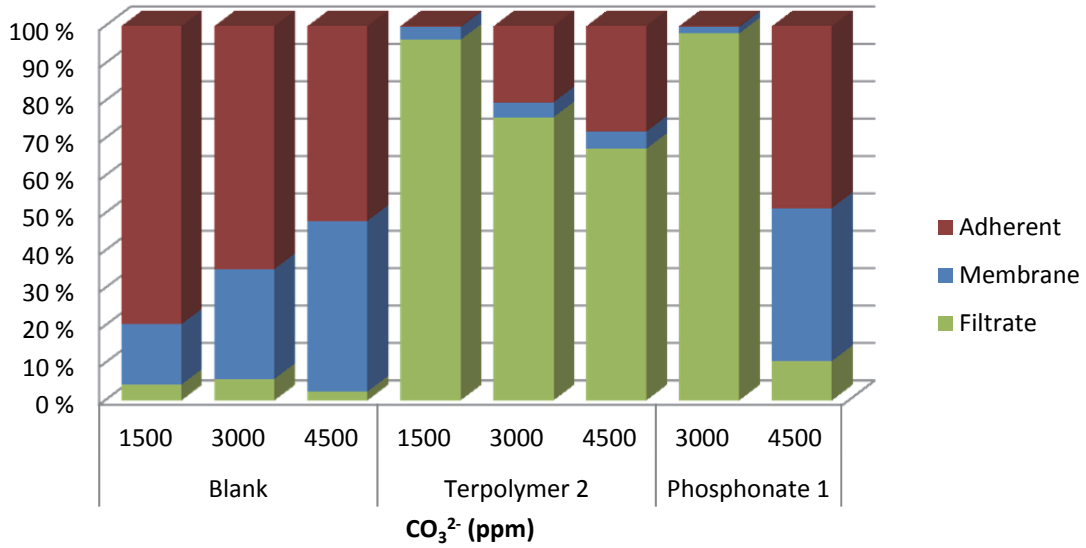

Figure 4.7. The effect of different carbonate levels on the calcium distribution of the sample in absence and presence of scale inhibitor. The calcium level was held constant at 80 ppm as Ca^{2+}. Tests were carried out with inhibitor dosage of 18 ppm for the test period of 48 h at 50 °C and pH 9.2.

When the calcium level of the sample is increased, the amount of adherent precipitation is increased in the blank. The same behavior is noticed when the carbonate level is decreased. This means that decrease in the excess carbonate in the blank results in favoring the adherent precipitate, and the supersaturation ratio is irrelevant. It can also be concluded from this data that a change in the calcium level affects the amount of adherent precipitate more than a change in the carbonate level.

When an antiscalant is present in the sample, the amount of adherent precipitate grows with the increasing supersaturation ratio. The reason for this is the same as discussed in context with the performance of PASPs and Polyacrylate in the screening test (see *Chapter 4.1.1* on page 44) the inhibitor slows the bulk precipitation process and the precipitation on the surface is promoted. Yet again the Terpolymer 2 is more resistant to the changes in the test conditions than Phosphonate 1. It appears that the phosphonate antiscalant performs well as long as the primary nucleation does not occur. As soon as crystals are present the failure is rapid. In the case of Terpolymer 2 the secondary nucleation is inhibited to a much greater extent. This finding is consistent with the conclusions of Rieger et al. [3] about the inhibition mechanisms of polycarboxylates. When the calcium ions are bridged into the polymer network, they are stabilized better than in the case of phosphonate antiscalants.

4.1.7 The effect of the ionic strength on the static tests

The role of ionic strength on the performance of the antiscalant has been mentioned before and is discussed next by comparing the results of the static test made in this study to some earlier test results at Kemira. The test conditions differ quite much but the biggest difference is that in the earlier test the ionic strength is low. In the earlier test,

the calcium concentration is 640 ppm as Ca^{2+}, carbonate concentration is 960 ppm as CO_3^{2-}. These tests were carried out at pH 8.6 and temperature 50 °C and the test period was 20 h. The pH was adjusted with NH_4Cl buffer solution. The final test solution had a chloride concentration of about 4500 ppm, which is low in comparison with the chloride concentration of about 36000 ppm in the tests of this study. The test results of the earlier test were compared with the test results of pH 8.8 from *Table 4.6*. The % inhibition values of these two tests are compared in *Table 4.9*. The antiscalant dosage of the earlier results is 20 ppm and the dosage of the results of this study is 18 ppm.

Table 4.9. Comparison of low ionic strength results of earlier test and the pH 8.8 results from Table 4.6.

Sample	% inhibition (this study)	% inhibition (earlier test)
Terpolymer 2	97 %	61 %
Polymaleate	101 %	91 %
Polyacrylate	2 %	101 %
Phosphonate 1	101 %	87 %
Polyaspartate 3	6 %	88 %

The differences between these two test results are significant. The results are almost completely contrary to each other. Only the Phosphonate 1 and Polymaleate perform almost similarly in both cases. The results of Polyaspartate 3 and Polyacrylate in the earlier test indicate that the high ionic strength in the tests of this study was the main reason for their poor performance. As mentioned before, the homopolymers might coil up in high TDS conditions as there is no compound to hold the polymer backbone straight. On the other hand, these homopolymers seem to be better threshold inhibitors in low TDS conditions than the Terpolymer 2.

The reason for the poorer performance of Terpolymer 2 in the earlier test might be the higher calcium level in this test, which means that the supersaturation ratio of the earlier test is likely higher than in the test of this study. Also the poorer performance of Phosphonate 1 indicates this. When the calcium level is high and the ionic strength low, the non-ionic compound in the Terpolymer 2 lessen the threshold inhibition properties of the antiscalant. The main idea of the non-ionic part is to hold the polymer backbone straight and to increase steric hindrance, which both improve more the dispersing and crystal modification properties of the polymer. In the threshold inhibition the non-ionic part of the polymer is inactive and might be the reason for the lower inhibition rates of Terpolymer 2 than those of pure PMA and PAA antiscalants at low TDS test conditions.

It is notable that the PMA antiscalant performs also in the high TDS conditions. When comparing the structures of PMA, PAA, and PASP (*Figure 2.7)* it is noteworthy that the maleate monomer has functional carboxylate groups on both sides of the polymer backbone and the acrylate, and aspartic acid only on the other. This means that in the polymaleate there are functional groups regularly on both sides of the polymer backbone even if the stereochemistry of the polymer is not controlled. It might be that

this results in less coiling in the PMA antiscalant and the performance is quite good also in the high TDS conditions.

4.1.8 Error sources and reliability of the method

The repeatability of the method has already been discussed in context with the results and it appears that the method is quite reliable. Due to large amount of samples the same test was rarely repeated in order to confirm the results, but when parallel tests were made they were in good consistency with each other in most cases. Only the results at high temperature had increased variance in the duplicates. The reason for this error was explicit and visual; the elevated temperature caused more agglomeration of the precipitate and a representative sampling for filtration was difficult.

The systematic error of measurements caused by the inaccuracies of scales, pipettes, volumetric flasks, and so on can be assumed to be minor. The majority of the error comes from the random error in the treatment of the sample after the reaction period and from the random error of the ICP. The error in the sample treatment comes from the difficulty of making the sample homogeneous before filtering and the error of ICP measurements has generally been estimated to be ± 5 %. It is hard to distinguish between these two error sources.

The total error of the method is estimated statistically. As the same sample was not prepared multiple times, the error in the distribution of calcium into filtrate, membrane, and adherent parts is not reasonable to be estimated statistically. However, all the samples of *Tables 4.1-4.8* with the supposed total calcium concentration of 80 ppm can be concerned as a single series of measurements, if only the total values of calcium are taken into account. The average, $\bar{x}$, and standard deviation, s, are calculated with Microsoft Excel for the results of *Tables 4.1-4.8* as follows.

$$\bar{x} = \frac{1}{N}\sum_{i=1}^{N} x_i = 79.1 \text{ ppm},$$

where N is the total amount of measurements. The standard deviation for the same values is

$$s = \sqrt{\frac{\sum(x_i - \bar{x})}{N-1}} = 6.6 \text{ ppm}.$$

The error limit of the method can be estimated using these values. $6.6 \text{ ppm}/79.1 \text{ ppm} \times 100\ \% = 8.3\ \%$, so the error limit of the method can be estimated to be ± 9 %. The same calculations can be made for the control samples prepared. The results of the control samples are summed up in *Table 4.10*.

Table 4.10. Results of the control samples.

Sample	Total calcium (ppm)	
Control	85.5	
	78.2	
	81.1	
	82.2	
	85.0	
	$\bar{x}$=82.4	*s*=3.0

From the results of *Table 4.10*, the error limit in the case of control samples can be calculated; $3.0\ \text{ppm}/82.4\ \text{ppm} \times 100\ \% = 3.6\ \% \approx 4\ \%$. In the control samples, the error resulting from the sample treatment after the reaction period is negligible and the error comes mainly from the error of ICP. From the error limits of the control samples can be estimated that about half of the total error of ± 9 % comes from the ICP.

4.2 Dynamic tests

The main aim of the dynamic tests was to estimate the suitability and reliability of the used methods for antiscalant testing. No large scale comparisons were made among different antiscaling chemistries, but when the data for the same antiscalant is available from static and dynamic tests, the results are compared and discussed. The used methods were a rotating disk procedure and dynamic tube blocking procedure.

4.2.1 Rotating disk results

The rotating disk tests were carried out at the temperature 50 °C and pH 9.2. The reaction period was 1.5 h, the calcium concentration of the sample was 80 ppm as Ca^{2+}, carbonate concentration 3000 ppm as CO_3^{2-}, and NaCl concentration 1 M. The used inhibitor dosage was 18 ppm. The results of rotating disk tests are summarized in *Table 4.11*.

Table 4.11. Results of the rotating disk tests. Tests were performed at 50 °C and pH 9.2 with the reaction period of 1.5 h. Inhibitor dosage of 18 ppm was used.

Sample	Filtrate (ppm as Ca^{2+})	Membrane (ppm as Ca^{2+})	Adherent (ppm as Ca^{2+})	Total (ppm as Ca^{2+})
Copolymer 2	66.0	1.5	24.6	92.1
Copolymer 3	70.5	2.4	18.6	91.5
Copolymer 4	70.0	1.5	14.3	85.7
Copolymer 6	62.5	4.9	25.5	92.8
Polyaspartate 3	3.4	2.0	73.7	79.0
Phosphonate 1	84.5	1.3	1.1	86.9
Phosphonate 2	81.0	9.8	2.4	93.2
Phosphonate 3	58.0	2.6	21.6	82.2
Polyacrylate	102.0	1.7	1.5	105.2
Terpolymer 2	65.8	2.3	16.8	84.8
Terpolymer 3	73.0	2.6	19.6	95.2
Terpolymer 4	74.0	3.1	19.0	96.1
Terpolymer 5	81.5	1.4	15.5	98.4

It is obvious from the data of *Table 4.11* that the sum of filtrate, membrane and adherent constantly exceeds the average control value of 82.4 ppm. This is due to the evaporation of water from the uncovered polystyrene cup during the 90 min test period. This results in too high values of the filtrate part of the sample. Because of this it is not reasonable to calculate % inhibition or % filtrate values for these results. However, as the evaporated amount of water can be considered to be the same in every sample, the results are comparable. The results of *Table 4.11* are presented in *Figure 4.8* and *Figure 4.9* and compared with the results of the static screening test for the same samples. The results of the new experimental antiscalants are presented in *Figure 4.8* and the results of some commercially available antiscalants in *Figure 4.9*.

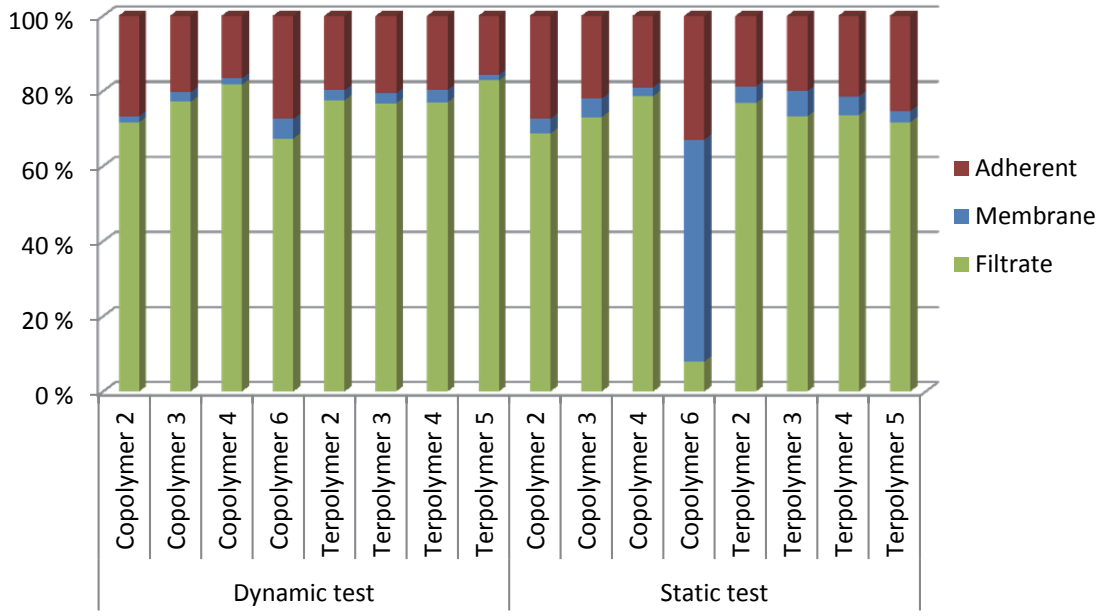

Figure 4.8. Comparison of the new laboratory scale products in static and dynamic conditions. Tests were performed at 50 °C and pH 9.2 with the inhibitor dosage of 18 ppm. The reaction period in the dynamic tests was 1.5 h and in the static tests 48 h.

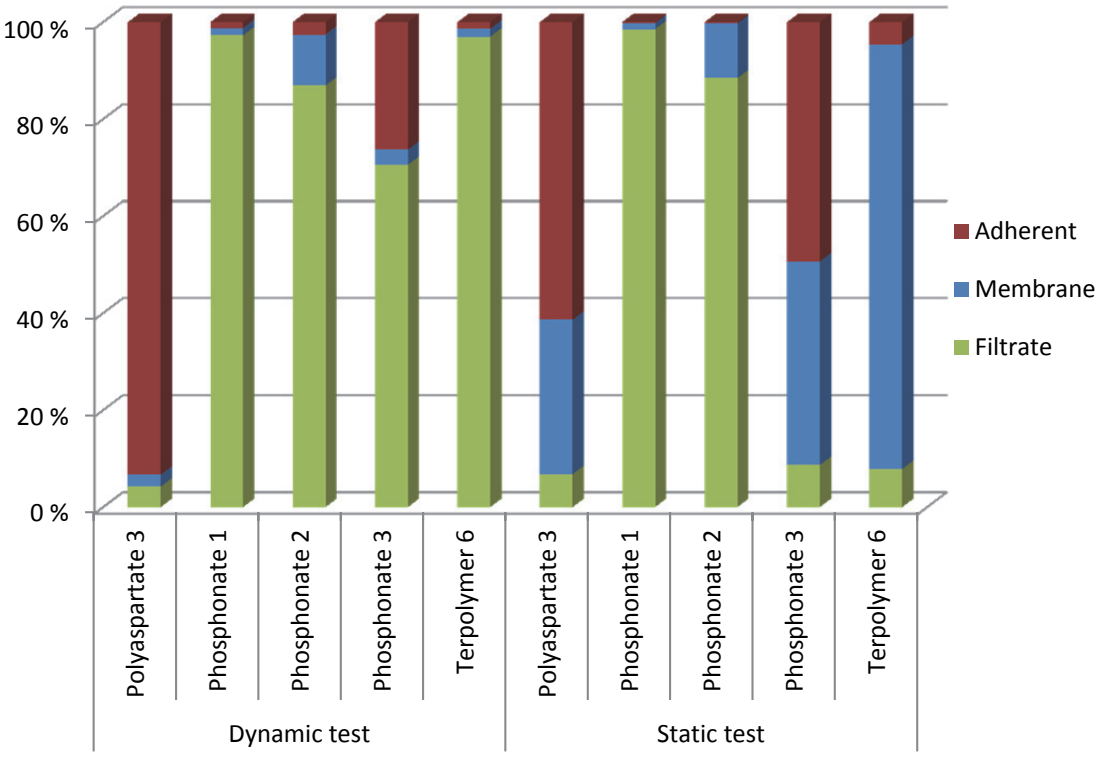

Figure 4.9. Comparison of commercially available products in static and dynamic conditions. Tests were performed at 50 °C and pH 9.2 with the inhibitor dosage of 18 ppm. The reaction period in the dynamic tests was 1.5 h and in the static tests 48 h.

The test conditions of the static and dynamic test were otherwise the same but the reaction period in the dynamic case was only 1.5 h as it was 48 h in the static case. The per-

formances of all the other new products but Copolymer 6 (*Figure 4.8*) are similar in both cases which indicate that accelerated kinetics is achieved with the addition of a metal surface, a seeding stage and the stirring. The performance of the Copolymer 6, which is a maleate/non-ionic copolymer, is quite different in the static and dynamic case. This could be due to dynamic conditions or the shorter reaction period. The percentages of adherent parts of the Copolymer 6 samples are quite similar in static and dynamic test, and it is the percentages of the membrane and filtrate parts that change. The same behavior can be seen for the other Copolymer and Terpolymer samples of *Figure 4.8* but to a smaller extent, as the amount of bulk precipitation in the 48 h static test was generally quite low. It seems that the addition of a metal surface, a seeding stage and the dynamic conditions accelerate the adhesion process relatively more than the bulk precipitation process.

Also the results of Terpolymer 6 presented in *Figure 4.9* are consistent with this conclusion, whereas the Polyaspartate 3 shows completely opposite behavior as the filtrate percentage remains the same and the membrane precipitation converts into adherent precipitation. This could be simply due to the overall poor performance of the Polyaspartates in any test performed in this study and the slight inhibition properties that the PASP has in these conditions only promote the adhesion process rather than delay the precipitation process. When only the adherent part is examined, the Phosphonate 3 (PBTC) is the only antiscalant which performs significantly better in the dynamic test. This is likely due to the rapid failure of the phosphonates in the longer tests, which was detected in the static test results.

Problems of the method

Although the rotating disk results presented above seem to be reasonable when compared with the static results some problems stood out. The reproducibility of the test was questionable when using different stirrers and disks. A number of blanks were prepared to study the reproducibility of the method. The results of the blanks are presented in *Table 4.12*.

Table 4.12. Results of the blanks in the rotating disk tests. Tests were performed at 50 °C with the reaction period of 1.5 h.

Sample	Filtrate (ppm as Ca^{2+})	Membrane (ppm as Ca^{2+})	Adherent (ppm as Ca^{2+})	Total (ppm as Ca^{2+})	Stirrer and disk used
Blank 1	1.5	16.0	61.7	79.2	1
Blank 2	7.0	19.6	56.5	83.0	2
Blank 3	2.0	6.5	65.8	74.3	1
Blank 4	1.5	24.9	45.0	71.4	2
Blank 5	2.0	45.3	18.0	65.3	3

As it can be seen from the results of *Table 4.12* the rotating disk method does not seem very repeatable. There is big variance in all three parts of the sample and the total amount of calcium is below the control value, which is opposite behavior to the samples

containing an inhibitor. The reasons for this are multiple. First, as the free calcium concentration is small, the evaporation of the water does not affect the total calcium result. Second, the adherent deposition is on the surface of the polystyrene cup to a great extent. In the presence of an inhibitor the adherent deposition occurs almost completely on the metal disk. It is likely that the adherent deposition on the surface of the polystyrene cup is not dissolved properly, at least in the blanks 4 and 5. This might be due to the smaller volume of acid solution used in the dissolution than the volume of the sample leaving part of adherent scale remaining above the fluid level of the acid solution. Third, the differences between different disks and stirrers may affect the overall precipitation quite a lot. If one disk spins with a slightly different speed or if the rod of one disk swings more than other, the delicate equilibrium between the filtrate, membrane and adherent may change as was discussed in *Chapter 2.4*. Also the preparation of representative filtrate and membrane samples is harder than in the static case, as the uncovered polystyrene cup cannot be inverted in order to make the sample homogeneous before filtering.

The best way to avoid or diminish these problems would be to always use the same disk with the same stirrer and to run parallel samples with all three stirrers and then calculate average of these three parallel runs. This way the differences caused by the equipment would be eliminated. It should also be confirmed that the same disk with the same stirrer gives reproducible results. The two repeated blanks of *Table 4.12* are not sufficient to draw conclusions about the reproducibility.

Seeding stage

The role of the seeding stage to the accelerated kinetics of the precipitation process was studied by analyzing the adherent calcium amount on the metal disk after the seeding stage. It was found out that only about 1 % of the calcium used in the seeding was adhered on the metal surface, when the seeding was performed as described in Appendix 1. In order to increase this amount, the extension of the seeding stage would be justified. With more prescale on the disk, the adhesion process could be more repeatable.

4.2.2 Dynamic tube blocking results

The dynamic tube blocking (DTB) tests were all performed at pH 9.2, at the pressure of 200 psig and the temperature of 50 °C. The other variables were adjusted in order to receive test conditions in which the scaling would occur at appropriate rate and so that the precipitation occurs as scale growth on the surfaces of the scaling coil rather than in the liquid phase. These variables included the concentration of NaCl, the concentrations of calcium and carbonate and the flow rates of the solutions. A prescale step was chosen to be included in all tests.

The calcium concentration was set to 80 ppm, carbonate concentration to 1500 ppm and NaCl concentration to 0.5 M. The prescale step was set to end at Δp=2.2 psi, 0.5 psi above the initial pressure difference and the cleaning step was set to start at Δp=5 psi. The flow rate was 3 ml/min per pump. First, a test was run with 5 minute steps and then

the *MIC* value was confirmed with another run of fewer 10 minute steps. In the second run the first step was only 5 minutes with a rather high inhibitor dosage so that the prescaling would certainly stop. Nine different antiscalants were tested this way. The *MIC* values of these tests are listed in *Table 4.13*.

Table 4.13. MIC values of different antiscalants in the DTB tests at 50 °C and pH 9.2. 80 ppm Ca^{2+}, 1500 ppm CO_3^{2-}, and 0.5 M NaCl was used.

Antiscalant	***MIC***
Copolymer 1	15 ppm
Copolymer 3	30 ppm
Copolymer 5	> 100 ppm
Polyaspartate 3	> 100 ppm
Phosphonate 1	3 ppm
Polyacrylate	10 ppm
Polymaleate	7.5 ppm
Terpolymer 1	15 ppm
Terpolymer 2	15 ppm

The graphs of the Phosphonate 1, Copolymer 5, Polyacrylate, and Polyaspartate 3 are plotted in *Figure 4.10*. The graphs of all the test runs can be found in Appendix 3.

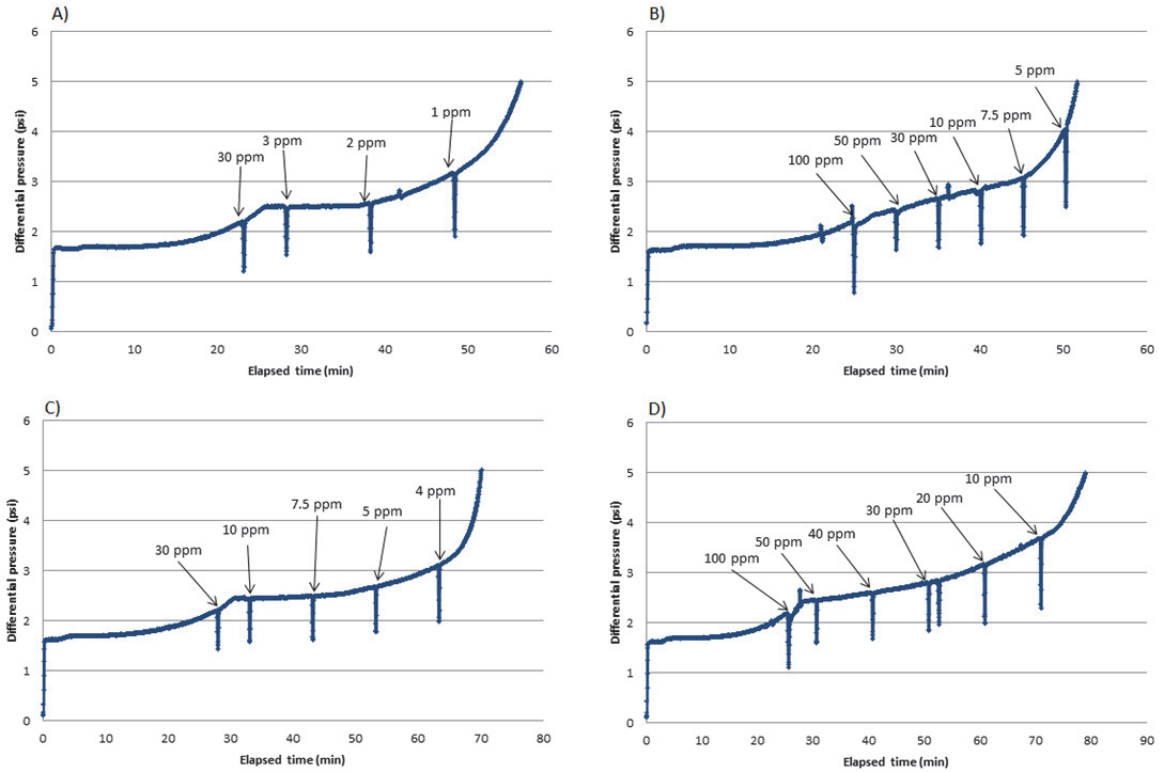

Figure 4.10. Result graphs of selected antiscalants in the DTB test run at 50 °C. A) Phosphonate 1, B) Copolymer 5, C) Polyacrylate, D) Polyaspartate 3

The ATMP antiscalant Phosphonate 1(*Figure 4.10A*) was superior to other antiscalants in the DTB run in the conditions used. This was expected as it was superior also in the static jar tests with similar conditions and as the antiscalants with good threshold inhibi-

tion properties, like phosphonates, are supposed to perform well in the once through systems with short residence times. The Polymaleate is the best of the polymer antiscalants which is likely due to the low molecular weight of this product. The effect of the molecular weight can also be seen in the results of Copolymer 1, Copolymer 3, and Copolymer 5, which all are MA/AA copolymers with the molecular weights of 1600, 3050 and 50000 Da, respectively. These findings are in consistency with the conclusions of Loy et al. [32] that the smaller polymer components diffuse and adsorb faster than larger ones. The favoring of the threshold inhibition properties over the crystal modification and dispersing properties of this method can be best seen from the results of the Copolymer 5 (*Figure 4.10B*). With the high molecular weight, it did not manage to stop the scaling in the DTB run even with the highest dosage and had the worst performance in this test whereas in the static test with long residence time (see *Figure 4.1*) it was much better as the crystal modification and dispersing properties could retard the precipitation process over a longer time period.

An interesting result is that the Polyacrylate (*Figure 4.10C*) which performed poorly in all of the static tests (apart from the test of *Table 4.9* with low ionic strength) is the second best polymer antiscalant in this test. This can be due to good threshold inhibition properties of the product or the lowering of the NaCl concentration form 1 M to 0.5 M. As has been discussed before, the ionic strength seems to have great influence on the pure polyacrylate and the halving of the NaCl concentration could critically ease its performance. It is also notable that the pure polymaleate and polyacrylate performed better in this test than all of the copolymers and terpolymers. In the case of Polymaleate, this is likely due to the lower molecular weight and in the case of Polyacrylate the lowered ionic strength could be the main explanation.

The Polyaspartate 3 (*Figure 4.10D*) had a poor performance also in this test but the result graph confirms the earlier speculations that it has some inhibition properties even though it could not be seen in the results of static tests (apart from the test of *Table 4.9*) and the rotating disk method. Although the Polyaspartate 3 could not stop the scaling in the DTB run even with the highest dosage the retardation of the scaling can be clearly seen.

4.3 Results of the computational methods

The computational model WatSIM from French Creek was utilized to estimate the scaling potential of selected test conditions from the static tests. The aim of these calculations was to understand the effect of different variables on the scaling potential and to learn what additional information can be achieved with the modeling software.

The scaling potential indices of calcium carbonate at the static test solutions of pH 9.2 and 10.7 with the carbonate concentration of 3000 ppm as CO_3^{2-} were calculated. The calculations were performed for the temperatures 50 °C, 75 °C, and 95 °C and for the calcium levels of 40 ppm, 80 ppm, and 160 ppm. Other input values for the calculations were the sodium ion concentration as parts per million, chloride ion concentration

as parts per million and the M and P alkalinities as $CaCO_3$ (mg/l). The Na^+ and Cl^- concentrations were calculated using the 1 M concentration of NaCl in the static tests. Also the Na^+ from the sodium carbonate and sodium bicarbonate solutions and the Cl^- from the calcium chloride solution were taken into account. The alkalinities were determined with titration as described in *Chapter 3.4*.

The alkalinity titration for the sample of pH 9.2 yielded two end points. At the first end point, which is the P end point, the consumption of the acid, V_{Acid}, was 2.1155 ml. For the second end point, which is the M endpoint V_{Acid} = 7.2218 ml. For the sample of pH 10.7, also two end points appeared. The V_{Acid} values for the P and M end points were 4.5975 ml and 9.6661 ml, respectively. The alkalinity values are calculated with equation 43. For the pH 9.2 sample,

$$P\ (\text{mg/l}\ as\ CaCO_3) = \frac{0.1\ \text{eq/l} \times 2.1155\ \text{ml}}{10\ \text{ml}} \times 50000\ \text{mg/eq} = 1057.75\ \text{mg/l}$$
$$M\ (\text{mg/l}\ as\ CaCO_3) = \frac{0.1\ \text{eq/l} \times 7.2218\ \text{ml}}{10\ \text{ml}} \times 50000\ \text{mg/eq} = 3610.9\ \text{mg/l}$$

and for the pH 10.7 sample,

$$P\ (\text{mg/l}\ as\ CaCO_3) = \frac{0.1\ \text{eq/l} \times 4.5975\ \text{ml}}{10\ \text{ml}} \times 50000\ \text{mg/eq} = 2298.75\ \text{mg/l}$$
$$M\ (\text{mg/l}\ as\ CaCO_3) = \frac{0.1\ \text{eq/l} \times 9.6661\ \text{ml}}{10\ \text{ml}} \times 50000\ \text{mg/eq} = 4833.05\ \text{mg/l}.$$

It should be noted that the titrations were performed at room temperature although the calculations with WatSIM were performed at higher temperatures. This might cause a minor error in the results of the saturation level calculations but the effect of temperature on the alkalinity values is assumed to be insignificant as the effect of pH plays a major role.

The validity of the titration results can be checked with the relations of *Table 3.4*. In both cases P < ½M, therefore the carbonate alkalinity is 2P and the bicarbonate alkalinity M-2P. For the sample of pH 9.2

$$c(CO_3^{2-}) = 2 \times 1057.75\ \text{mg/l as}\ CaCO_3 = 2115.5\ \text{mg/l as}\ CaCO_3$$
$$c(HCO_3^-) = 3610.9 - 2115.5\ \text{mg/l as}\ CaCO_3 = 1495.4\ \text{mg/l as}\ CaCO_3.$$

The conversion of the carbonate alkalinity can be made with equation 44,

$$c(CO_3^{2-}) = 0.6 \times 2115.5\ \text{mg/l as}\ CO_3^{2-} = 1269.3\ \text{mg/l as}\ CO_3^{2-}$$

The conversion of the bicarbonate alkalinity can be made with equation 45

$c(HCO_3^-) = 1.22 \times 1495.4 \text{ mg/l as } HCO_3^- = 1824.39 \text{ mg/l as } HCO_3^-$.

The bicarbonate concentration can be further converted to carbonate concentration by using the molecular weights of carbonate and bicarbonate ions.

$$c(HCO_3^-) = 1824.39 \times \frac{60 \text{ g/mol}}{61 \text{ g/mol}} = 1794.48 \text{ mg/l as } CO_3^{2-}$$

The sum of the carbonate and bicarbonate alkalinities yields now $1269.3 + 1794.48 = 3063.8$ mg/l as CO_3^{2-}, which is quite close to the supposed value of 3000 mg/l as CO_3^{2-}. The same calculation was performed for the sample of pH 10.7 and yielded $2758.5 + 282.66 = 3041.2$ mg/l as CO_3^{2-} for the total concentration of carbonate ions.

The input values used in the saturation level calculations are summed up in *Table 4.14*.

Table 4.14. The input values used in the WatSIM for the saturation level calculations.

pH	T (°C)	Ca^{2+} (ppm)	P alkalinity (mg/l as $CaCO_3$)	M alkalinity (mg/l as $CaCO_3$)	Na^+ (ppm)	Cl^- (ppm)
9.2	50	40	1058	3611	24600	35600
		80				
		160				
	75	40				
		80				
		160				
	95	40				
		80				
		160				
10.7	50	40	2298	4833	24600	35600
		80				
		160				
	75	40				
		80				
		160				
	95	40				
		80				
		160				

In the actual static jar tests, the sodium ion concentration actually changes a bit when the pH is adjusted from 9.2 to 10.7 but the change is so minor that the sodium ion concentration value was not changed between the calculations. Also the chloride ion concentration changes a bit when the calcium concentration is changes but again the change is regarded as insignificant.

The results for the calculations of the selected scaling potential indices are presented in *Table 4.15*. The data of the input values and all the scaling potential indices and other values that WatSIM calculates are available for the conditions of pH 9.2 and calcium concentration of 80 ppm with all three temperatures in Appendix 4.

Table 4.15. Calculated values of selected scaling potential indices with the initial values of Table 4.14.

pH	T (°C)	Ca^{2+} (ppm)	Saturation level (Calcite)	Langelier saturation index	Momentary Excess (Calcite, ppm)
9.2	50	40	30.41	2.67	72.57
		80	60.50	2.98	146.44
		160	119.81	3.28	241.37
	75	40	20.78	2.92	74.03
		80	41.37	3.22	119.93
		160	82.08	3.52	127.56
	95	40	14.01	3.08	59.53
		80	27.91	3.38	71.67
		160	55.47	3.68	74.07
10.7	50	40	38.11	4.32	71.18
		80	75.91	4.62	144.02
		160	150.58	4.92	281.47
	75	40	21.67	4.62	69.46
		80	43.22	4.92	128.23
		160	85.97	5.22	146.33
	95	40	11.62	4.91	51.62
		80	23.21	5.21	76.08
		160	46.26	5.51	81.77

The results for the saturation level calculation are quite unexpected. The increase in the calcium level or the pH value increases the saturation level as it should, but the increase in the temperature decreases the saturation level, which is opposite to what is expected. The Langelier saturation index (*LSI*) results are increasing logically with the increasing pH, calcium level and temperature. Nevertheless, as was discussed in *Chapter 2.5.1* the ion association is not taken into account in the Langelier saturation index and the values calculated in this case might be systematically too large. However, the increase of the *LSI* from 2.67 at the lowest temperature, pH and calcium level to 5.51 at the highest temperature, pH and calcium level gives a more realistic picture from the relative scaling potential of the aqueous solutions than the corresponding increase in the saturation level from 30.41 to 46.26. The Momentary Excess values seem to correspond quite closely with the saturation level values.

The illogical behavior of the saturation level with increasing temperature might be brought on by the lack of data for the equilibrium constants at these temperatures. This

is unlikely as this kind of data is easily available. Also the relatively high pH or the high TDS value could be out of range of the model used in the software, as it is designed to be used in municipal applications which rarely have high TDS values or high pH that are present in the pulp and paper applications. However, it is not possible to verify these presumptions as the details of the model are unknown. The data of Appendix 4 shows that with increasing temperature the calculations yield smaller value for the free carbonate ions. The reason for this is hard to explain without knowing the species in which the carbonate is bound according to the calculations of WatSIM. The amount of free calcium ions seems reasonable. Although the *LSI* values of these calculations seem the most logical, the problem of using this index arises when also the sodium chloride concentration is altered. The *LSI* value remains the same with altering total ionic strength though the activities of calcium and carbonate ions are obviously affected by the ionic strength.

5. CONCLUSIONS

The formation of the calcium carbonate scale is a common problem in many industrial processes using large quantities of water and it can be solved or eased with the use of antiscalants. The scaling problems in the pulp and paper mills are often more difficult to solve than in many other industries, where scaling is encountered. The reason for this is the alkaline conditions of the pulp mill combined with high temperature and high amount of dissolved and suspended solids, which disable the function of many antiscalants that function well in other applications. In order to determine the performance of different antiscalants in the conditions of pulp and paper mills, adequate laboratory testing methods have to be established.

In order to determine the performance of a scale inhibitor as accurately as possible it is important to test the product with both static and dynamic laboratory tests with varying test conditions. It is also important that the tests are quite easy and quick to perform yet giving enough information to conclude the performance of the antiscalant. Additional information or evaluation of laboratory test results can be achieved with computational models. In this thesis one static method and two dynamic methods were used. The static method was a quite simple static jar test and the dynamic methods were a rotating disk procedure and a dynamic tube blocking procedure. The utilized computational model was French Creek's WatSIM.

The static jar test proved to be a reliable and repeatable method for the evaluation of the performances of different antiscalants. In the method the concentration of the unprecipitated calcium, the amount of the precipitated calcium carbonate in the liquid phase, and the amount of the precipitated calcium adhered on the surface of the jar are measured. The error limit of the method was estimated to be ±9 %. In addition to the reliable results, the advantage of the method is that several test parameters are easily adjustable. These parameters include the temperature, pH, supersaturation ratio, and reaction period. The disadvantage of the method is that the static conditions which represent homogeneous nucleation are far away from the real test conditions of the unit operations of pulp and paper mills.

The results of the dynamic rotating disc procedure seemed to give information about the performance of different antiscalants in the dynamic conditions. In this procedure the static jar test is basically transferred to dynamic conditions by an addition of a rotating stainless steel disk. The advantages of this method in comparison with the static jar test were the addition of the dynamic conditions, a seeding stage and a metal surface. The seeding stage and the metal surface simulate the heterogeneous nucleation. These additions bring the test closer to a real application, where the system is rarely static or

completely clean. In addition, the advantage of the rotating disk procedure was that the precipitation process could be accelerated and the results from 1.5 h rotating disk tests were in consistency with 48 h static tests. However, there were problems with the repeatability of the test results when parallel stirrers were used. The results for the blanks without an inhibitor differed quite much when different disks and stirrers were used. Also the efficiency of the seeding stage could be better if the seeding stage was extended. Before the rotating disk procedure can be utilized in a large scale product testing, the problems of the method have to be solved.

The dynamic tube blocking procedure enables the testing of the antiscalants in high pressure and temperature dynamic conditions. In this method, a calcium solution and a carbonate solution flow through a narrow scaling coil which is blocked when scaling occurs. The level of blockage is quantified by measuring the pressure difference over the scaling coil. The method proved to give additional information about the threshold inhibition properties of the antiscalants at the temperature of 50 °C. At higher temperatures, the adjustment of the process parameters such way that the blockage of the scaling coil would be controlled turned out to be challenging and could not be completed in the scope of this study.

With the computational model WatSIM, various scaling potential indices can be calculated. These include among others the Langelier saturation index and Saturation Level. When analyzing the calculation results of the software for the typical high TDS, high carbonate level and alkaline conditions of paper making, it became evident that the model is not suitable for the use in these conditions. The calculated Saturation Level values decreased with increasing temperature, which was opposite to what was expected. The calculated LSI values were logical but did not include the effect of the high TDS content on the activities of calcium and carbonate ions.

The functionality of different commercially available antiscaling chemistries and some new experimental products in the alkaline and high TDS conditions of paper making were evaluated with the static jar test, rotating disk procedure, and dynamic tube blocking procedure. The results of these tests confirmed the presumption made in *Chapter 2.3.1* that phosphonates are better threshold inhibitors whereas the dispersing properties of polycarboxylates are better. As long as the nucleation does not occur the phosphonates can inhibit the precipitation completely but when the nucleation occurs the failure is fast as the crystal modification and dispersing properties are poor. A good polycarboxylate antiscalant cannot inhibit the nucleation as well as phosphonates but can slow down the crystal growth process much better.

The differences between different polycarboxylate antiscalants were drastic. The best performing polycarboxylates were a pure polymaleate antiscalant referred to as Polymaleate and a new experimental maleate/acrylate/non-ionic terpolymer referred to as Terpolymer 2. The pure polyacrylate antiscalant referred to as Polyacrylate showed very little inhibition in all of the static tests of this thesis but had rather good threshold inhibition properties in the dynamic tube blocking test. It has also performed well in the some earlier tests with low TDS content, which indicates that the high TDS content dis-

ables the function of a pure polyacrylate. The behavior of the polyaspartic acid antiscalant referred to as Polyaspartate 3 had similar behavior with Polyacrylate in different tests but it had poorer threshold inhibition properties in the dynamic tube blocking procedure. Also the molecular weight of the polycarboxylate antiscalants played a major role in its performance. A low molecular weight seems to promote the threshold inhibition properties and high molecular weight the dispersing properties.

There is no single answer for what is the best antiscalant in the applications of paper making but the results gained with the methods of this study show that the advantages and disadvantages of different antiscalants can be distinguished with these methods. It seems that maleate/acrylate/non-ionic terpolymer type of antiscalants have the best tolerance for the changes in the test conditions which indicates that they would be a good choice for example for the digester scale inhibition where the complete inhibition of the scale is unlikely. In order to link the laboratory test results to real applications, experience from the performance of the antiscalants in the pilot and mill scale trials has to be gained.

In order to answer the few questions which arose from the test results of this thesis, further study should be made. The further study should consider how critical the TDS value is to the performance of the antiscalants and how the morphology of the precipitation is affected by different test parameters and antiscalants. Also the thermal stability of the antiscalants and the effect of impurities such as iron and aluminum ions on the performance of the antiscalants are worth studying.

The main objective of the study was to establish adequate laboratory testing methods for Kemira's Fiber and Biorefinery Chemistry laboratory. Other objectives included the improvement of their overall knowledge about the scaling phenomenon of the calcium carbonate and the gathering of information about the performance of different antiscalants in the conditions of paper making. The objectives of the study were reached and the overall success of the work was good although some of the topics require further study.

REFERENCES

1. Ketrane, R., Saidani, B., Gil, O., Leleyter, L., Baraud, F. Efficiency of five scale inhibitors on calcium carbonate precipitation from hard water: Effect of temperature and concentration. Desalination 249(2009), pp. 1397–1404.
2. Martinod, A., Euvrard, M., Foissy, A., Neville, A. Progressing the understanding of chemical inhibition of mineral scale by green inhibitors. Desalination 220(2008), pp. 345–352.
3. Rieger, J., Thieme, J., Schmidt, C. Study of Precipitation Reactions by X-ray Microscopy: $CaCO_3$ Precipitation and the Effect of Polycarboxylates. Langmuir 16(2000)22, pp. 8300–8305.
4. Koutsoukos, P.G., Aikaterini, N.K., Kanellopoulou, D.G. Solubility of salts in water: Key issues for crystal growth and dissolution processes. Pure and Applied Chemistry 79(2007)5, pp. 825–850.
5. Sitholé, B. Scale deposit problems in pulp and paper mills. African Pulp and Paper Week, Durban, South Africa, October 8–11 2002. Available at: http://www.tappsa.co.za/archive/APPW2002/Title/Scale_deposit_problems/scale_deposit_problems.html.
6. Clément, S., Gouiller, A., Ottenio, P., Nivelon, S., Huber, P., Nortier, P. Speciation and supersaturation model in papermaking streams. Process Safety and Environmental Protection 89(2011)1, pp. 67–73.
7. NACE TM0374-2007. Laboratory Screening Test to Determine the Ability of Scale Inhibitors to Prevent the Precipitation of Calcium Sulfate and Calcium Carbonate from Solutions (for Oil and Gas production Systems). 2007. National Association of Corrosion Engineers. 8 p.
8. Hui, F., Lédion, J. Evaluation methods for the scaling power of water. Journal European of Water Quality 33(2002)1, pp. 55–74.
9. Ferguson, R.J. Developing Scale Inhibitor Dosage Models. French Creek Software Online Library [WWW]. [Cited 8/11/2011]. Available at: http://www.frenchcreeksoftware.com/online-library/Developing-Scale-Inhibitor-Dosage-Models.
10. Brečević, L., Kralj, D. On Calcium Carbonates: from Fundamental Research to Application. Croatica Chemica Acta 80(2007)3–4, pp. 467–484.

11. Patent EP1392609. Method for inhibiting calcium salt scale. Dequest AG, Zug. (Thompson, J.O., Verrett, S.P., Severtson, S.J., LOY, J.E.). Appl. No 02739705.8, 5.6.2002. (24.11.2010). 62 p.

12. Engel, T., Reid, P. Physical Chemistry. San Francisco, USA 2006. Pearson Benjamin Cummings. 1061 p.

13. Mullin, J.W. Crystallization. 4th edition. Woburn, USA 2001. Reed Educational and Professional Publishing Ltd. 594 p.

14. Melia, T.P., Moffitt, W.P. Secondary nucleation from aqueous solution. Industrial & Engineering Chemistry Fundamentals 3(1964)4, pp. 313–317.

15. Myerson, A.S. Handbook of industrial crystallization. 2nd edition. Boston, USA 2002. Butterworth-Heinemann. 313 p.

16. Crystallization. The Free Dictionary by Farlex [WWW]. [Cited 9/11/2011]. Available at: http://encyclopedia2.thefreedictionary.com/crystallization.

17. Nehrke, G. Calcite Precipitation from Aqueous Solution: Transformation from Vaterite and Role of Solution Stoichiometry. Dissertation. Utrecht 2007. Utrecht University. Geologica Ultraiectina 273(2007), 144 p.

18. Dalas, E., Koutsoukos, P.G. Calcium Carbonate Scale Formation on Heated Metal Surfaces. Geothermics 18(1989)1–2, pp. 83–88.

19. MacAdam, J., Parsons, S.A. The Effect of Metal Ions on Calcium Carbonate Precipitation and Scale Formation. Sustainability in Energy and Buildings 2009, Part 3, pp. 137–146.

20. Beck, R., Andreassen, J-P. The onset of spherulitic growth in crystallization of calcium carbonate. Journal of Crystal Growth 312(2010)15, pp. 2226–2238.

21. Brečević, L., Nielsen, A.E. Solubility of amorphous calcium carbonate. Journal of Crystal Growth 98(1989)3, pp. 504–510.

22. Bischoff, J.L., Fitzpatrick, J.A., Rosenbauer, R.J. The solubility and stabilization of ikaite (CaCO3•6H2O) from 0°C to 25°C: Environmental and paleoclimatic implications for thinolite tufa. The Journal of Geology 101(1993)1, pp. 21–33.

23. Kralj, D., Brečević, L. Dissolution kinetics and solubility of calcium carbonate monohydrate. Colloids and Surfaces A: Physicochemical and Engineering Aspects 96(1995)3, pp. 287–293.

24. Plummer, L.N., Busenberg, E. The solubilities of calcite, aragonite and vaterite in CO_2-H_2O solutions between 0 and 90°C, and an evaluation of the aqueous model for the system $CaCO_3$-CO_2-H_2O. Geochimica et Cosmochimica Acta 46(1982)6, PP. 1011–1040.

25. Wojtowicz, J.A. Calcium Carbonate Precipitation Potential. Journal of the Swimming Pool and Spa Industry 2(2001)2, pp. 23–29.

26. Macdonald, R.W., North, N.A. The Effect of Pressure on the Solubility of $CaCO_3$, CaF_2, and $SrSO_4$ in Water. Canadian Journal of Chemistry 52(1974)18, pp. 3181–3186.

27. Duan, Z., Li, D. Coupled phase and aqueous species equilibrium of the H_2O-CO_2-NaCl-$CaCO_3$ system from 0 to 250°C, 1 to 1000bar with NaCl concentrations up to saturation of halite. Geochimica et Cosmochimica Acta 72(2008)20, pp. 5128–5145.

28. Kralj, D., Kontrec, J., Brečević, L., Falini, G., Nöthig-Laslo, V. Effect of Inorganic Anions on the Morphology and Structure of Magnesium Calcite. Chemistry 10(2004)7, pp. 1647–1656.

29. Tai, C.Y., Chen, P.C. Nucleation, Agglomeration and Crystal Morphology of Calcium Carbonate. AIChE Journal 41(1995)1, pp. 68–77.

30. Ferguson, R.J., Ferguson, B.R., Stancavage, R.F. Modeling Scale Formation and Optimizing Scale Inhibitor Dosages in Membrane Systems. AWWA Membrane Technology Conference, March 30 2011, Long Beach, CA, USA. Available at: http://www.frenchcreeksoftware.com/AWWA-2011/Modeling_Scale_Formation_and_Optimizing_Scale_Inhibitor_Dosages_in_Membrane_Systems.pdf.

31. Guo, J., Severtson, S.J. Inhibition of Calcium Carbonate Nucleation with Aminophosphonates at High Temperature, pH and Ionic Strength. Industrial & Engineering Chemistry Research 43(2004)17, pp. 5411–5417.

32. Loy, J.E., Guo, J., Severtson, S.J. Role of Adsorption Fractionation in Determining the $CaCO_3$ Scale Inhibition Performance of Polydisperse Sodium Polyacrylate. Industrial & Engineering Chemistry Research 43(2004)8, pp. 1882–1887.

33. Handbook of Industrial Water Treatment, Chapter 25 [WWW]. [Cited 11/9/2011]. Available at: http://www.gewater.com/handbook/index.jsp.

34. Zhang, G., Ge, J., Sun, M., Pan, B., Mao, T., Song, Z. Investigation of scale inhibition mechanisms based on the effect of scale inhibitor on calcium carbonate crystal forms. Science in China Series B: Chemistry 50(2007)1, pp. 114–120.

35. ChemBlink online database [WWW]. [Cited 11/10/2011]. Available at: http://www.chemblink.com.

36. Verschueren, K. Handbook of Environmental Data on Organic Chemicals, Volume 1. 5th edition. Hoboken, USA 2009. John Wiley & Sons. Available at: http://www.knovel.com/web/portal/browse/display?_EXT_KNOVEL_DISPLAY_bookid=2437&VerticalID=0.

37. Joentgen, W., Müller, N., Mitschker, A., Schmidt, H. Polyaspartic Acids. In: Steinbüchel, A. (ed.). Biopolymers. Vol. 7, 2003, Weinheim, Germany, Wiley-VCH. pp. 171-181.

38. Patent US5866012. Multifunctional maleate polymers. National Starch and Chemical Investment Holding Corporation, Wilmington, Delaware, USA. (Austin, A-M.B., Belcher, J.H., Carrier, A.M., Standish, M.L.). Appl. No. 885541, 30.6.1997. (2.2.1999). 13 p.

39. Chemland product list [WWW]. [Cited 11/10/2011]. Available at: http://clpolymers.com/product.htm.

40. Amjad, Z., Zuhl, R.W. Effect of heat treatment on the performance of deposit control polymers as calcium carbonate inhibitors. Corrosion 2007, Nashville, Tennesee, USA, March 11–15 2007. NACE International.

41. Erickson, D.L. Evaluating polymers and phosphonates for use as inhibitors for calcium, phosphate and iron in steam boilers. AWT Conference 2002. Available at: http://www.uswaterservices.com/downloads/AWT%20Conference%202002.pdf.

42. Abdel-Aal, N., Sawada, K. Inhibition of adhesion and precipitation of $CaCO_3$ by aminopolyphosphonate. Journal of Crystal Growth 256(2003)1–2, pp. 188–200.

43. Hardness, Calcium titration using EDTA, Method 8204, Hach Water Analysis Handbook [WWW]. [Cited 11/10/2011]. Available at: http://www.hach.com/wah.

44. Chen, T., Neville, A., Yuan, M. Calcium carbonate scale formation – assessing the initial stages of precipitation and deposition. Journal of Petroleum Science and Engineering 46(2005)3, pp. 185–194.

45. Ma, Y.F., Gao, Y.H., Feng, Q.L. Effects of pH and temperature on $CaCO_3$ crystallization in aqueous solution with water soluble matrix of pearls. Journal of Crystal Growth 312(2010)21, pp. 3165–3170.

46. PMAC Automated Scale Rig Instruction Manual. Process Measurement and Control Systems Limited, Scotland.

47. WaterCycle User Manual. French Creek Software Online Library [WWW]. [Cited 11/8/2011]. Available at: http://www.frenchcreeksoftware.com/Manuals/WaterCycle-Rx-User-Manual.pdf.

48. Lowenthal, R.E., Marais, G.V.R. Carbonate chemistry of aquatic systems. USA 1976. Ann Arbor Science Publishers, INC. 432 p.

49. Ferguson, R.J. A Kinetic model for calcium carbonate deposition. Materials Performance 23(1984)11, pp. 25–34.

50. Truesdell, A. H., Jones, B.F. WATEQ, A Computer Program for Calculating Chemical Equilibria of Natural Waters. U.S. Geological Survey, 1973. National Technical Information Service PB-220 464, 77 p.

51. Patent EP0517453. Controlling scale in black liquor evaporators. Calgon Corporation, Pittsburgh, Pennsylvania, USA. (Gill, J.S.). Appl. No. 92304951.4, 29.5.1992. (13.12.1995). 21 p.

52. Evans, B., Wright, R., Haskins, W., Laakso, A-P. Filling SC Papers with PCC; A Holistic Approach. Pira Conference, Fillers and Pigments for Papermakers, November 9–10, 2005, Atlanta, GA, USA. Available at: http://www.specialtyminerals.com/publications/paper-filling-smi-publications.

53. Grist S. R., Canty R. J. Carbon dioxide in pulp/paper mill stocks: fix or fizz? 60th Appita Annual Conference and Exhibition, April 3–5, 2006, Melbourne, Australia. Available at: http://www.coveyconsulting.com.au/Documents/paper_sg_rc_co2_in_pulp-paper_mill_stocks.pdf.

54. Norweco, Alkalinity titration method [WWW]. [Cited 11/10/2011]. Available at: http://www.norweco.com/html/lab/test_methods/2320bfp.htm.

55. California Department of Public Health. Alkalinity Conversions [WWW]. [Cited 11/10/2011]. Available at: http://www.cdph.ca.gov/certlic/drinkingwater/Documents/Drinkingwaterlabs/AlkalinityConversions.pdf.

56. Hostomsky, J., Jones, A.G. Calcium carbonate crystallization, agglomeration and form during continuous precipitation from solution. Journal of Physics D: Applied Physics 24(1991)2, pp. 165–170.

APPENDIX 1: ROTATING DISK PROCEDURE

Steps:

1. Make sure disks are clean from the end of the last run. Cleaning step detailed below.

2. Pre-scale (seeding) step:
    a. Add 25 ml anionic solution to clear **polystyrene** cup. (Anionic solution = 6000 ppm carbonate and 2 M NaCl containing solution)
    b. Immerse disk (to about the bottom of the vortex formed) and start stirrer at 250 RPM.
    c. Add 25 mL $CaCl_2$ (160 ppm as Ca^{2+}) to separate cup. Pour this into cup that is spinning with anionic solution.
        i. Avoid getting solution onto shaft
        ii. Ensure that no bubbles are trapped on bottom of disk
    d. Raise disk immediately after the $CaCl_2$ addition.
    e. Let the disk spin at high speed (e.g. 2000 rpm) until dry in appearance.
    f. While spinning, rinse with distilled water (top and bottom of disk).
    g. After distilled water, rinse with acetone (top and bottom of disk).
    h. Allow to stand for 5 minutes.

3. Scale step:
    a. Add 75 mL anionic solution to clear **polystyrene** cup.
    b. Add inhibitor as desired.
    c. Immerse disk (about 2 cm above bottom of cup) and start stirrer at 250 RPM.
        i. Do not allow disk to touch the cup walls
        ii. Ensure no bubbles are present on the bottom of the disk.
    d. Add 75 mL $CaCl_2$ (160 ppm as Ca^{2+}) to separate cup. Pour this into cup that is spinning with anionic solution
        i. Avoid getting solution onto shaft
        ii. Ensure no bubbles are present on the bottom of the disk
    e. Spin at 250 RPM for 90 minutes
    f. Disk should be positioned so that vortex does not touch surface (near the 110 mL graduation level in cup.)
    g. Raise disk and spin at high speed until dry in appearance**. Save these cups for analysis**. These contain what we call “filtrate” and “membrane” samples.
    h. Rinse disk (top and bottom) with distilled water.

i. While spinning rapidly, rinse with acetone.
j. Allow to dry.

4. Dissolution Step
    a. Pour 100 mL of 7% HNO_3 into the same cup in which the scale step was performed and swirl to dissolve the scale from the surfaces of the cup
    b. Immerse disk in the same cup and rotate at 250 RPM for 15 minutes.
        i. Ensure that no bubbles are present on bottom of the disk
    c. Raise disk out of solution and spin rapidly to remove excess liquid.
    d. **Save these cups for analysis**. These cups contain the “adherent” sample.

5. Cleaning step:
    a. Rinse disk (top and bottom) with distilled water
    b. Rinse with acetone at high spinning speed and allow drying.

APPENDIX 2: SCREENING TEST RESULTS

Test was performed with inhibitor dosage of 18 ppm as solids at 50 °C and pH 9.2. The test period was 48 h, calcium level 80 ppm, carbonate level 3000 ppm and NaCl concentration 1 M.

Sample	Filtrate (ppm as Ca2+)	Membrane (ppm as Ca2+)	Adherent (ppm as Ca2+)	Total (ppm as Ca2+)
Blank	7.8	31.0	57.0	95.8
	4.6	23.4	51.7	79.7
	1.5	21.8	49.8	73.1
	6.2	34.2	39.6	79.9
Control	85.5			85.5
	78.2			78.2
	81.1			81.1
	82.2			82.2
	85.0			85.0
Copolymer 1	56.0	3.6	25.4	85.0
Copolymer 2	59.0	3.4	23.6	86.0
Copolymer 3	62.0	4.2	18.7	84.9
Copolymer 4	67.5	2.1	16.3	85.8
	72.0	2.6	13.8	88.4
Copolymer 5	41.7	6.9	37.4	86.0
Copolymer 6	6.0	44.1	24.6	74.7
Polyaspartate 1	6.6	9.8	65.8	82.2
Polyaspartate 2	5.5	12.3	66.5	84.3
Polyaspartate 3	4.3	71.0	11.9	87.2
	4.5	24.8	49.6	78.9
	5.8	23.4	43.3	72.5
Phosphonate 1	88.5	2.3	0.3	91.1
	78.7	1.4	0.2	80.2
Phosphonate 2	84.0	10.7	0.3	95.0
Phosphonate 3	7.5	36.3	42.6	86.4
Polyacrylate	5.0	1.4	72.4	78.8
	5.6	1.6	67.2	74.4
Polymaleate	55.5	0.9	19.0	75.4
	56.5	0.7	20.4	77.7
Terpolymer 1	64.3	4.3	11.5	80.0
Terpolymer 2	67.8	4.2	15.2	87.1
	57.4	3.0	15.4	75.8
Terpolymer 3	61.5	5.6	16.8	83.9
Terpolymer 4	61.0	4.1	17.8	82.9
Terpolymer 5	59.5	2.5	21.1	83.0
Terpolymer 6	6.0	66.8	3.5	76.2

APPENDIX 3: DTB RESULTS AT 50 °C

Phosphonate 1

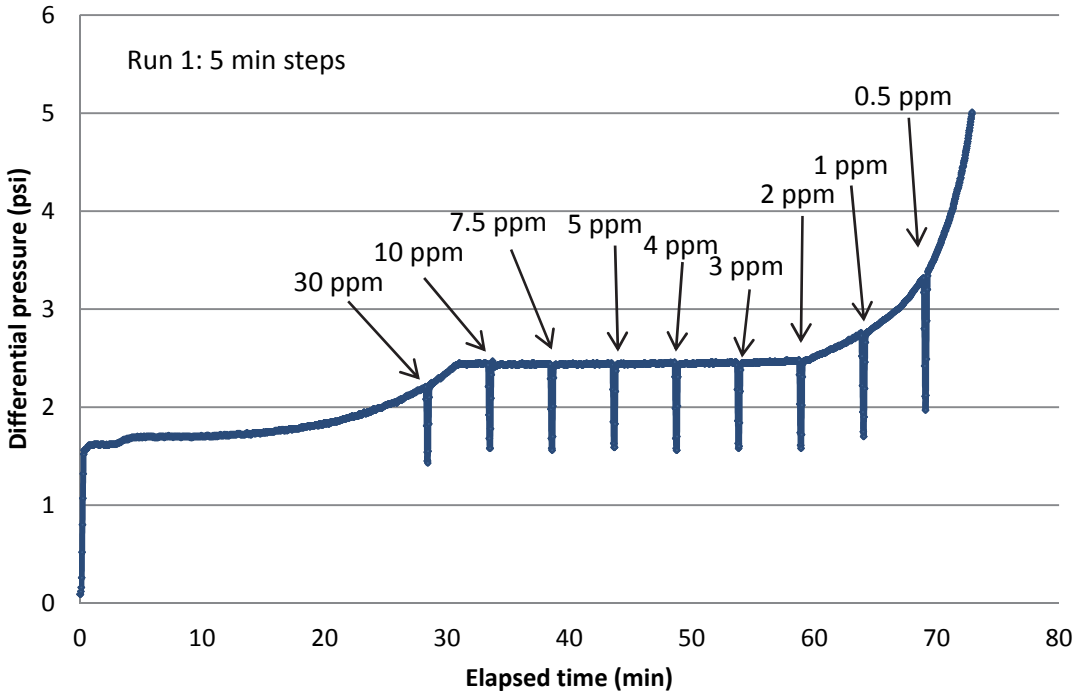

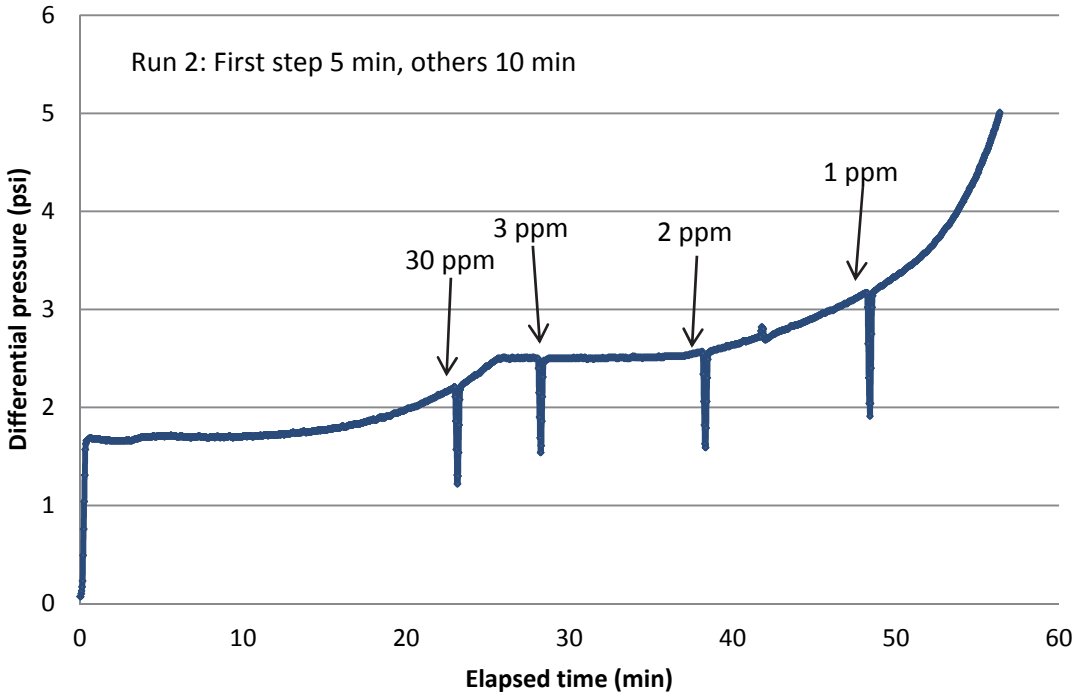

Polymaleate

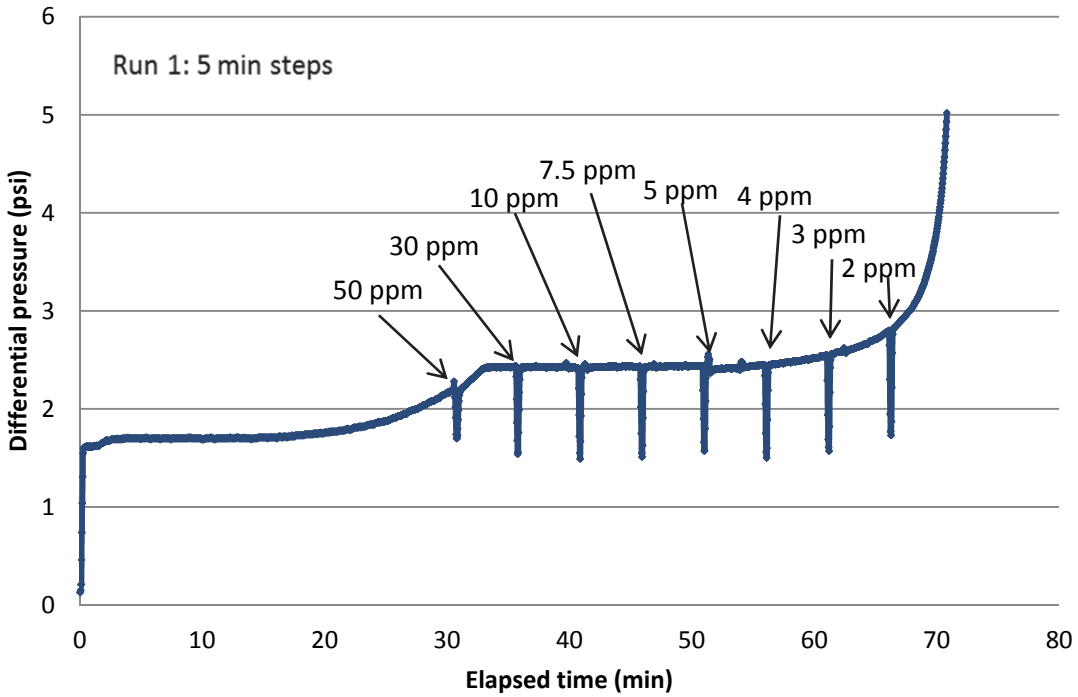

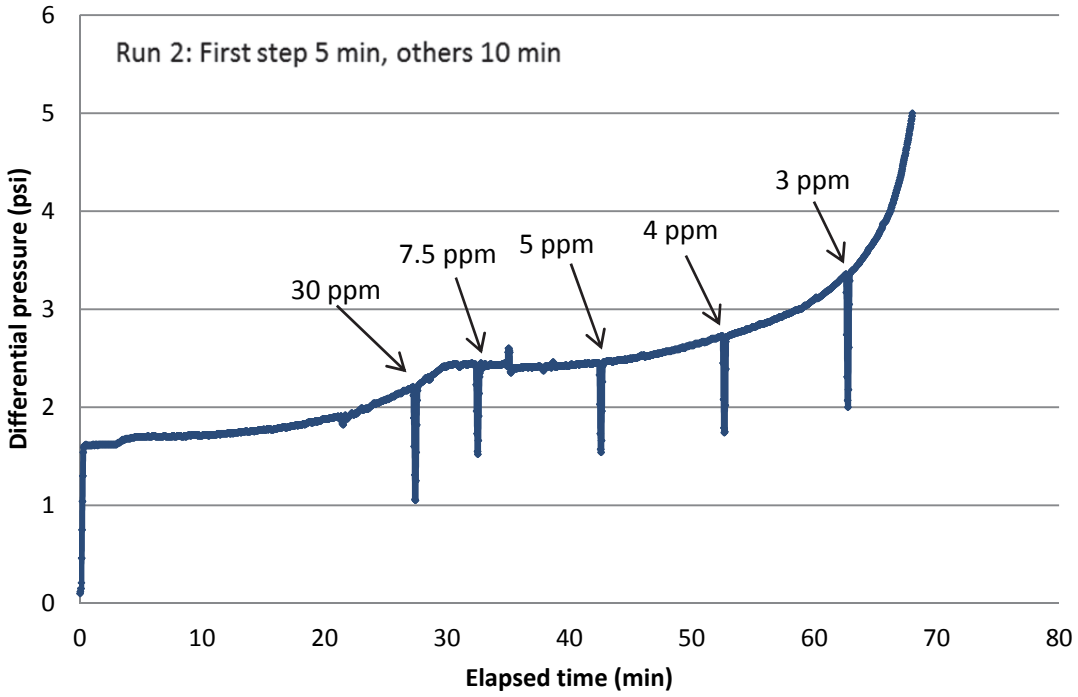

Polyacrylate

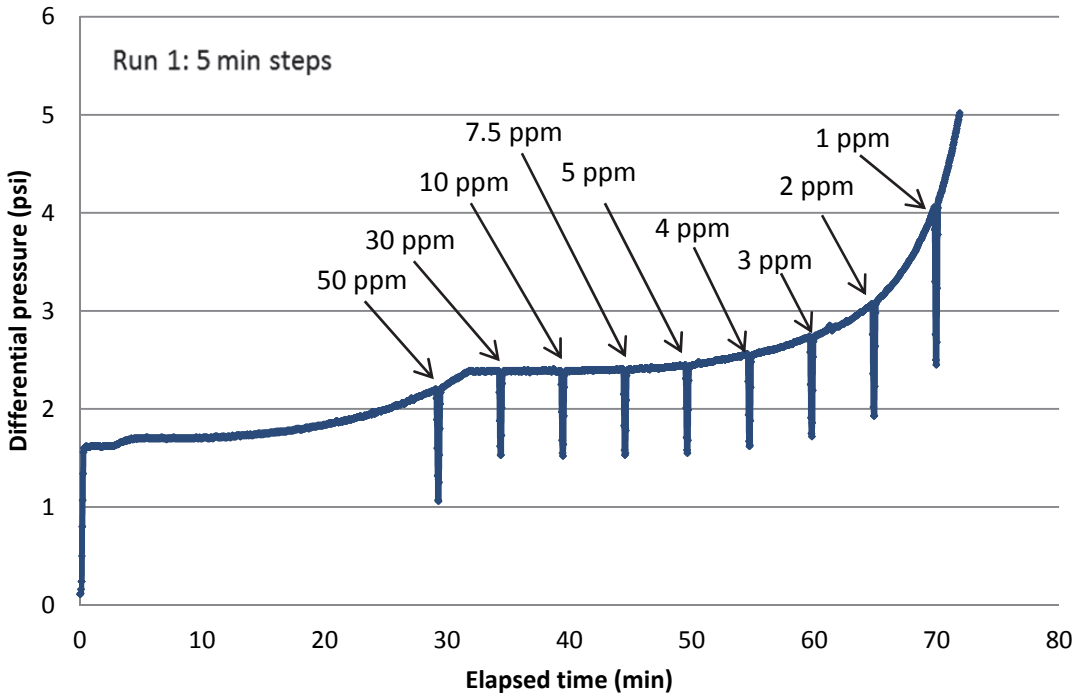

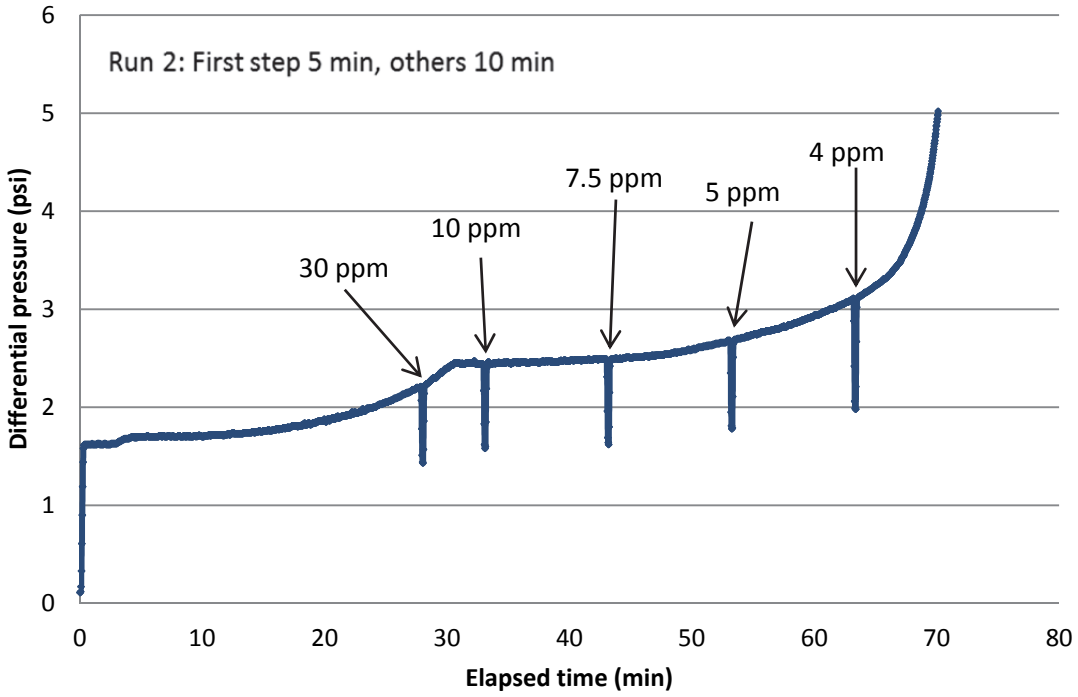

Polyaspartate 3

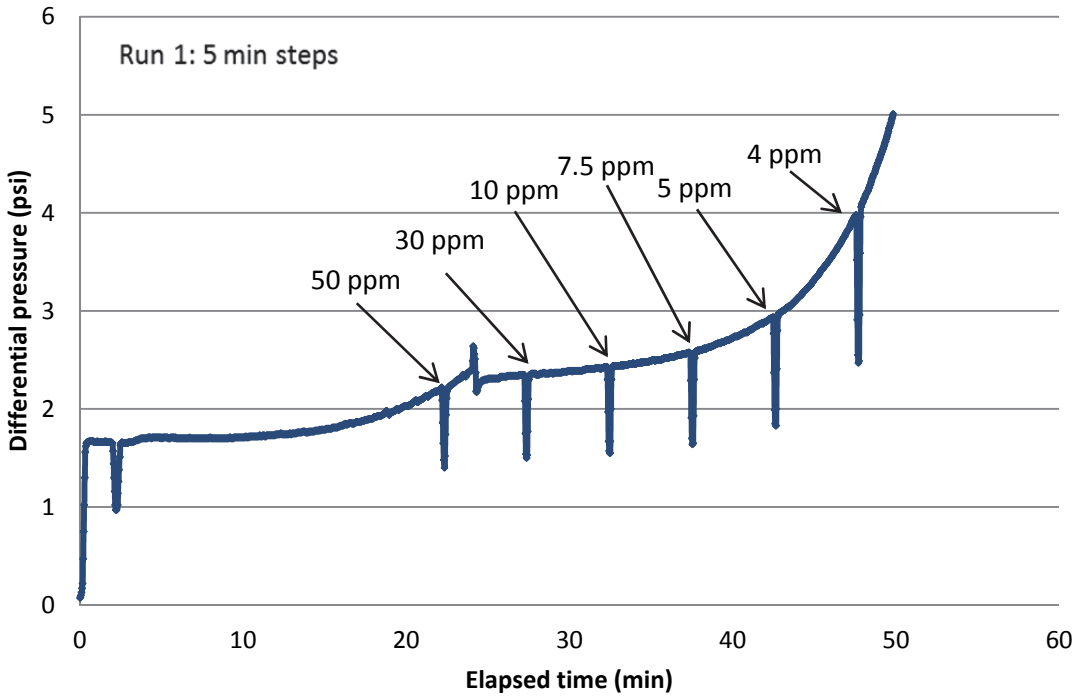

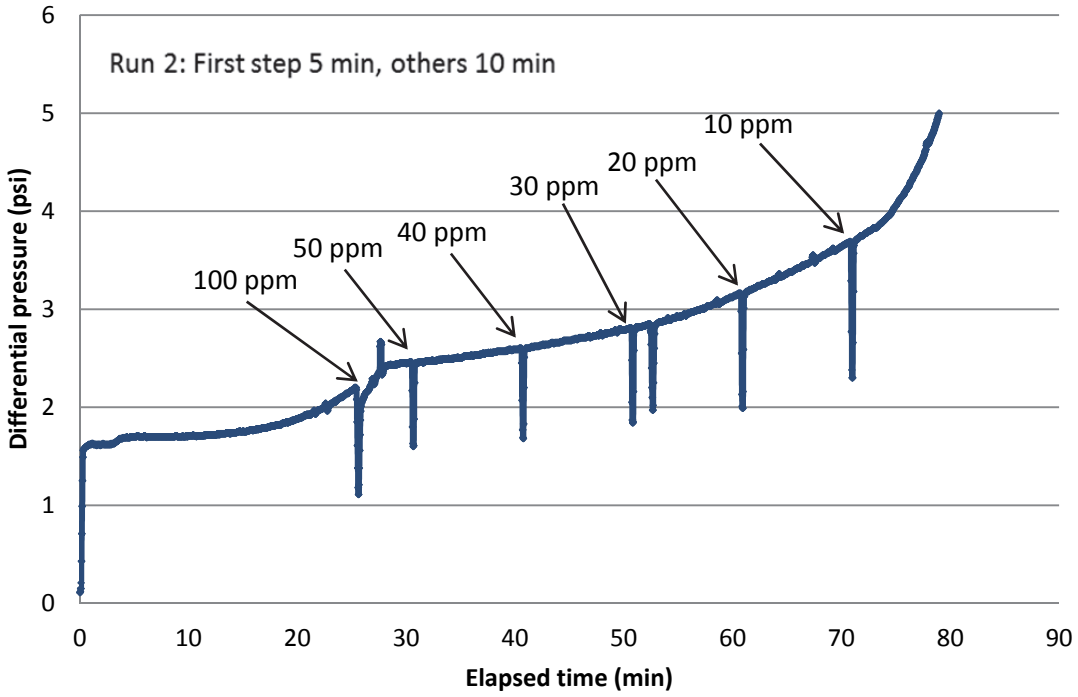

Copolymer 1

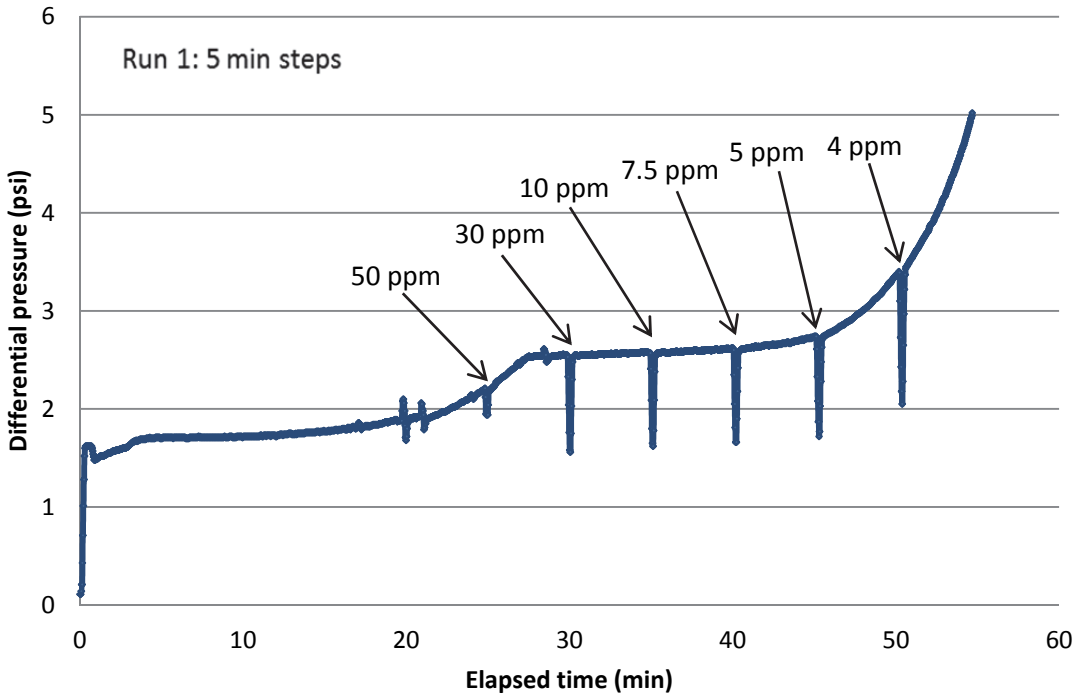
Run 1: 5 min steps
Differential pressure (psi)
Elapsed time (min)
50 ppm
30 ppm
10 ppm
7.5 ppm
5 ppm
4 ppm
0
1
2
3
4
5
6
0
10
20
30
40
50
60

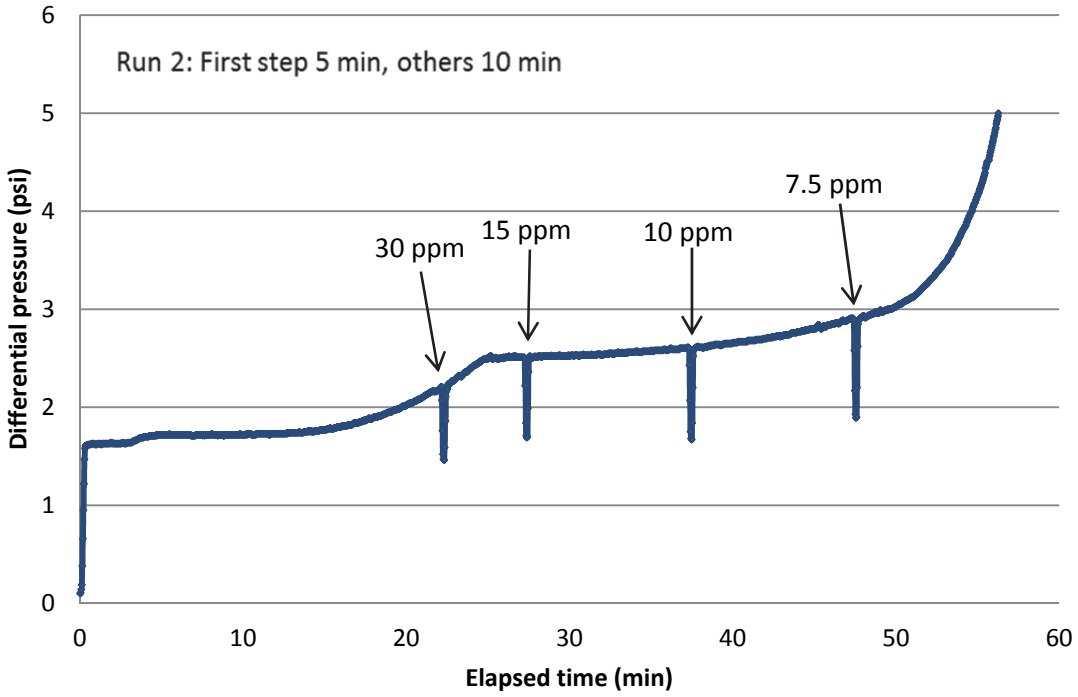
Run 2: First step 5 min, others 10 min
Differential pressure (psi)
Elapsed time (min)
30 ppm
15 ppm
10 ppm
7.5 ppm
0
1
2
3
4
5
6
0
10
20
30
40
50
60

Copolymer 3

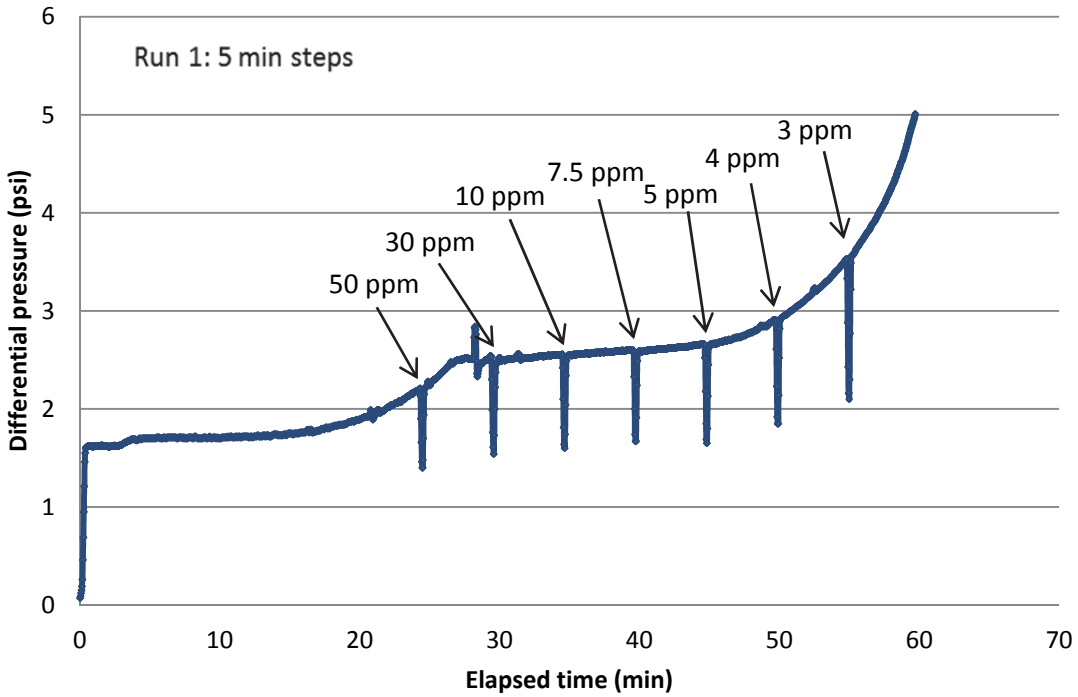
Run 1: 5 min steps
Differential pressure (psi)
Elapsed time (min)
50 ppm
30 ppm
10 ppm
7.5 ppm
5 ppm
4 ppm
3 ppm
0
1
2
3
4
5
6
0
10
20
30
40
50
60
70

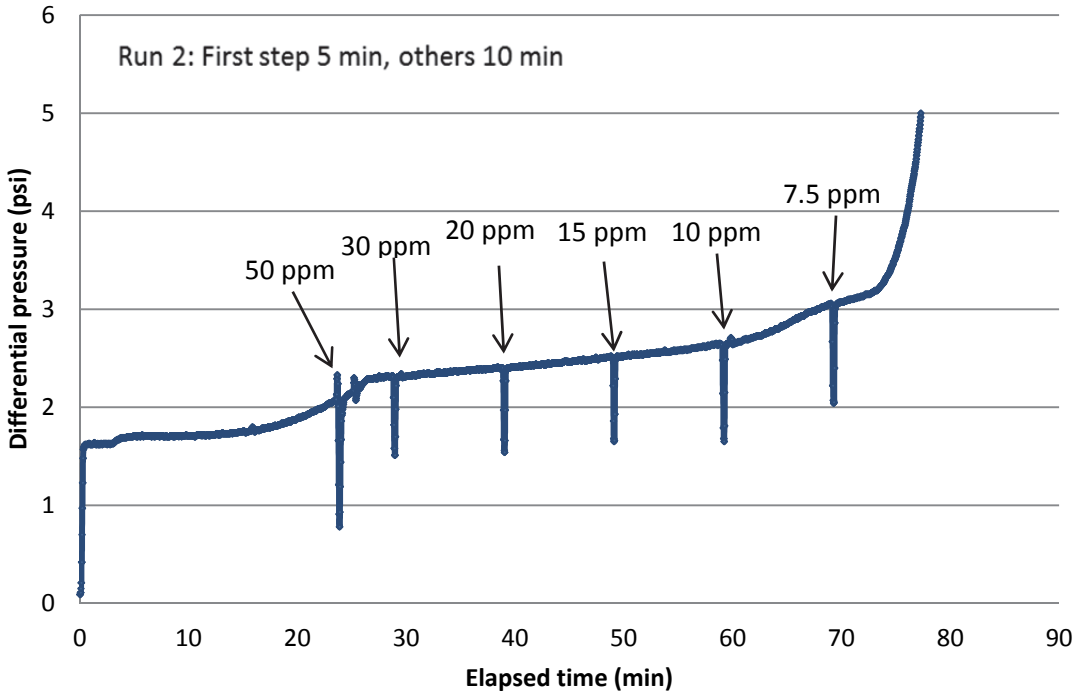
Run 2: First step 5 min, others 10 min
Differential pressure (psi)
Elapsed time (min)
50 ppm
30 ppm
20 ppm
15 ppm
10 ppm
7.5 ppm
0
1
2
3
4
5
6
0
10
20
30
40
50
60
70
80
90

Copolymer 5

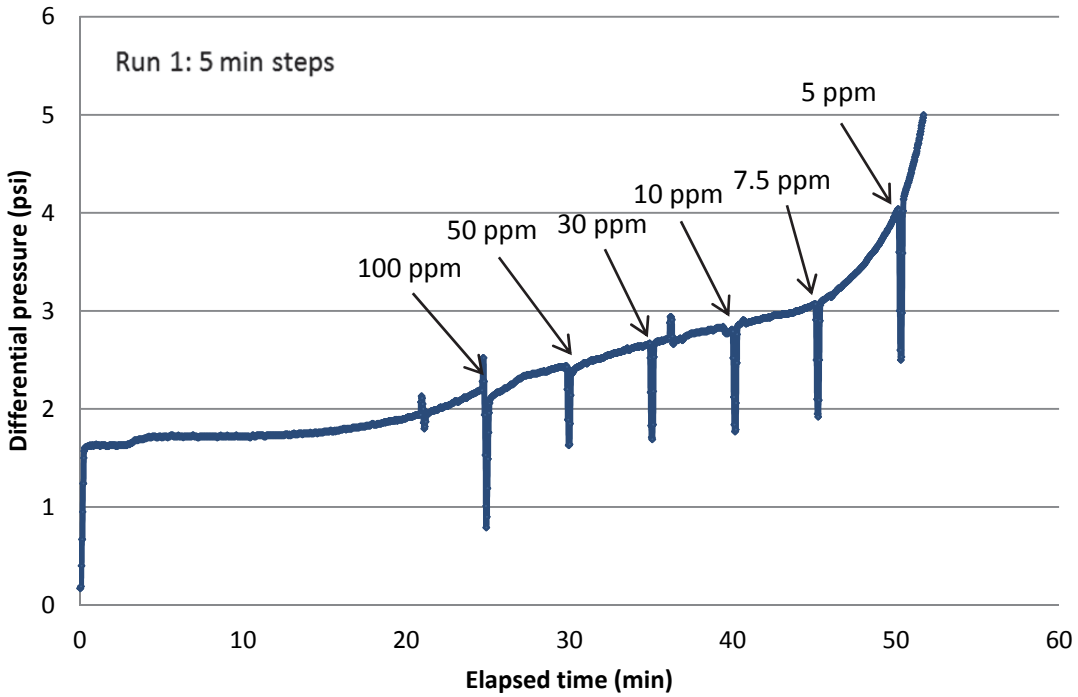
Run 1: 5 min steps
Differential pressure (psi)
Elapsed time (min)
100 ppm
50 ppm
30 ppm
10 ppm
7.5 ppm
5 ppm
0
1
2
3
4
5
6
0
10
20
30
40
50
60

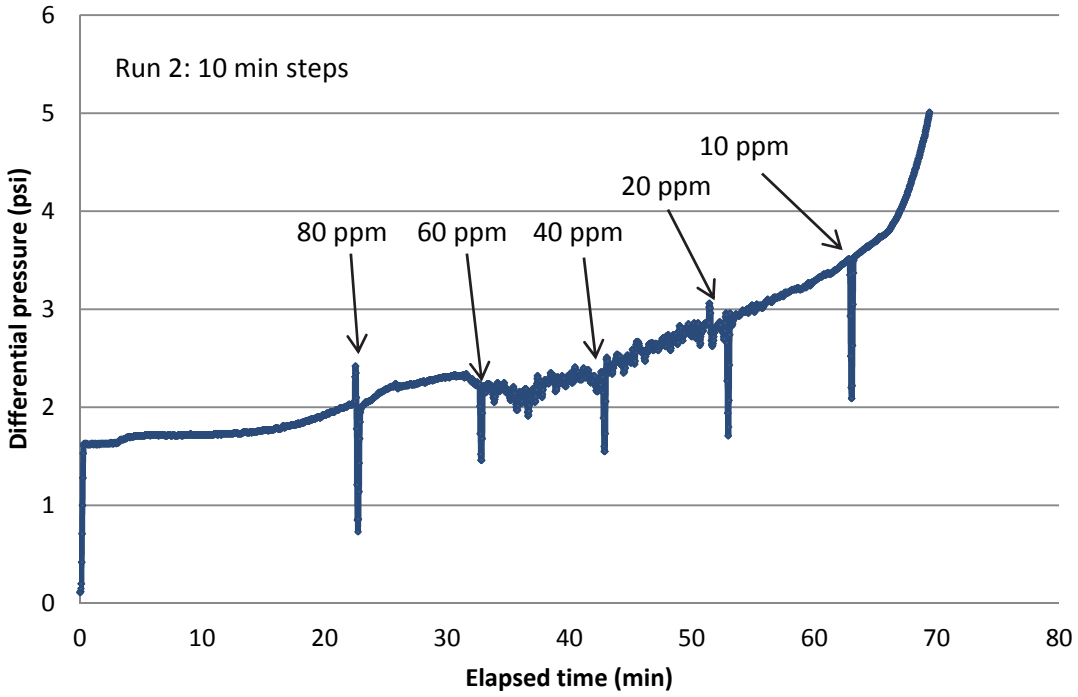
Run 2: 10 min steps
Differential pressure (psi)
Elapsed time (min)
80 ppm
60 ppm
40 ppm
20 ppm
10 ppm
0
1
2
3
4
5
6
0
10
20
30
40
50
60
70
80

Terpolymer 1

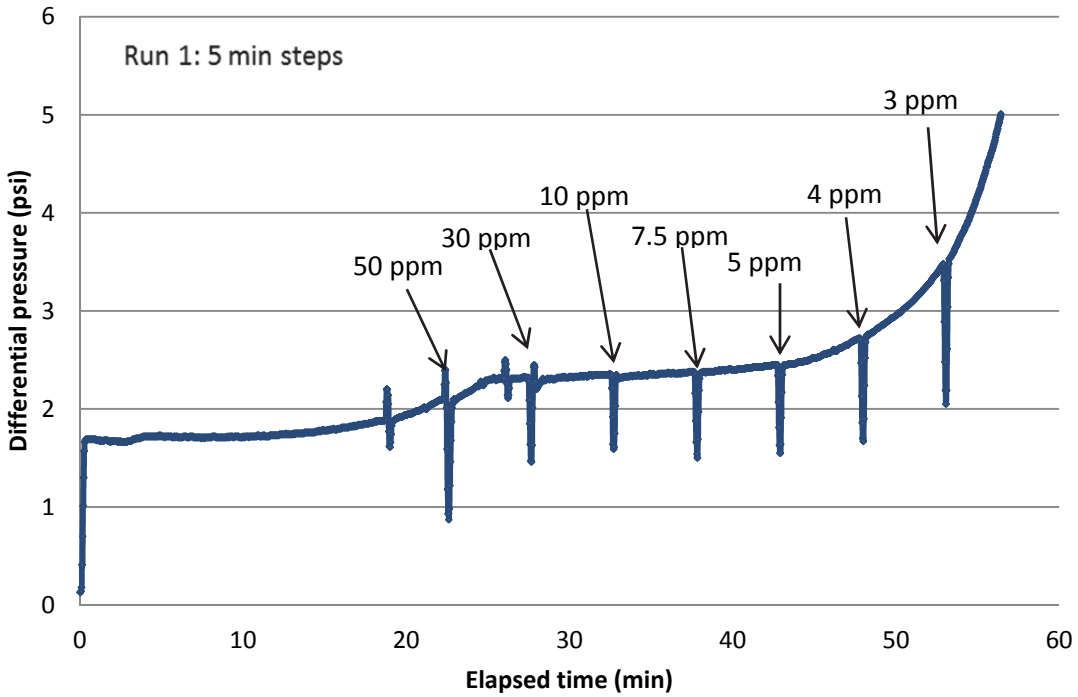

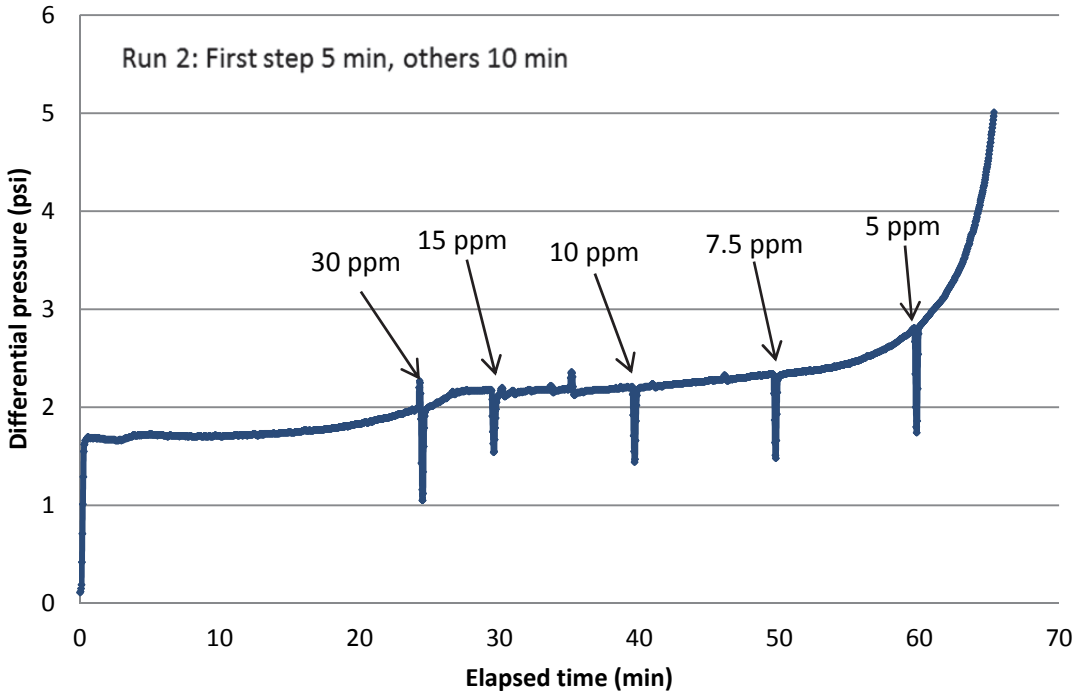

Terpolymer 2

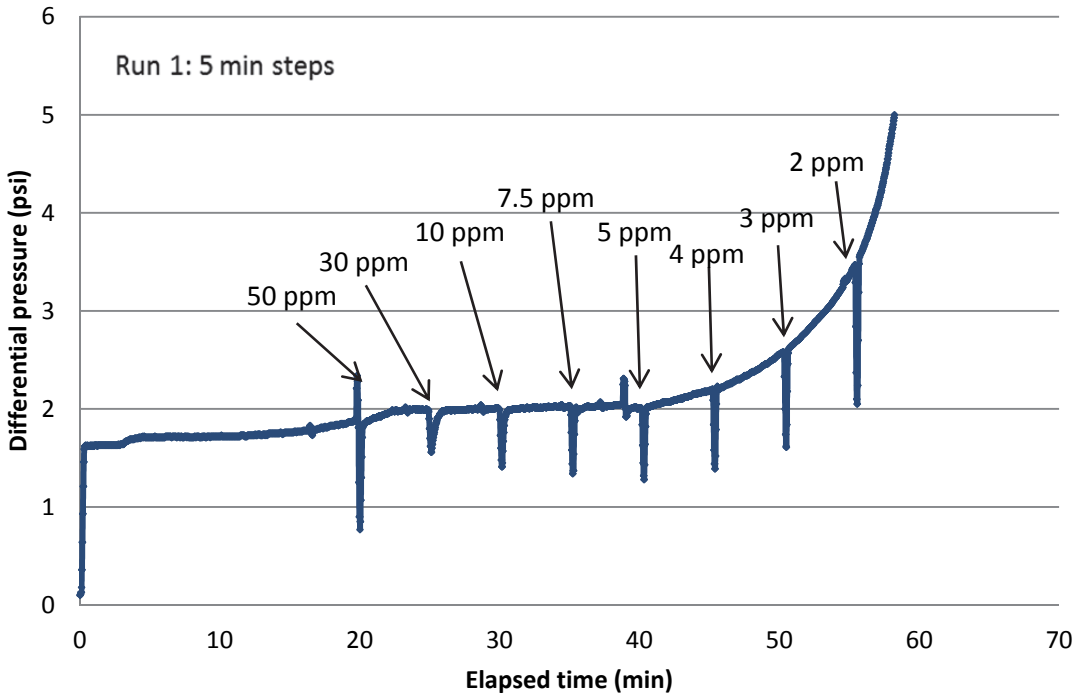

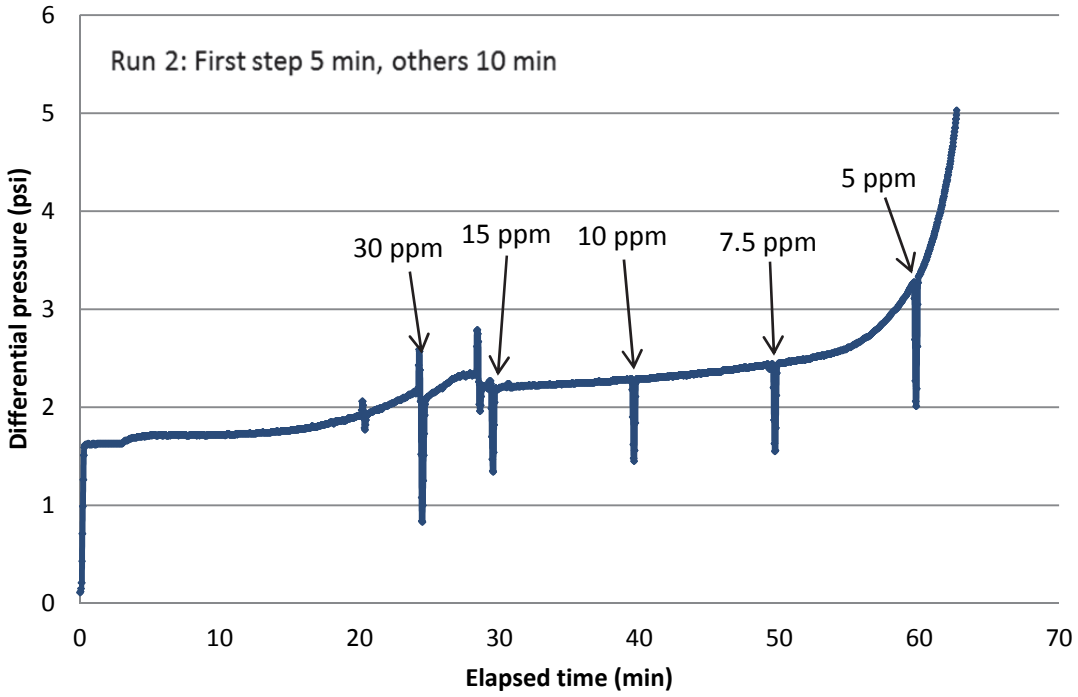

APPENDIX 4: WATSIM CALCULATIONS

Input data: pH 9.2 T=50 °C

CATIONS		**ANIONS**	
Calcium (as Ca)	80.00	Chloride (as Cl)	35600
Magnesium (as Mg)	0.00	Sulfate (as SO_4)	0.00
Sodium (as Na)	24600	"M" Alkalinity (as $CaCO_3$)	3611
Potassium (as K)	0.00	"P" Alkalinity (as $CaCO_3$)	1058
Ammonia (as NH_3)	0.00	Oxalic acid (as C_2O_4)	0.00
Iron (as Fe)	0.00	Cyanide (as HCN)	0.00
Manganese (as Mn)	0.00	Phosphate (as PO_4)	0.00
Aluminum (as Al)	0.00	Pyrophosphate (as PO_4)	0.00
Zinc (as Zn)	0.00	Silica (as SiO_2)	0.00
Boron (as B)	0.00	Nitrate (as NO_3)	0.00
		Fluoride (as F)	0.00

PARAMETERS		**COMMENTS**
pH	9.20	
Temperature (°C)	50.00	
Calculated T.D.S.	62478	
Calculated Cond.	58516	

RAW WATER DEPOSITION POTENTIAL INDICATORS: pH 9.2 T=50 °C

SATURATION LEVEL		FREE ION MOMENTARY EXCESS (ppm)	
Calcite ($CaCO_3$)	60.50	Calcite ($CaCO_3$)	146.44
Aragonite ($CaCO_3$)	51.13	Aragonite ($CaCO_3$)	145.42
Anhydrite ($CaSO_4$)	0.00	Anhydrite ($CaSO_4$)	-2.6%E+3
Gypsum ($CaSO_4*2H_2O$)	0.00	Gypsum ($CaSO_4*2H_2O$)	-3.1%E+3
Calcium phosphate	0.00	Calcium phosphate	-0.00297
Hydroxyapatite	0.00	Hydroxyapatite	-1.2%E+3
Fluorite (CaF_2)	0.00	Fluorite (CaF_2)	-84.99
Silica (SiO_2)	0.00	Silica (SiO_2)	-186.84
Brucite ($Mg(OH)_2$)	0.00	Brucite ($Mg(OH)_2$)	-12.12
Magnesium silicate	0.00	Magnesium silicate	-373.84
Iron hydroxide ($Fe(OH)_3$)	0.00	Iron hydroxide ($Fe(OH)_3$)	>-0.001
Siderite ($FeCO_3$)	0.00	Siderite ($FeCO_3$)	-0.00116
Strengite ($FePO_4*2H_2O$)	0.00	Strengite ($FePO_4*2H_2O$)	>-0.001
Calcium oxalate (CaC_2O_4)	0.00	Calcium oxalate (CaC_2O_4)	-3.20
Ca pyrophosphate (CaP_2O_7)	0.00	Ca pyrophosphate (CaP_2O_7)	-0.335
Zinc phosphate ($Zn_3(PO_4)_2$)	0.00	Zinc phosphate ($Zn_3(PO_4)_2$)	-0.318

SIMPLE INDICES		BOUND IONS	TOTAL	FREE
Langelier	2.98	Calcium	80.00	61.02
Ryznar	3.25	Carbonate	2251	152.56
Puckorius	2.61	Phosphate	0.00	0.00
Larson-Skold Index	12.12			
C.C.P.P.	199.60			

CHEMICAL PROPERTIES		OPERATING CONDI-	
D.I.C. (mg/L C)	544.36	Temperature (°C)	50.00
Pb solubility(ug/L)	0.00176	Time(mins)	3.00
Cu solubility(mg/L)	0.151		
Zn solubility(mg/L)	97.29		
PPO_4 solubility(mg/L)	310.39		
PO_4 solubility(mg/L)	499.79		

Input data: pH 9.2 T=75 °C

CATIONS		ANIONS	
Calcium (as Ca)	80.00	Chloride (as Cl)	35600
Magnesium (as Mg)	0.00	Sulfate (as SO_4)	0.00
Sodium (as Na)	24600	"M" Alkalinity (as $CaCO_3$)	3611
Potassium (as K)	0.00	"P" Alkalinity (as $CaCO_3$)	1058
Ammonia (as NH_3)	0.00	Oxalic acid (as C_2O_4)	0.00
Iron (as Fe)	0.00	Cyanide (as HCN)	0.00
Manganese (as Mn)	0.00	Phosphate (as PO_4)	0.00
Aluminum (as Al)	0.00	Pyrophosphate (as PO_4)	0.00
Zinc (as Zn)	0.00	Silica (as SiO_2)	0.00
Boron (as B)	0.00	Nitrate (as NO_3)	0.00
		Fluoride (as F)	0.00

PARAMETERS		COMMENTS
pH	9.20	
Temperature (°C)	75.00	
Calculated T.D.S.	62456	
Calculated Cond.	54462	

RAW WATER DEPOSITION POTENTIAL INDICATORS: pH 9.2 T=75 °C

SATURATION LEVEL		FREE ION MOMENTARY EXCESS (ppm)	
Calcite ($CaCO_3$)	41.37	Calcite ($CaCO_3$)	119.93
Aragonite ($CaCO_3$)	34.08	Aragonite ($CaCO_3$)	118.04
Anhydrite ($CaSO_4$)	0.00	Anhydrite ($CaSO_4$)	-2.2%E+3
Gypsum ($CaSO_4*2H_2O$)	0.00	Gypsum ($CaSO_4*2H_2O$)	-3.4%E+3
Calcium phosphate	0.00	Calcium phosphate	-0.00191
Hydroxyapatite	0.00	Hydroxyapatite	-1.5%E+3
Fluorite (CaF_2)	0.00	Fluorite (CaF_2)	-94.52
Silica (SiO_2)	0.00	Silica (SiO_2)	-306.99
Brucite ($Mg(OH)_2$)	0.00	Brucite ($Mg(OH)_2$)	-6.19
Magnesium silicate	0.00	Magnesium silicate	-465.67
Iron hydroxide ($Fe(OH)_3$)	0.00	Iron hydroxide ($Fe(OH)_3$)	>-0.001
Siderite ($FeCO_3$)	0.00	Siderite ($FeCO_3$)	-0.00144
Strengite ($FePO_4*2H_2O$)	0.00	Strengite ($FePO_4*2H_2O$)	>-0.001
Calcium oxalate (CaC_2O_4)	0.00	Calcium oxalate (CaC_2O_4)	-3.45
Ca pyrophosphate (CaP_2O_7)	0.00	Ca pyrophosphate (CaP_2O_7)	-0.332
Zinc phosphate ($Zn_3(PO_4)_2$)	0.00	Zinc phosphate ($Zn_3(PO_4)_2$)	-0.358

SIMPLE INDICES		BOUND IONS	TOTAL	FREE
Langelier	3.22	Calcium	80.00	66.65
Ryznar	2.76	Carbonate	2550	78.72
Puckorius	2.08	Phosphate	0.00	0.00
Larson-Skold Index	11.43			
C.C.P.P.	199.65			

CHEMICAL PROPERTIES		OPERATING CONDITIONS	
D.I.C. (mg/L C)	544.20	Temperature (°C)	75.00
Pb solubility(ug/L)	< 0.001	Time(mins)	3.00
Cu solubility(mg/L)	0.00904		
Zn solubility(mg/L)	2.09		
PPO_4 solubility(mg/L)	309.06		
PO_4 solubility(mg/L)	815.77		

Input data: pH 9.2 T=95 °C

CATIONS		ANIONS	
Calcium (as Ca)	80.00	Chloride (as Cl)	35600
Magnesium (as Mg)	0.00	Sulfate (as SO_4)	0.00
Sodium (as Na)	24600	"M" Alkalinity (as $CaCO_3$)	3611
Potassium (as K)	0.00	"P" Alkalinity (as $CaCO_3$)	1058
Ammonia (as NH_3)	0.00	Oxalic acid (as C_2O_4)	0.00
Iron (as Fe)	0.00	Cyanide (as HCN)	0.00
Manganese (as Mn)	0.00	Phosphate (as PO_4)	0.00
Aluminum (as Al)	0.00	Pyrophosphate (as PO_4)	0.00
Zinc (as Zn)	0.00	Silica (as SiO_2)	0.00
Boron (as B)	0.00	Nitrate (as NO_3)	0.00
		Fluoride (as F)	0.00

PARAMETERS		COMMENTS
pH	9.20	
Temperature (°C)	95.00	
Calculated T.D.S.	62480	
Calculated Cond.	50752	

RAW WATER DEPOSITION POTENTIAL INDICATORS: pH 9.2 T=95 °C

SATURATION LEVEL		FREE ION MOMENTARY EXCESS (ppm)	
Calcite ($CaCO_3$)	27.91	Calcite ($CaCO_3$)	71.67
Aragonite ($CaCO_3$)	22.58	Aragonite ($CaCO_3$)	70.63
Anhydrite ($CaSO_4$)	0.00	Anhydrite ($CaSO_4$)	-2.1%E+3
Gypsum ($CaSO_4*2H_2O$)	0.00	Gypsum ($CaSO_4*2H_2O$)	-3.7%E+3
Calcium phosphate	0.00	Calcium phosphate	-0.00154
Hydroxyapatite	0.00	Hydroxyapatite	-1.8%E+3
Fluorite (CaF_2)	0.00	Fluorite (CaF_2)	-103.44
Silica (SiO_2)	0.00	Silica (SiO_2)	-435.02
Brucite ($Mg(OH)_2$)	0.00	Brucite ($Mg(OH)_2$)	-1.45
Magnesium silicate	0.00	Magnesium silicate	-547.56
Iron hydroxide ($Fe(OH)_3$)	0.00	Iron hydroxide ($Fe(OH)_3$)	>-0.001
Siderite ($FeCO_3$)	0.00	Siderite ($FeCO_3$)	-0.00188
Strengite ($FePO_4*2H_2O$)	0.00	Strengite ($FePO_4*2H_2O$)	>-0.001
Calcium oxalate (CaC_2O_4)	0.00	Calcium oxalate (CaC_2O_4)	-3.81
Ca pyrophosphate (CaP_2O_7)	0.00	Ca pyrophosphate (CaP_2O_7)	-0.350
Zinc phosphate ($Zn_3(PO_4)_2$)	0.00	Zinc phosphate ($Zn_3(PO_4)_2$)	-0.401

SIMPLE INDICES		BOUND IONS	TOTAL	FREE
Langelier	3.38	Calcium	80.00	70.23
Ryznar	2.44	Carbonate	2644	45.74
Puckorius	1.73	Phosphate	0.00	0.00
Larson-Skold Index	11.23			
C.C.P.P.	199.67			

CHEMICAL PROPERTIES		OPERATING CONDITIONS	
D.I.C. (mg/L C)	544.19	Temperature (°C)	95.00
Pb solubility(ug/L)	< 0.001	Time(mins)	3.00
Cu solubility(mg/L)	0.00126		
Zn solubility(mg/L)	0.127		
PPO_4 solubility(mg/L)	317.68		
PO_4 solubility(mg/L)	1294		

s